1988-06

An advanced study of natural convection immersion cooling of 3 x 3 array of simulated components in an enclosure filled with dielectric liquid

Benedict, Terry J.

Monterey, California. Naval Postgraduate School

NAVAL POSTGRADUATE SCHOOL
Monterey, California

THESIS

AN ADVANCED STUDY OF NATURAL CONVECTION IMMERSION COOLING OF A 3 x 3 ARRAY OF SIMULATED COMPONENTS IN AN ENCLOSURE FILLED WITH DIELECTRIC LIQUID

by

Terry J. Benedict

June 1988

Co-advisors: Matthew D. Kelleher
Yogendra Joshi

Approved for public release; distribution is unlimited

REPORT DOCUMENTATION PAGE

1a. REPORT SECURITY CLASSIFICATION UNCLASSIFIED	1b. RESTRICTIVE MARKINGS
2a. SECURITY CLASSIFICATION AUTHORITY	3. DISTRIBUTION / AVAILABILITY OF REPORT Approved for public release; distribution is unlimited
2b. DECLASSIFICATION / DOWNGRADING SCHEDULE	
4. PERFORMING ORGANIZATION REPORT NUMBER(S)	5. MONITORING ORGANIZATION REPORT NUMBER(S)
6a. NAME OF PERFORMING ORGANIZATION Naval Postgraduate School 6b. OFFICE SYMBOL (*If applicable*) Code 69	7a. NAME OF MONITORING ORGANIZATION Naval Postgraduate School
6c. ADDRESS (*City, State, and ZIP Code*) Monterey, California 93943-5000	7b. ADDRESS (*City, State, and ZIP Code*) Monterey, California 93943-5000
8a. NAME OF FUNDING / SPONSORING ORGANIZATION 8b. OFFICE SYMBOL (*If applicable*)	9. PROCUREMENT INSTRUMENT IDENTIFICATION NUMBER
8c. ADDRESS (*City, State, and ZIP Code*)	10. SOURCE OF FUNDING NUMBERS PROGRAM ELEMENT NO / PROJECT NO / TASK NO / WORK UNIT ACCESSION NO

11. TITLE (*Include Security Classification*)
AN ADVANCED STUDY OF NATURAL CONVECTION IMMERSION COOLING OF A 3 x 3 ARRAY OF SIMULATED COMPONENTS IN AN ENCLOSURE FILLED WITH DIELECTRIC LIQUID

12. PERSONAL AUTHOR(S)
Benedict, Terry J.

13a. TYPE OF REPORT	13b. TIME COVERED	14. DATE OF REPORT (*Year, Month, Day*)	15. PAGE COUNT
Master's Thesis	FROM _____ TO _____	1988, June	115

16. SUPPLEMENTARY NOTATION
The views expressed in this thesis are those of the author and do not reflect the official policy or position of the Department of Defense or the U.S. Government.

17 COSATI CODES			18. SUBJECT TERMS (*Continue on reverse if necessary and identify by block number*)
FIELD	GROUP	SUB-GROUP	Electronic Cooling; Protruding Heat Sources; Flow Visualization; Convective Heat Transfer; Immersion Cooling; Dielectric Liquids

19. ABSTRACT (*Continue on reverse if necessary and identify by block number*)

An experimental study has been conducted to examine the three-dimensional natural convection heat transfer from an array of simulated electronic components immersed in a chamber filled with Fluorinert FC-75, a commercially available dielectric liquid. The top and bottom walls of the chamber were maintained at uniform temperature while all other surfaces were insulated. The simulated components were in the form of a 3 x 3 array of discrete protruding aluminum blocks, each with geometrical dimensions of a 20 Pin Dual-inline-Package. The components were electrically powered resulting in a range of energy dissipation levels from 0.1 to 3.1 watts. Flow visualization in steady state was accomplished using Magnesium particles illuminated by a Helium Neon laser plane. Component surface temperature measurements allowed determination of the heat transfer characteristics. Timewise fluctuations

20. DISTRIBUTION / AVAILABILITY OF ABSTRACT ☒ UNCLASSIFIED/UNLIMITED ☐ SAME AS RPT ☐ DTIC USERS	21. ABSTRACT SECURITY CLASSIFICATION Unclassified
22a. NAME OF RESPONSIBLE INDIVIDUAL Prof. Matthew D. Kelleher	22b. TELEPHONE (*Include Area Code*) (408) 646-2530 22c. OFFICE SYMBOL Code 69Kk

#19 - ABSTRACT - (CONTINUED)

of temperature at several locations were measured with increasing power levels.

Approved for public release; distribution is unlimited

An Advanced Study of Natural Convection Immersion Cooling of a 3 x 3 Array of Simulated Components in an Enclosure Filled with Dielectric Liquid

by

Terry J. Benedict
Lieutenant, United States Navy
B.S., United States Naval Academy, 1982

Submitted in partial fulfillment of the
requirements for the degree of

MASTER OF SCIENCE IN ENGINEERING SCIENCE

from the

NAVAL POSTGRADUATE SCHOOL
June 1988

ABSTRACT

An experimental study has been conducted to examine the three-dimensional natural convection heat transfer from an array of simulated electronic components immersed in a chamber filled with Fluorinert FC-75, a commercially available dielectric liquid. The top and bottom walls of the chamber were maintained at uniform temperature while all other surfaces were insulated. The simulated components were in the form of a 3 x 3 array of discrete protruding aluminum blocks, each with geometrical dimensions of a 20 Pin Dual-inline-Package. The components were electrically powered resulting in a range of energy dissipation levels from 0.1 to 3.1 watts. Flow visualization in steady state was accomplished using Magnesium particles illuminated by a Helium Neon laser plane. Component surface temperature measurements allowed determination of the heat transfer characteristics. Timewise fluctuations of temperature at several locations were measured with increasing power levels.

TABLE OF CONTENTS

LIST OF TABLES

LIST OF FIGURES

NOMENCLATURE

SYMBOL	DESCRIPTION	UNITS
A	Area	m^2
α	Thermal Diffusivity	m^2/sec
β	Thermal Expansion Coefficient	1/K
c_p	Specific Heat	$J/kg-^oC$
δ	Uncertainty in the Variables	Various
g	Acceleration of Gravity	m/sec^2
Gr	Grashof Number	Dimensionless
h	Heat Transfer Coefficient	W/m^2-^oC
k	Thermal Conductivity	$W/m-^oC$
L	Characteristic Length	m
Nu	Nusselt Number	Dimensionless
Nu_c	Nusselt Number at the Center	Dimensionless
ν	Kinematic Viscosity	m^2/sec
Pr	Prandtl Number	Dimensionless
Q_{con}	Energy Loss by Conduction	W
Q_{conv}	Energy Added to the Fluid	W
Q_{in}	Energy Input to the Heaters	W
R	Resistance of the Precision Resistor	ohms
R_{con}	Total Thermal Resistance	$^oC/W$
Ra_t	Temperature Based Rayleigh Number	Dimensionless
Ra_f	Flux Based Rayleigh Number	Dimensionless

ρ	Density	kg/m^3
T_b	Back Surface Temperature of Board	^oC
T_c	Average Heat Exchanger Temperature	^oC
T_f	Average Film Temperature	^oC
T_s	Back Surface Temperature of the Component	^oC
V_{in}	Input Voltage	Volts
V_h	Voltage Across the Heaters	Volts

ACKNOWLEDGMENTS

The author would like to express his sincere gratitude to Professors Joshi and Kelleher for their guidance, advice and friendship in this endeavor.

He wishes to thank all the members of the Mechanical Engineering support shop for their superior efforts and professional advice on the many difficult problems encountered.

The author would like to thank the Educational Media Department Photography lab personnel for their efforts that went above and beyond the norm. These people are true professionals.

Last but not least, a very special word of thanks to my wife, Kim, whose understanding, support and patience made this thesis and the entire tour an enjoyable experience.

I. INTRODUCTION

A. STATEMENT OF PROBLEM

As microelectronic components continue to decrease in size and increase in component density, the problem of heat dissipation becomes increasingly more critical in the design of circuits and components. A five-order-of-magnitude increase in circuit integration in the last 25 years has been associated with successive revolutions in components technology.

With the recent development of CMOS, industry has seen an almost three-order-of-magnitude reduction in size, an order-of-magnitude increase in the characteristic component dimensions and perhaps, most importantly, a precipitous drop in transition switching energy from 10^{-9} J in 1960 to nearly 10^{-13} J in present day devices. It is anticipated that power dissipation of 100 W in a 10 million component chip could be encountered by 1990. This would result in component heat fluxes in excess of 100 W/cm^2 [Bar-Cohen, 1987, pp. 159-175]. The strong requirement to keep components at low temperature levels, 100^{o}C to 125^{o}C, does exist, since for every 20^{o}C decrease in components temperature, the components failure rates are cut in half [Oktay, 1986, pp. 36-42].

B. BACKGROUND

Air cooling is the standard design in today's systems. Advances in air cooling technology now include impingement cooling and combined conduction and air cooling technology which offers even higher cooling rates than natural or forced convection air cooling. However, air as a heat transfer medium is extremely limited not only in its ability to transfer heat but also in its capacity to carry the transferred energy with a reasonable temperature increase [Baker, 1972, pp. 213-222].

Special component surfaces have been investigated. Features such as Turbulence Promoting Fins (TPF) have significantly higher cooling enhancements when used with special gases such as Helium as the closed cycle coolant [Kishimoto et al., 1983, pp. 286-93]. By doing so, a 300% greater dissipation rate can be reached than in an open cycle with air as the coolant.

Forced convection in liquids offers greater heat transfer coefficients than does natural convection in liquids or air. However, forced convection introduces two major problems: (i) greater amounts of expensive coolant are required and (ii) pumps and external plumbing increase the size and reduce the reliability by introducing the possibility of vibration related failures to the system [Baker, 1973, pp. 163-173].

Boiling can produce very large scale heat transfer coefficients, but it also introduces major problems: (i) boiling restricts the physical design of the system, (ii) if the surface is very smooth, as most electronic components are, a high degree of superheat may be required so that nucleation can occur. The occurrence of periodic boiling due to the high local heat flux may result in severe local turbulence and mechanical damage and (iii) boiling may result in the concentration of impurities at the nucleation site [Baker, 1973, pp. 163-173].

C. STUDIES ON NATURAL CONVECTION COOLING OF ELECTRONIC DEVICES

1. Numerical Studies

Of the different heat transfer modes mentioned above, immersion cooling by natural convection offers not only high heat transfer potential, but also a practical means of controlling circuit temperatures. However, only limited heat transfer data are available for immersion cooling of discrete, protruding heat sources [Liu et al., 1987, pp. 309-30]. Early studies of natural convection heat transfer were motivated by applications such as energy conservation and solar energy collection. The pertinent length scales were several order of magnitude higher then those applicable in cooling of electronic equipment. However, recent studies have focused on computational and

experimental studies of natural convection cooling in electronic components.

[Han et al., 1984, pp. 21-28] have used numerical simulation to investigate the transient laminar natural convection in a rectangular enclosure with a localized constant heat flux source. [Acharya et al., 1983, pp. 855-66] have investigated the natural convection phenomenon in an inclined square box shaped enclosure which has energy sources in it. [Jaluria, 1985, pp. 883-92] investigated the interacting natural convection flows generated by flush, isolated thermal energy sources, such as electronic components, located on a vertical adiabatic surface. [Jaluria, 1982, pp. 223-27] also analytically studied the natural convection flow due to multiple isolated heated elements located on a vertical surface. [Torok, 1984, pp. 49-57] used the finite element technique to predict component and board temperatures and heat fluxes.

[Kuhn et al., 1986, pp. 55-62] have investigated the transient three-dimensional natural convective flow and heat transfer within a rectangular box following a sudden temperature change on a rectangular portion of one vertical wall. They found that when two elements are symmetrically placed on the wall, the distance between them has only a slight effect on the mean heat transfer distribution. However, it does have a significant effect on the local Nusselt number. [Shakerin et al., 1986, pp. 17-22]

investigated the natural convection flow adjacent to a heated wall with single and repeated, two-dimensional, rectangular roughness elements. [Oosthuizen et al., 1987, pp. 1-7] studied the heat transfer rates from an element of square cross-sectional shape held at a uniform temperature and mounted on a vertical adiabatic wall of a tilted square enclosure. They found that the mean heat transfer rate from the block did not vary continuously with the angle of inclination.

[Liu et al., 1987, pp. 486-97] have conducted a finite difference numerical study of natural convection flow in a rectangular enclosure of an array of simulated components that are mounted on a vertical wall. The results of this numerical study have been presented for enclosure widths of 18 and 30 mm. It was concluded that:

- The temperature field in the enclosure is characterized by boundary layer regions surrounding individual components.
- There are only small interferences among the components, especially for the lower rows.
- The maximum temperatures on the components surfaces are located on the upper horizontal surfaces of the components. Lower temperatures have been found on the lower horizontal faces of the components in the bottom row.
- The results for the 30 mm width are essentially the same as those for the 18 mm, indicating only a minor dependence on the enclosure width.

[Liu et al., 1987, pp. 309-30] have also observed a local oscillatory surface temperature response in the same

enclosure. Their study found that the components surface temperatures have a tendency to fluctuate within a range of approximately $3^{o}C$ with a period of 4 seconds.

2. Experimental Studies

Numerous experimental studies have been conducted concurrently with the numerical studies described above. Two of the earliest studies were conducted by [Baker, 1972, pp. 213-22] and [Baker, 1973, pp. 163-73]. The purpose of these investigations was to examine liquid immersion techniques for cooling miniature heat sources, specifically effects of component size on the convective heat transfer. [Goel et al., 1986, pp. 1341-46] experimentally investigated the two-dimensional natural convection flow from a long, finite size heat source located on a vertical or inclined plate in air. The principal items of interest were the nonboundary layer effects that arise in the flow, particularly in the vicinity of the source. Flow separation was observed at large inclinations.

[Milanez et al., 1986, pp. 1347-52] experimentally studied the interaction of two horizontal, wide strips on a vertical adiabatic wall in both air and water. They found the results of their experiment in good agreement with past numerical studies. [Ortega et al., 1986, pp. 5-15] presented the results for a series of experiments in air designed to measure the natural convective heat transfer rates and the thermal characteristics of a rectangular array

of cubical roughness elements mounted on an insulated plane wall, with and without a shrouding wall. [Parks et al., 1987, pp. 91-109] simulated microelectronic circuits with thin foil heaters for both flush and protruding components. They found that the protruding heaters have approximately 15% higher coefficients and that the upper heaters have varying coefficients depending upon the array configuration.

A number of studies have been conducted at the Naval Postgraduate school. [Knock, 1983] studied the effect of the location of a single protruding heater in an enclosure filled with water. [Pamuk, 1987] investigated the heat transfer characteristics of an array of nine protruding components immersed in a dielectric fluid in an uninsulated chamber. [Hazard, 1987] studied the natural convection liquid cooling of a vertically arranged components array with and without a shrouding wall.

D. OBJECTIVES

This experimental work was motivated by the numerical study of [Liu et al., 1987, pp. 486-97] and the recent experimental studies of [Pamuk, 1987]. The objectives for this thesis are:

- To design and build a circuit card of nine simulated components and determine the rate of heat transfer for various power inputs.
- To determine the natural convection flow patterns developed in the chamber by means of flow visualization.
- To correlate the data in terms of dimensionless heat transfer parameters such as Rayleigh vs. Nusselt number.

II. EXPERIMENTAL APPARATUS

A. GENERAL CONSIDERATIONS

This experimental study is a continuation of past experiments conducted at the Naval Postgraduate School [Knock, 1983; Pamuk, 1987; Hazard, 1987]. The purpose of this work was to examine natural convection heat transfer and fluid flow from a 3 x 3 element array of simulated electronic components. A major change from the previous experiments was the design of the simulated circuit card. In [Pamuk, 1987] an arrangement of vertical components was used. The present study utilized a horizontal arrangement. A decision to increase the card thickness was made to reduce the contamination of the dielectric fluid by the loose insulating material previously used and also to reduce the conduction loss through the card.

The experimental apparatus consists of a chamber filled with a dielectric fluid. Top view of the chamber is provided in Figure 2.1. The top and bottom surfaces of the chamber are maintained at a prescribed temperature by means of two heat exchangers and two separate chilled water circulation baths. One vertical wall of the chamber simulates a circuit card. It contains nine simulated components in a 3 x 3 array, while all other vertical walls are insulated. The geometrical arrangement of the simulated

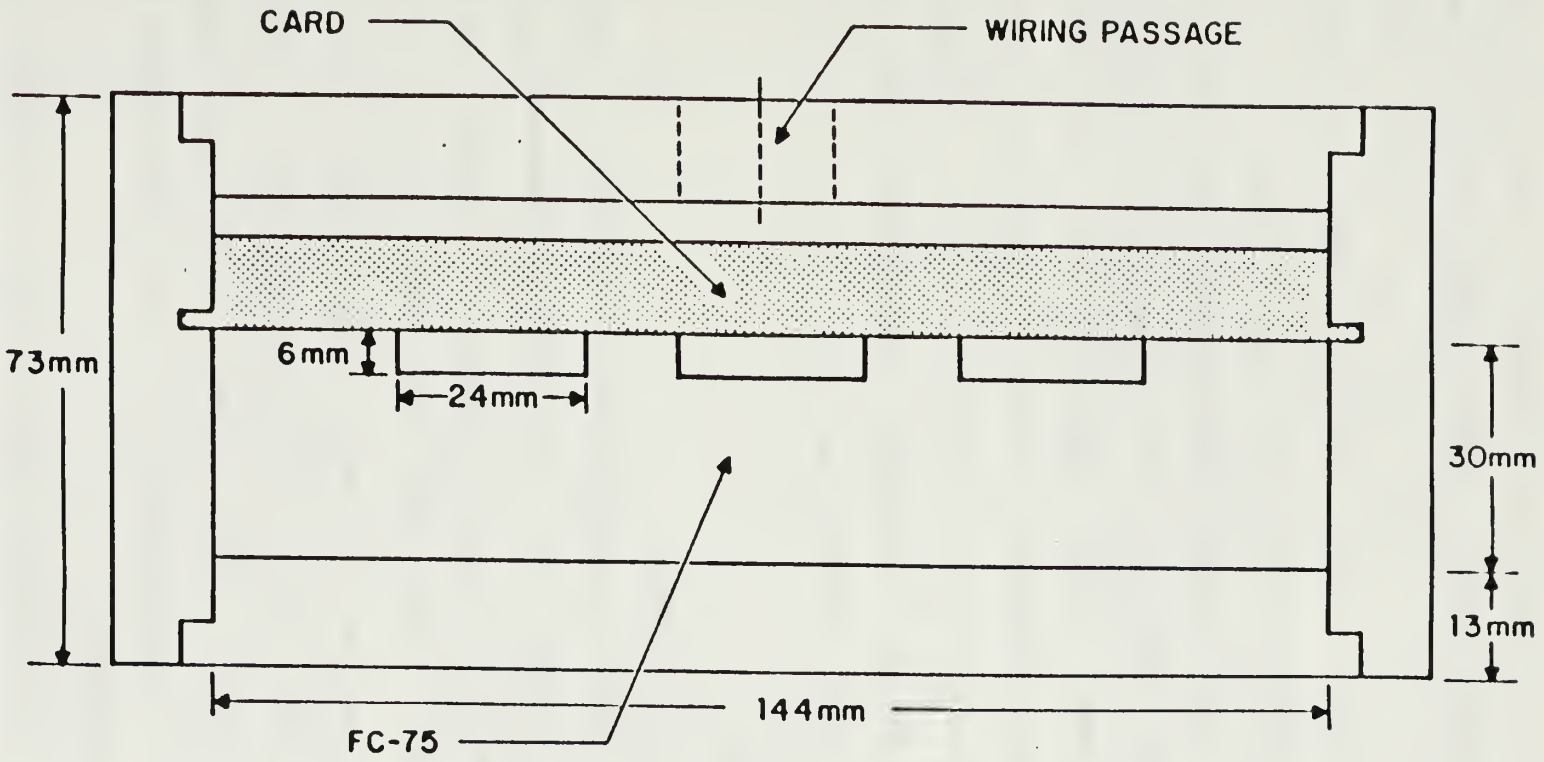

Figure 2.1 Top View of Chamber

components on the card is seen in Figure 2.2. The components were chosen to simulate an array of 20 pin Dual-inline-packages (DIPS). Their dimensions are identical to those used by [Liu et al., 1987, pp. 486-97; Liu et al., 1987, pp. 309-30; Pamuk, 1987] in order to permit future comparisons of experiments and computations.

The heating elements were made of aluminum and heated by means of small foil type resistance heaters attached to the bottom surfaces. The temperatures of the faces of the elements were measured by means of embedded thermocouples. Data were recorded and processed using an automatic data acquisition system. The major components of the system are described in the following section.

B. COMPONENTS

1. Heating Element

Each heating element was a block of aluminum 6mm by 8mm by 24mm (Figure 2.3). The temperatures at the faces of the blocks were measured by means of thermocouples placed within grooves (0.5mm deep) on each surface. The front surface thermocouple was passed through the block by means of a 1.02mm hole drilled through the block. All grooves were filled with high thermal conductivity epoxy and smoothed prior to attachment to the simulated circuit card.

2. Thermocouples

All thermocouples were 10-mil (0.254mm) copper-constantan. These small wires were chosen to minimize the

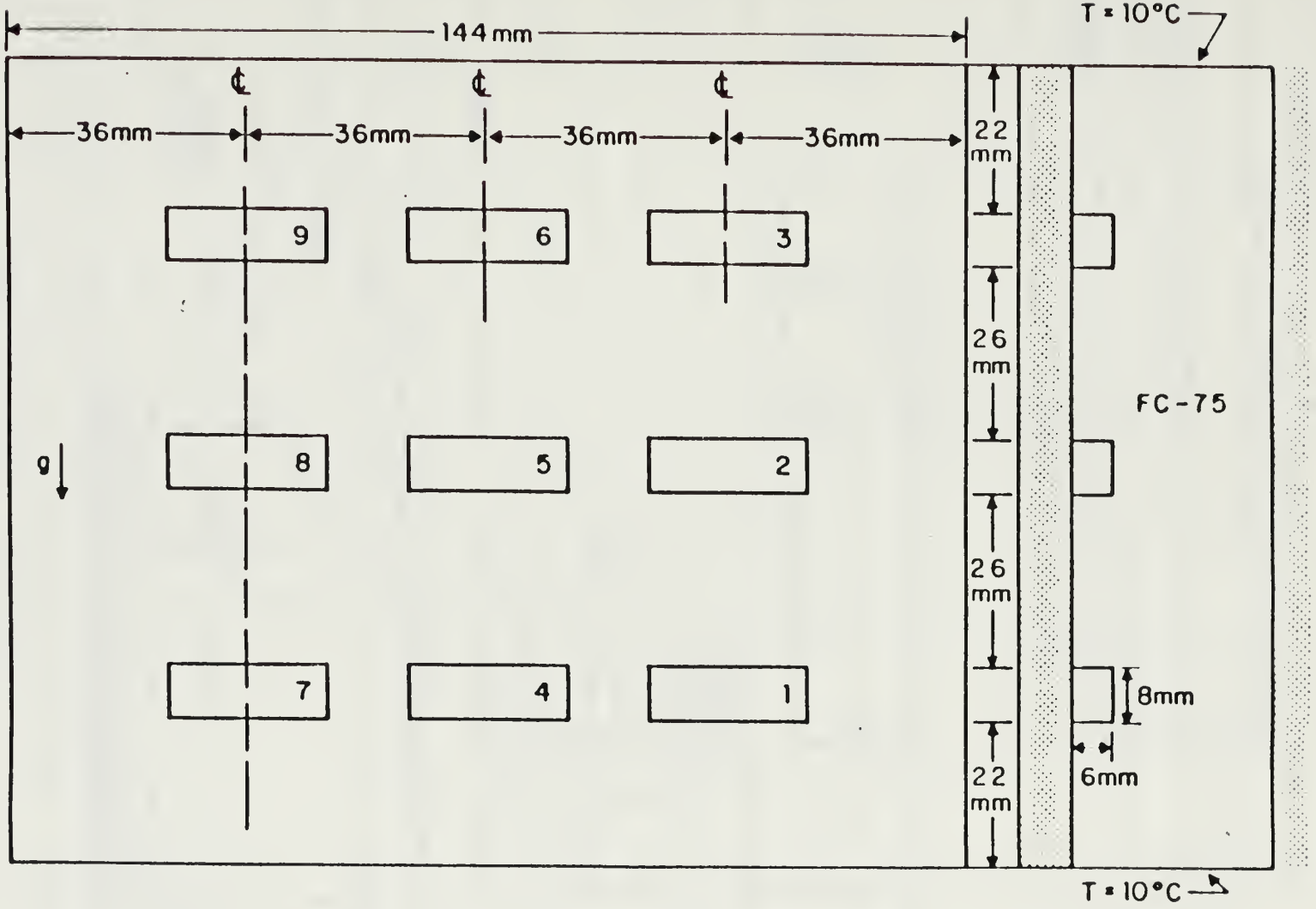

Figure 2.2 Simulated Circuit Card

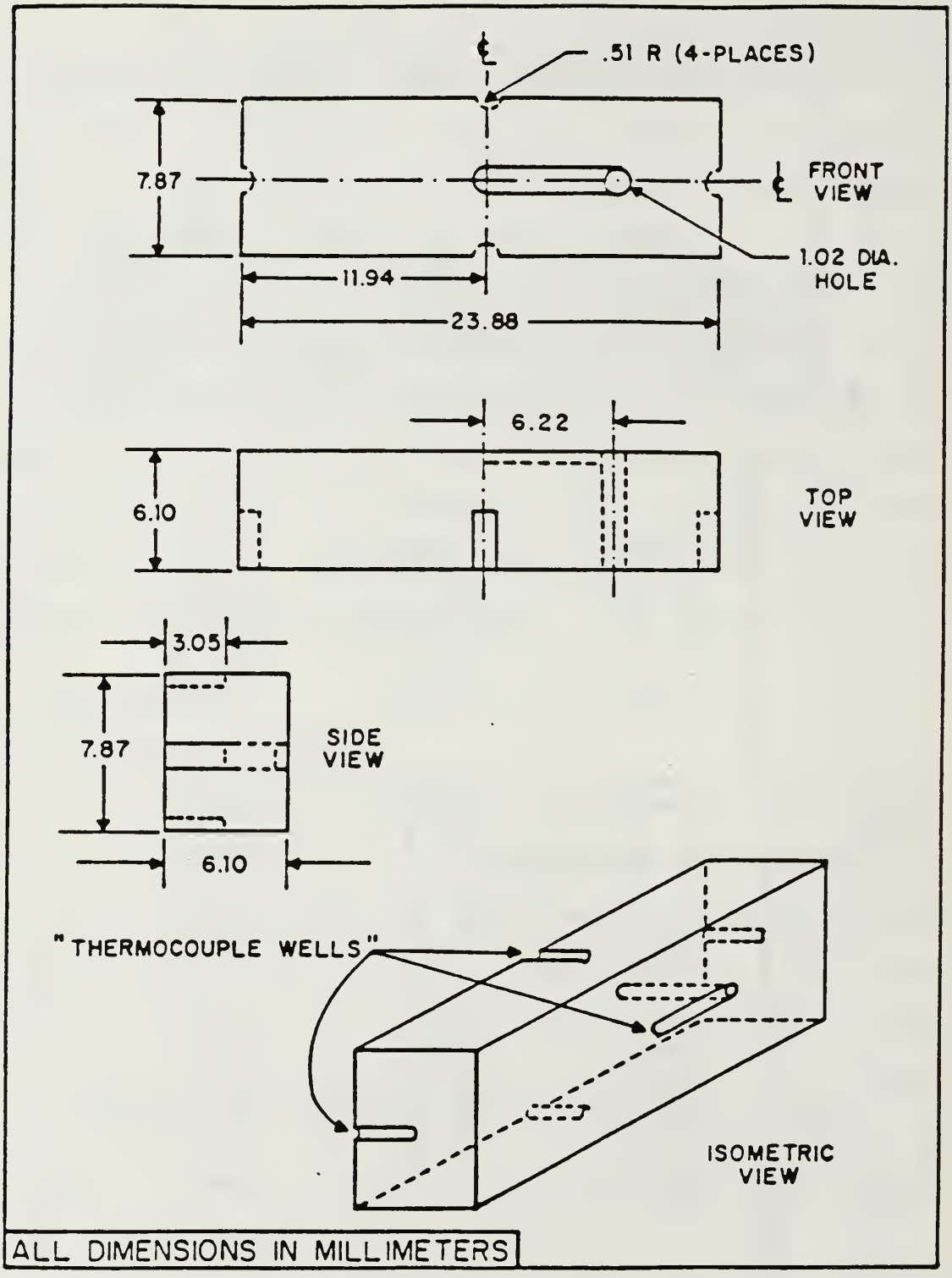

Figure 2.3 Heating Element

material removed from the block. The thermocouples were manufactured by using an arc welder designed for such purposes. The setting for both current time and gas pressure (argon) was kept at 'medium.' Due to the extremely small diameter of the wire the gas pressure was carefully regulated to less than 5 psig. The thermocouples were also checked for continuity due to the fact that the arc welder tended to embrittle the copper wire at the bead.

3. Heaters

A nearly constant heat flux condition was maintained at the base of the block by use of thin (0.18mm) foil type heaters (Figure 2.4). Each of the heaters was measured to have a resistance between 10.5 and 10.6 ohms. These heaters were designed to align with the blocks. Holes were provided within the heaters to pass the various thermocouple wires.

The power leads of the heaters were gold plated to ensure a low electrical contact resistance. Wires from the power supply were attached to the leads by means of soldering. After ensuring proper alignment, the heaters were bonded to the blocks by means of a high thermal conductivity epoxy.

4. Simulated Circuit Card

Three grooves of 0.5mm depth were made on the front of the card in order to allow the heaters to be mounted below the surface and thus prevent the dielectric fluid from seeping under the blocks and introducing a variable, unknown

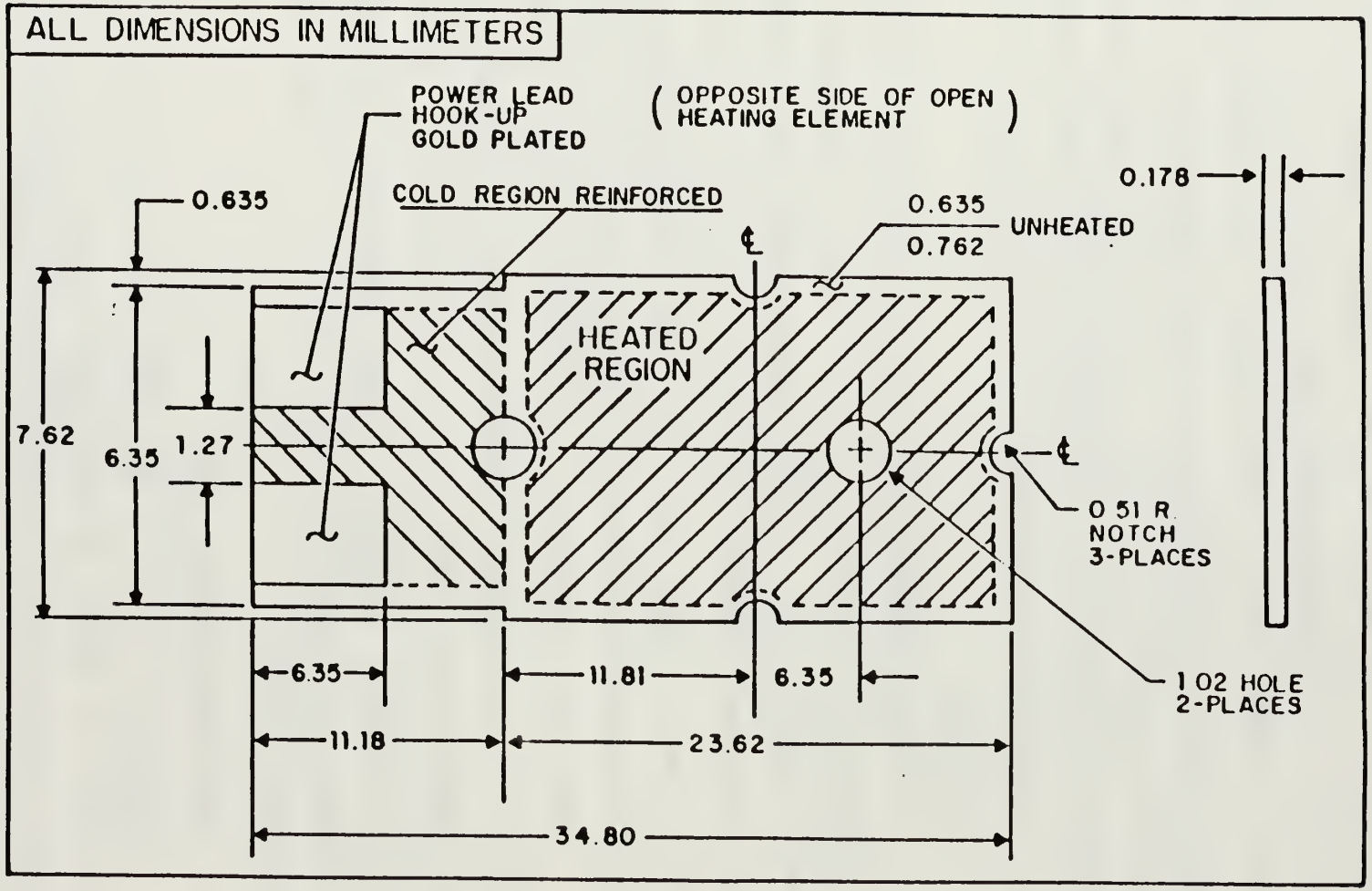

Figure 2.4 Foil Type Heaters

resistance. The heating elements were bonded to the circuit card with a low thermal conductivity epoxy.

5. Test Chamber

The test chamber was constructed of plexiglass (13mm thick) and had inside dimensions of 120mm in height, 144mm in length, and 30mm in width. The wires were fed through the grooves in the back of the circuit card to a "Tygon" tube on the back wall. The chamber also contained two small pressure equalization outlets, located at the top and the bottom of the front vertical surface.

6. Heat Exchangers

The two aluminum heat exchangers measure 38mm by 65mm by 274mm. The details of the heat exchangers are available in [Knock, 1983]. Aluminum plates 3mm thick were used as top and bottom surfaces. These plates were grooved 2.5mm to provide slots for the thermocouples. This left a 0.5mm wall thickness of aluminum between the thermocouple bead and the surface in contact with the dielectric fluid. The resulting conductive thermal resistance was found to be negligible. The heat exchangers were each attached to individual coolant baths by means of "Tygon" tubing. Four 10 mil (0.254mm) thermocouples, two on the top and two on the bottom, were used to read the heat exchanger temperatures.

7. Flow Visualization

Visualization was accomplished with magnesium powder, 325 mesh. Magnesium has a density of 1.92 g/cm^3 compared to 1.76 g/cm^3 for FC-75, resulting in a large suspension time of the particles. The beams from the light sources were spread into plane sheets which illuminated the particles suspended in the FC-75. This technique allowed for the visualization of a single plane of the flow field. Other planes were examined by the realignment of the apparatus. A four milli-watt helium neon laser and a cylindrical lens were used for the time lapse camera photos (Figure 2.5).

8. Assembly

After sliding the card into the slot in the chamber, both the thermocouple and power wires were run out through the 1.27cm diameter extension pipe on the back of the chamber to the connected "Tygon" tubing of approximately 1.0 meter in length.

Rubber o-rings were placed in grooves located on the top and bottom surfaces of the chamber and the thin aluminum plates were set in place. The heat exchangers were then set on the plates and clamped by means of specially made aluminum clamps to ensure a proper seal. The inlet and outlet tygon tubes were attached to the constant temperature baths for each heat exchanger. Finally, the pressure

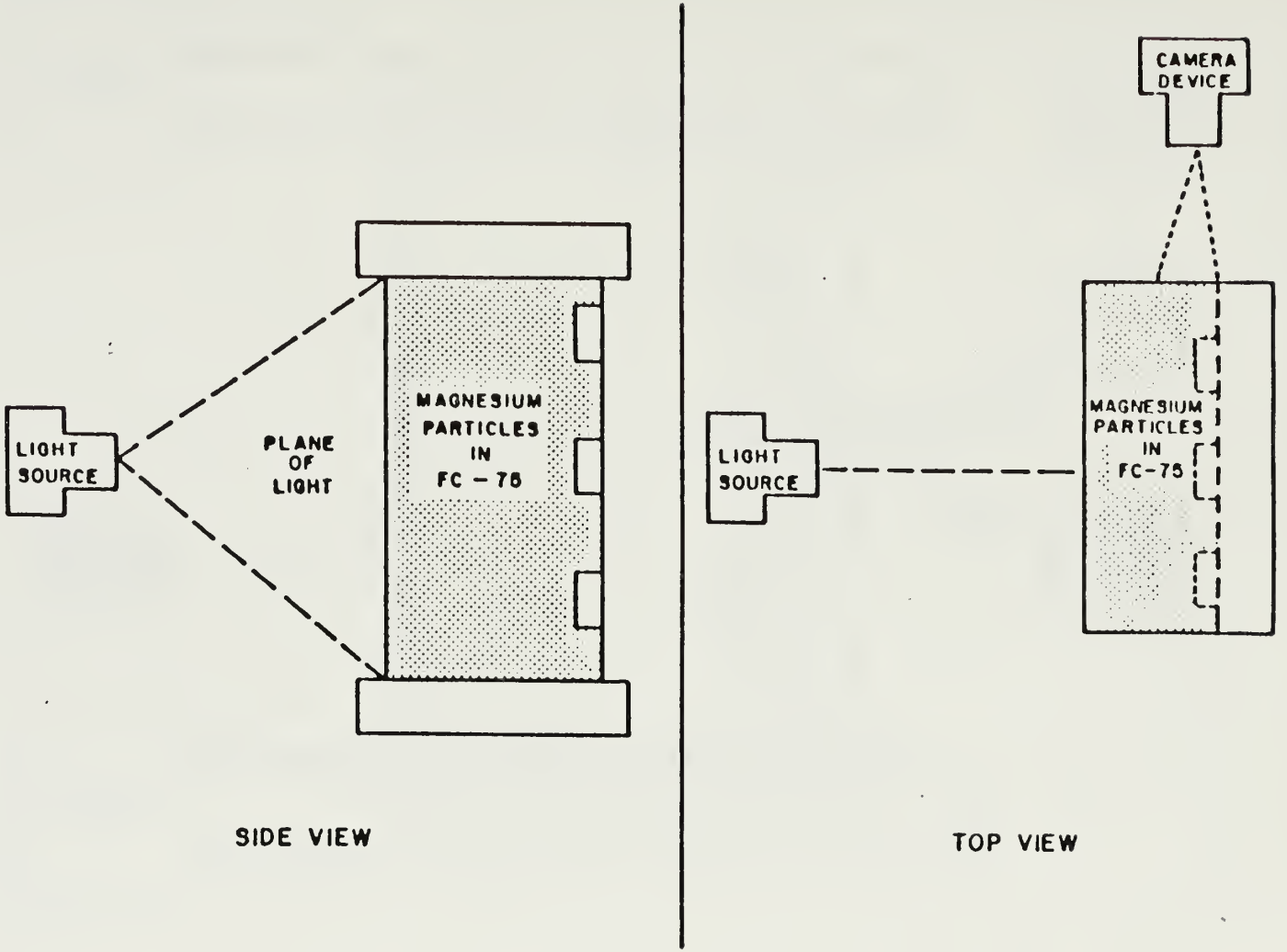

Figure 2.5 Flow Visualization Set-Up

equalization tubes were attached to the chamber. A schematic of the entire assembly is shown in Figure 2.6.

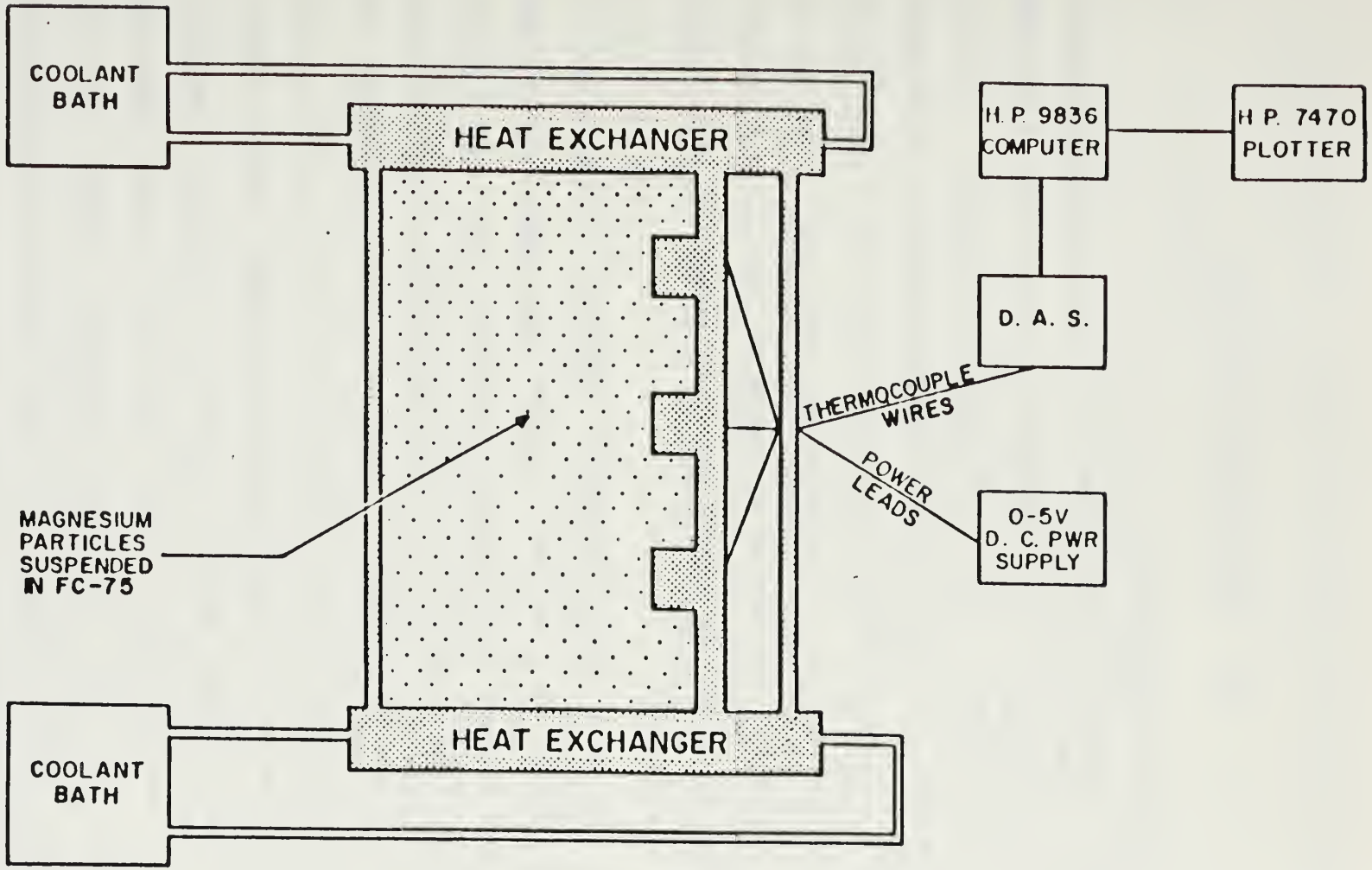

Figure 2.6 Schematic of Entire Assembly

III. EXPERIMENTAL PROCEDURE

A. APPARATUS PREPARATION

After assembling the apparatus, the chamber was filled with the dielectric fluid through the top vent tube by means of a small funnel and a hypodermic syringe. To damp disturbances, the entire apparatus was placed on a separate platform. This platform also served as a means of leveling the chamber by use of adjustable screw legs. Since the entire apparatus was sealed by means of four clamps it could be tilted in order to remove the last remaining air bubbles inside the chamber.

The use of a single constant temperature bath providing cooling water in series to the top and bottom heat exchangers proved inefficient to maintain both the top and the bottom heat exchangers at the same constant temperature. A second bath was added so that each heat exchanger was supplied individually and could be adjusted separately. The ten terminals on the power supply panel were used to supply power to the heaters on the simulated components. The first terminal was the main input, the next nine were the terminals to the individual heaters located on each component. These heaters were connected in series with the 2 ohm precision resistors. This arrangement was repeated

for each component. These nine units were then connected in parallel to the main input.

B. DATA ACQUISITION

Prior to energizing the power supply or the constant temperature baths all the thermocouples were scanned to measure the starting steady state temperatures. The constant temperature baths were set at 10°C by means of adjustment dials located on the baths. Throughout each experiment the bath supplying the top heat exchanger required constant monitoring. As the power levels increased, the bath temperature was reduced accordingly to maintain the top heat exchanger thermocouple readings at a constant 10°C.

The desired voltage was obtained by setting the power supply to the desired level. The reading on the power supply was verified by means of reading channel number 61, the main power input channel, on the data acquisition panel.

Approximately four hours were allotted for the system to achieve steady state. For this experiment, the steady state condition was defined as a majority of the thermocouple readings changing less than 0.2°C during three separate readings taken at ten minute intervals. The bath temperatures were checked to ensure they were at 10°C. If they were in agreement then the data was recorded by means of the program "ACQUIRE" (Appendix C). This program scanned all 76 channels and converted the emf signals from the

thermocouples to temperatures in degrees Celsius. The power to the heater was determined by utilizing the precision 2 ohm resistor. This resistor was connected in series with the heater and allowed the measurement of the current through this configuration. This current was then multiplied by the measured voltage of the heater to produce the power input to the component.

A second program "Fastscan" (Appendix C) was developed to scan three individual channels. Each of the three channels, numbers 1, 13, 32, was scanned individually at a rate of 3 scans per second for a period of 200 seconds. The main intention in doing so was to isolate any periodic behavior caused by the flow past these three thermocouples. A third program "Plot" (Appendix C) was developed to plot these results on a HP model 7470A plotter.

Flow visualization was conducted by means of 325 mesh Magnesium particles and a four milliwatt laser focused with a cylindrical lens. The magnesium particles were injected into the chamber by way of the bottom vent tube. A motor driven Nikon F3 camera with a Micro-Nikkor 55mm lens and a Nikon MT-2 Intervalometer was used for the long-time photography. The time exposure photographs of length 8 or 20 seconds were taken at the various power levels where heat transfer data had been obtained. The photographs were taken of the three columns of components by placing the camera at a ninety degree angle to the plane created by the laser.

This configuration was then reversed to obtain photographs of three separate planes in the chamber.

C. DATA ANALYSIS

1. Determination of the Nusselt Number

The Nusselt Number is defined as the following:

$$Nu = \frac{hL}{k_f} \tag{3.1}$$

where L is a characteristic length, taken here as the length of the component in the vertical direction, k_f is the thermal conductivity of the fluid, and h is the convective heat transfer coefficient. All fluid properties were taken to be a function of the average film temperature.

To evaluate the heat loss, one thermocouple was placed directly behind each of the heated blocks. A series of nine thermocouples were also attached to the back of the card. These temperatures were used to calculate the conduction loss through the back of the card.

One dimensional conduction resistance, R_{con}, for the simulated board was determined from:

$$R_{con} = \frac{L}{kA} \tag{3.2}$$

where L is the length along the conduction path i.e., the thickness of the board, k is the thermal conductivity of the material (Appendix A) and A is the area normal to the

conduction path. The area normal to the path of conduction was calculated as the area directly behind the components back, 192mm^2. By doing so spreading losses were neglected. The conduction loss is then:

$$Q_{con} = \frac{T_s - T_b}{R_{con}} \tag{3.3}$$

Power input to each component is calculated from:

$$Q_{in} = \frac{(V_{in} - V_h)V_h}{R} \tag{3.4}$$

where V_{in} is the input voltage applied to both the 2 ohm resistor and the heater which is in series with it. V_h is the voltage drop across the heater. The difference between V_{in} and V_h gives the voltage drop across the 2 ohm resistor.

The net energy added to the fluid in the chamber is the difference between Q_{in} and Q_{con} which by Newton's Law of cooling is:

$$Q_{conv} = Q_{net} = hA(T_{avg} - T_c)$$

$$= Q_{in} - Q_{con} \tag{3.5}$$

where,

A = The total wetted surface area of the components,

T_{avg} = Area weighted average surface temperature,

calculated by,

$$T_{avg} = \frac{\Sigma A_i T_i}{\Sigma A_i} \qquad (3.6)$$

where,

T_i = Temperature of the i^{th} surface of the components,

A_i = Area of the i^{th} surface of the components. The summation of the index i varies from 1 to 5,

and,

T_c = Average heat exchanger temperature.

Thus,

$$h = \frac{Q_{conv}}{A_{tot}(T_{avg} - T_c)} \qquad (3.6)$$

The above procedure was repeated for each of the nine components at each power level. The Nusselt Number was then calculated from Equation 3.1.

2. Determination of the Rayleigh Numbers

The definition of the temperature based Rayleigh number is:

$$Ra_t = Gr_t * Pr \qquad (3.7)$$

where the Grashof Number (Gr_t) is defined as,

$$Gr_t = \frac{g\beta L^3 (T_{avg} - T_c)}{\nu^2} \tag{3.8}$$

and the Prandtl Number (Pr) is defined as,

$$Pr = \frac{\nu}{\alpha} \tag{3.9}$$

where,

$$\alpha = \frac{k_f}{(\rho c_p)}$$

All the properties in the above equations are calculated at the average film temperature:

$$T_f = \frac{T_{avg} + T_c}{2} \tag{3.10}$$

Therefore:

$$Ra_t = \frac{g\beta L^3 (T_{avg} - T_c)}{\nu\alpha} \tag{3.11}$$

3. Determination of the Flux Based Rayleigh Number

The definition of the flux based Rayleigh number is:

$$Ra_f = Gr_f * Pr \tag{3.12}$$

all film properties are calculated at the average film temperature as before and:

$$Gr_f = \frac{g\beta L^4 Q_{net}}{k_f \nu^2 A_{tot}} \quad . \quad (3.13)$$

Functional relationships for the properties at the film temperature are given in Appendix A, together with sample calculations. Uncertainty calculations are given in Appendix B.

IV. RESULTS

A. FLOW VISUALIZATION

Flow visualization was accomplished using Magnesium particles as a flow marker and a Helium Neon laser to illuminate the particles. The results provided insights into the flow patterns existing at various power dissipation levels. As expected, the particle traces suggest highly three-dimensional flow patterns at all power levels. Particles can be seen entering and leaving the plane of light in almost all the long time exposure photographs. A multitude of flow patterns was observed for the wide range of input power levels in the of 0.1 to 3.1 watts. Representative flow visualizations are presented in Figures 4.1 to 4.14.

1. Flow Patterns at Component Midplanes

The following flow patterns are in a vertical plane through the center of components 4, 5, 6 (Fig. 2.2). The laser was placed in front of the chamber and the camera located to the side (Fig. 2.5). The camera exposure time was set at 10 seconds. The three dark regions located on the left side of the photographs are the three rows of components as seen in side view. The top and bottom of the chamber and the horizontal walls can also be seen in the photos.

Figure 4.1 is the flow pattern for a power input of 0.1 watts and indicates a pattern that contains two individual eddies located between the rows of components along with an overall circular pattern that encompasses the entire chamber. A boundary layer like flow is seen in the vicinity of the heated components. A dark region located at the bottom of the photograph is evident in all photos taken throughout the experiment. This region is the stagnant, dense cold fluid layer in the vicinity of the bottom heat exchanger. This region proved to be impermeable at all power levels.

Figure 4.2 for power input of 0.3 watts indicates the same overall pattern with the exception of a constriction of the overall circular pattern at the approximate height of the second row of components. The slight increase in the upper eddy size is also evident.

Figure 4.3 for a power input of 1.5 watts indicates an increase in the thickness of the boundary layer emanating from the second row of components along with increased entrainment of the particles located below the second row of components. Also evident is the disappearance of the two distinct eddies seen earlier and strong evidence of three dimensionality in the flow as seen by the crossing of the particle paths.

Figure 4.1 Power @ 0.1 W
Side View

Figure 4.2 Power @ 0.3 W
Side View

Figure 4.3 Power @ 1.5 W
Side View

Figure 4.4, for a power input of 2.7 watts, shows a buoyant fluid layer adjacent to the components and random motion throughout the remaining chamber. Also seen are entrainment of particles at the approximate height of the second row of components, and evidence of an area, immediately above the black region at the photo's bottom, where particles are basically suspended.

Figure 4.5, at 3.1 watts, demonstrated a downward flow pattern in the vicinity of the bottom row. This downward flow was forced past the face of the bottom chip in this column. The flow also demonstrated a perpendicular entrainment of particles between the first and second row of components, and a large increase in the boundary layer at the third row of components.

Figures 4.6 and 4.7 show flow patterns in the vertical plane at the mid-span of components 7, 8 and 9. These two photographs were taken approximately 5 seconds apart at a power setting of 3.1 watts. They demonstrate the strongly time-dependent behavior of the flow. In Figure 4.6, entrainment into the upward moving buoyant layer is seen to be present almost as far down as the bottom of the lowest component. Far away from the components the core fluid exhibits no preferential direction of motion. In Figure 4.7 the flow pattern has changed. Near the lowest row of components the flow now appears almost quiescent. Also, the buoyant region appears thinner than in Figure 4.6.

Figure 4.4 Power @ 2.7 W
Side View

Figure 4.5 Power @ 3.1 W
Side View

Figure 4.6 Power @ 3.1 W
Side View,
Chips 7, 8, 9

Figure 4.7 Power @ 3.1 W
Side View,
Chips 7, 8, 9

2. Flow Patterns in Other Planes

Figure 4.8 is a schematic of the three planes that were investigated when the positions of the camera and the laser were reversed. Figures 4.9, 4.10 and 4.11 are at a power setting of 0.1 watts and demonstrate the flow patterns in the back, middle and front planes, respectively. In Figure 4.9, the back plane, the flow appears to be somewhat like a large circular pattern that is bounded by the physical dimensions of the chamber and exhibits no noticeable flow directly up the center of the chamber. Figure 4.10, the middle plane, indicates a strong upward flow in the center of the chamber and two areas of eddy formation located approximately mid-height in the chamber. Finally, Figure 4.11, the front plane, demonstrated approximately the same behavior as the middle plane; a general area of motion in the center of the chamber along with eddy formation areas on either side.

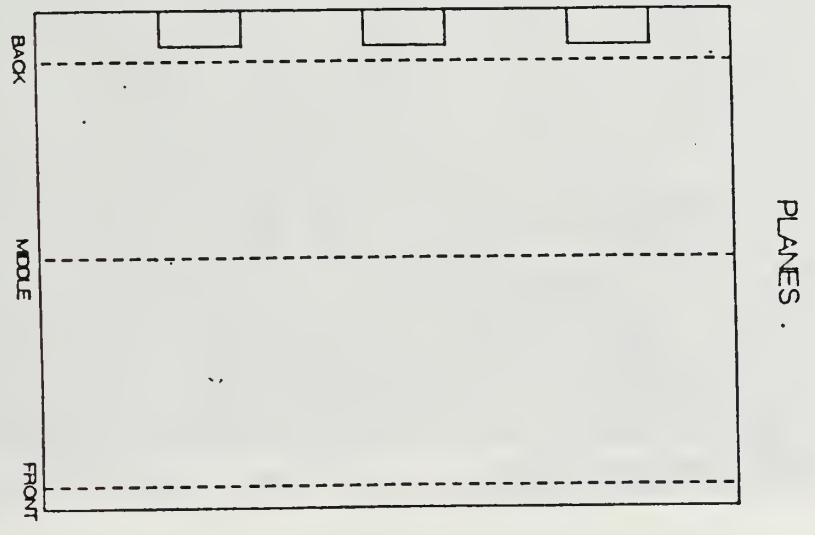

Figure 4.8 Top View of Planes

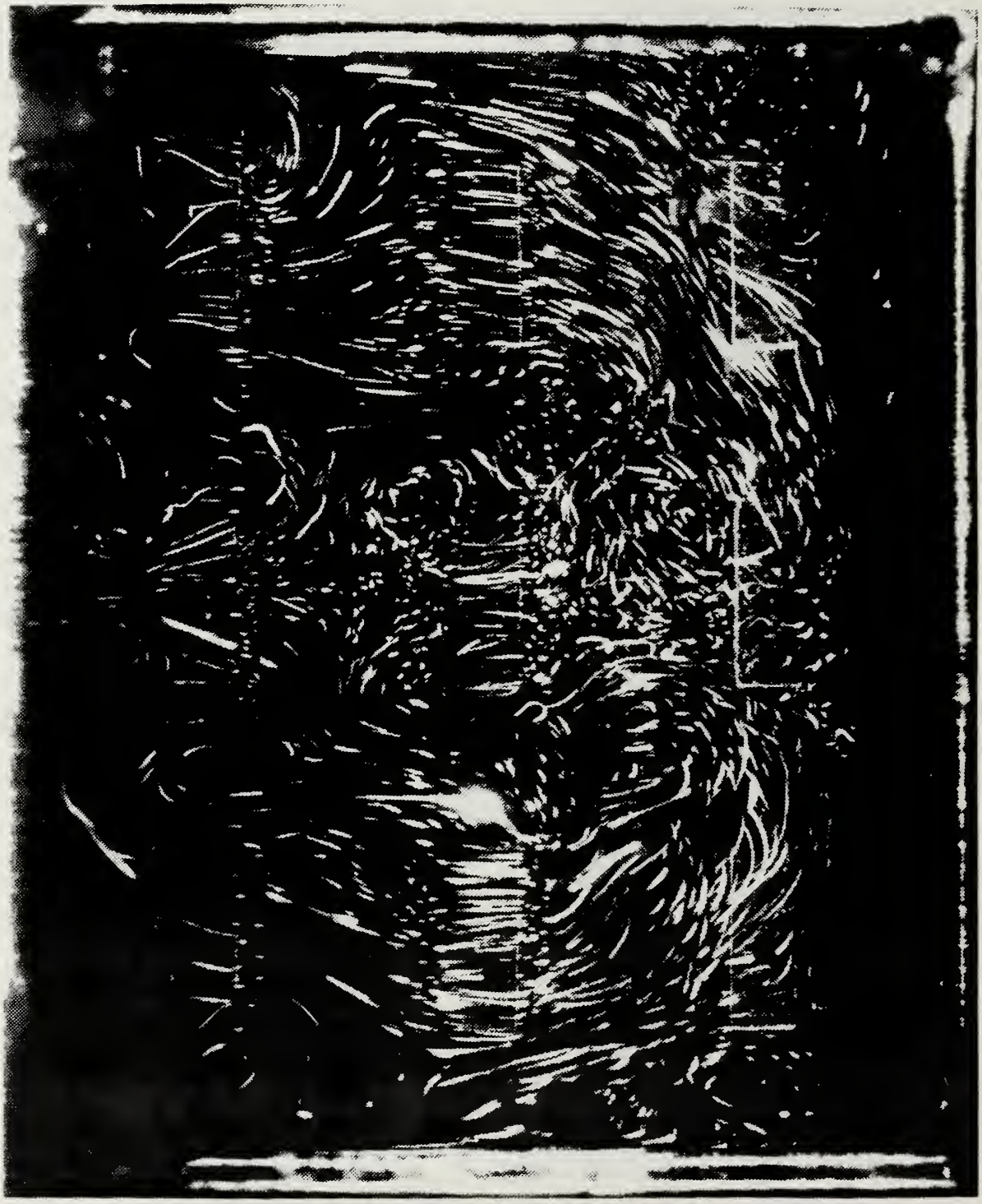

Figure 4.9 Back Plane @ 0.1 Watts

Figure 4.10 Middle Plane @ 0.1 Watts

Figure 4.11 Front Plane @ 0.1 Watts

Figures 4.12, 4.13 and 4.14 are the same three planes at a power setting of 3.1 watts. Figure 4.12, the back plane, indicates regions of upward flow near the components. These patterns characterize the boundary layer nature of transport in the vicinity of the elements. Relatively short particle traces in regions away from the components appear to result due to the strongly three-dimensional transport. The dark area in the very bottom of the photograph is again pointed out to demonstrate the cold isothermal layer developed by the bottom heat exchanger.

Figures 4.13 and 4.14 are views of the center and front planes respectively. The flow in both planes appears strongly time dependent. Figure 4.14 shows relatively longer particle traces than Figure 4.13, indicating stronger three dimensional effects near the components.

These 13 photographs illustrate the complex three-dimensional, time dependent flow patterns found in this study. Obtaining a detailed understanding of these effects is essential in achieving predictive capability for the heat transfer in these configurations.

B. REDUCTION OF HEAT TRANSFER DATA

The temperature and reduced data tables corresponding to the eight power levels are as follows: (see Figure 2.2 for identification of the component numbers).

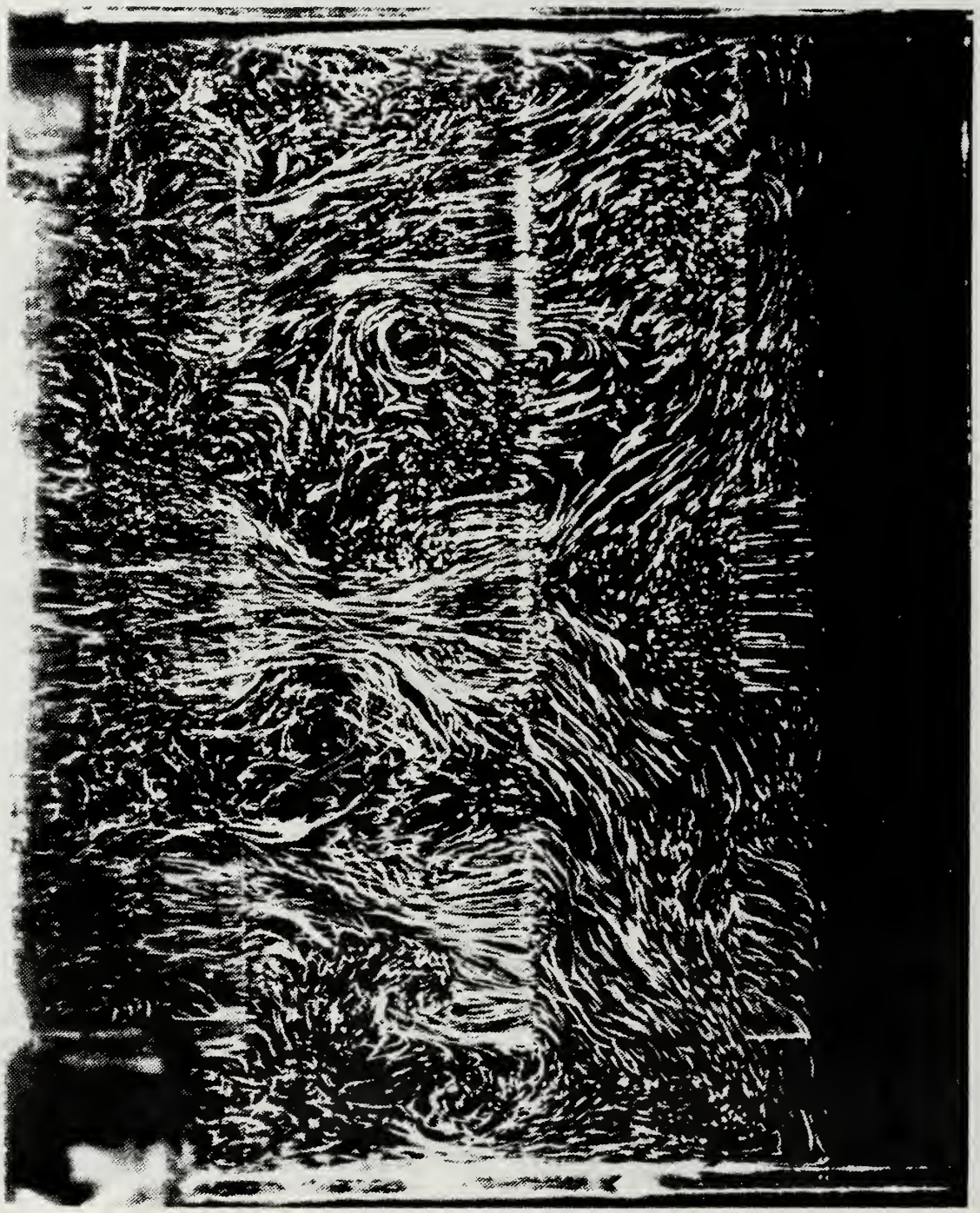

Figure 4.12 Back Plane @ 3.1 Watts

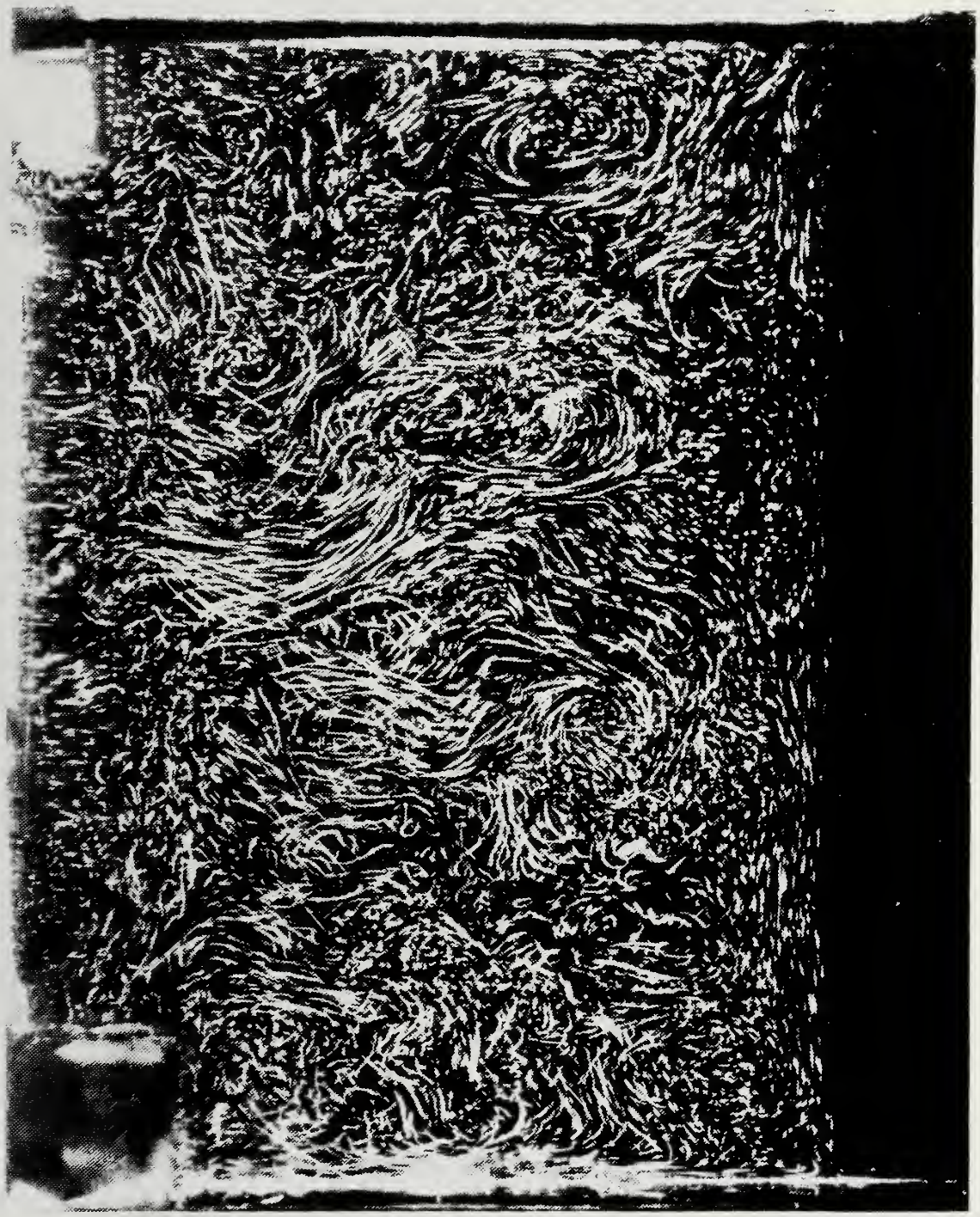

Figure 4.13 Middle Plane @ 3.1 Watts

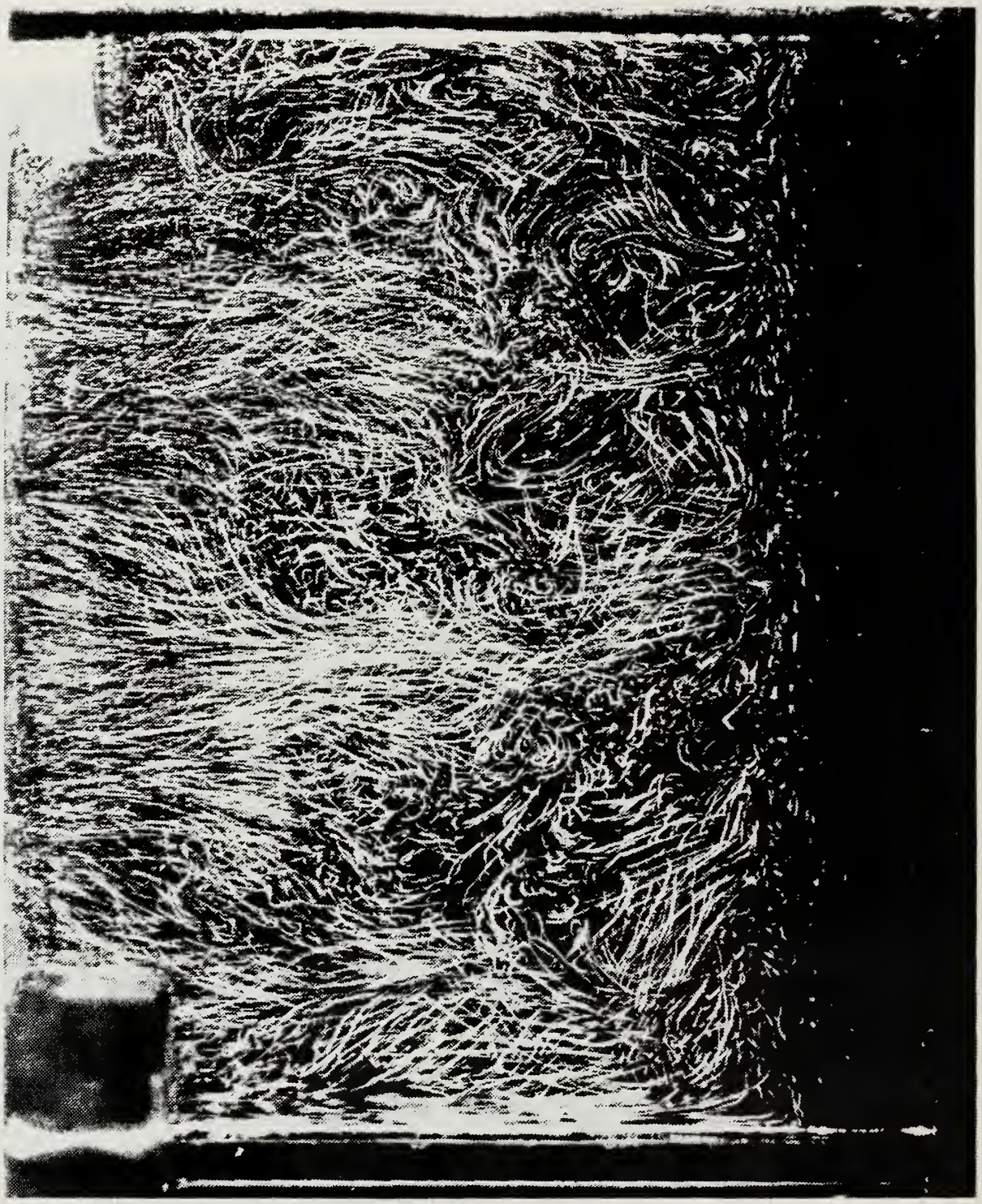

Figure 4.14 Front Plane @ 3.1 Watts

TABLE 1

TEMPERATURE DATA FOR INPUT POWER Q_{in} = 0.3 W

THESE RESULTS ARE STORED IN FILE: D80981130

AMBIENT TEMP WAS: 23 C
VOLTMETER READING WAS: 2.0382 #61
BATH TEMP WAS: 10 C
THIS RUN WAS RECORDED WITH FLOW VIZ

ALL TEMPERATURES ARE IN DEGREES CELCIUS

	CENTER	TOP	RIGHT	LEFT	BOTTOM	BACK
CHIP NO1:	16.54E+00	16.33E+00	16.15E+00	16.16E+00	16.11E+00	16.96E+00
POWER (WATTS):	29.93E-02					
CHIP NO2:	16.68E+00	16.31E+00	16.34E+00	16.19E+00	16.30E+00	17.53E+00
POWER (WATTS):	29.94E-02					
CHIP NO3:	16.74E+00	16.32E+00	16.46E+00	16.33E+00	16.63E+00	17.40E+00
POWER (WATTS):	29.83E-02					
CHIP NO4:	16.52E+00	16.33E+00	16.08E+00	15.82E+00	16.02E+00	16.33E+00
POWER (WATTS):	29.55E-02					
CHIP NO5:	16.52E+00	16.15E+00	16.12E+00	16.05E+00	16.30E+00	17.11E+00
POWER (WATTS):	29.67E-02					
CHIP NO6:	16.51E+00	16.50E+00	16.33E+00	16.33E+00	16.58E+00	18.13E+00
POWER (WATTS):	29.64E-02					
CHIP NO7:	16.64E+00	16.42E+00	16.12E+00	16.12E+00	16.32E+00	17.31E+00
POWER (WATTS):	30.01E-02					
CHIP NO8:	16.71E+00	16.42E+00	16.40E+00	16.40E+00	16.28E+00	18.02E+00
POWER (WATTS):	30.12E-02					
CHIP NO9:	16.65E+00	16.38E+00	16.23E+00	16.36E+00	16.41E+00	17.69E+00
POWER (WATTS):	29.87E-02					

HEAT EXCHANGERS TEMPERATURES:	RIGHT	LEFT
BOTTOM:	99.12E-01	99.39E-01
TOP:	10.38E+00	98.03E-01

BACK PLANE TEMPERATURES ARE :

T(55):	14.67E+00
T(56):	15.41E+00
T(57):	15.27E+00
T(72):	15.57E+00
T(73):	15.55E+00
T(74):	16.06E+00
T(75):	15.56E+00
T(76):	15.56E+00
T(77):	15.45E+00

TABLE 2

TEMPERATURE DATA FOR INPUT POWER Q_{in} = 0.7 W

THESE RESULTS ARE STORED IN FILE: D80982100

AMBIENT TEMP WAS: 23 C
VOLTMETER READING WAS: 3.2198 #61
BATH TEMP WAS: 10 C
THIS RUN WAS RECORDED WITH FLOW VIZ

ALL TEMPERATURES ARE IN DEGREES CELCIUS

	CENTER	TOP	RIGHT	LEFT	BOTTOM	BACK
CHIP NO1:	23.35E+00	22.53E+00	22.35E+00	22.39E+00	22.24E+00	24.06E+00
POWER (WATTS):	71.08E-02					
CHIP NO2:	23.36E+00	22.37E+00	22.43E+00	22.09E+00	22.39E+00	25.05E+00
POWER (WATTS):	71.11E-02					
CHIP NO3:	23.16E+00	22.36E+00	22.55E+00	22.14E+00	22.73E+00	24.58E+00
POWER (WATTS):	70.87E-02					
CHIP NO4:	23.23E+00	22.42E+00	22.31E+00	21.69E+00	22.16E+00	24.16E+00
POWER (WATTS):	70.18E-02					
CHIP NO5:	23.11E+00	21.96E+00	21.94E+00	21.85E+00	22.37E+00	24.19E+00
POWER (WATTS):	70.47E-02					
CHIP NO6:	22.69E+00	22.77E+00	22.18E+00	22.21E+00	22.60E+00	26.12E+00
POWER (WATTS):	70.38E-02					
CHIP NO7:	23.49E+00	22.76E+00	22.17E+00	22.15E+00	22.39E+00	24.55E+00
POWER (WATTS):	71.26E-02					
CHIP NO8:	23.32E+00	22.63E+00	22.47E+00	22.55E+00	22.47E+00	26.17E+00
POWER (WATTS):	71.55E-02					
CHIP NO9:	23.07E+00	22.54E+00	22.05E+00	22.38E+00	22.20E+00	25.41E+00
POWER (WATTS):	70.95E-02					

HEAT EXCHANGERS TEMPERATURES:	RIGHT	LEFT
BOTTOM:	98.18E-01	98.46E-01
TOP:	98.21E-01	93.58E-01

BACK PLANE TEMPERATURES ARE :

T(55):	17.67E+00
T(56):	18.76E+00
T(57):	19.05E+00
T(72):	19.08E+00
T(73):	18.90E+00
T(74):	19.11E+00
T(75):	19.02E+00
T(76):	18.79E+00
T(77):	18.71E+00

TABLE 3

TEMPERATURE DATA FOR INPUT POWER Q_{in} = 1.1 W

THESE RESULTS ARE STORED IN FILE: D80990745

AMBIENT TEMP WAS: 23 C
VOLTMETER READING WAS: 4.1107 #61
BATH TEMP WAS: 10 C
THIS RUN WAS RECORDED WITH FLOW VIZ

ALL TEMPERATURES ARE IN DEGREES CELCIUS

	CENTER	TOP	RIGHT	LEFT	BOTTOM	BACK
CHIP NO1:	28.62E+00	27.35E+00	27.13E+00	27.16E+00	26.93E+00	29.81E+00
POWER (WATTS):	11.57E-01					
CHIP NO2:	28.73E+00	27.05E+00	27.13E+00	26.72E+00	27.11E+00	31.43E+00
POWER (WATTS):	11.58E-01					
CHIP NO3:	28.47E+00	27.17E+00	27.49E+00	26.82E+00	27.69E+00	30.65E+00
POWER (WATTS):	11.54E-01					
CHIP NO4:	28.47E+00	27.04E+00	27.14E+00	26.18E+00	26.95E+00	30.13E+00
POWER (WATTS):	11.43E-01					
CHIP NO5:	28.21E+00	26.29E+00	26.42E+00	26.30E+00	27.03E+00	30.00E+00
POWER (WATTS):	11.48E-01					
CHIP NO6:	27.45E+00	27.90E+00	26.98E+00	27.00E+00	27.76E+00	33.28E+00
POWER (WATTS):	11.46E-01					
CHIP NO7:	29.12E+00	27.77E+00	27.03E+00	26.97E+00	27.25E+00	30.66E+00
POWER (WATTS):	11.60E-01					
CHIP NO8:	28.56E+00	27.45E+00	27.27E+00	27.40E+00	27.18E+00	33.20E+00
POWER (WATTS):	11.65E-01					
CHIP NO9:	28.13E+00	27.32E+00	26.60E+00	27.12E+00	26.72E+00	32.07E+00
POWER (WATTS):	11.55E-01					

HEAT EXCHANGERS TEMPERATURES:	RIGHT	LEFT
BOTTOM:	99.44E-01	99.77E-01
TOP:	10.05E+00	96.50E-01

BACK PLANE TEMPERATURES ARE :

T(55):	19.74E+00
T(56):	21.13E+00
T(57):	21.79E+00
T(72):	21.42E+00
T(73):	21.14E+00
T(74):	21.41E+00
T(75):	21.53E+00
T(76):	20.93E+00
T(77):	20.82E+00

TABLE 4

TEMPERATURE DATA FOR INPUT POWER Q_{in} = 1.5 W

THESE RESULTS ARE STORED IN FILE: D80992015

AMBIENT TEMP WAS: 23 C
VOLTMETER READING WAS: 4.6442 e-01
BATH TEMP WAS: 10 C
THIS RUN WAS RECORDED WITH FLOW VIZ

ALL TEMPERATURES ARE IN DEGREES CELCIUS

	CENTER	TOP	RIGHT	LEFT	BOTTOM	BACK
CHIP NO1:	32.81E+00	31.19E+00	31.03E+00	31.08E+00	30.78E+00	34.47E+00
POWER (WATTS):	14.77E-01					
CHIP NO2:	32.92E+00	30.93E+00	31.02E+00	30.42E+00	31.07E+00	36.44E+00
POWER (WATTS):	14.77E-01					
CHIP NO3:	32.36E+00	30.95E+00	31.32E+00	30.50E+00	31.66E+00	35.33E+00
POWER (WATTS):	14.72E-01					
CHIP NO4:	32.60E+00	30.86E+00	31.04E+00	29.86E+00	30.79E+00	34.86E+00
POWER (WATTS):	14.58E-01					
CHIP NO5:	32.28E+00	29.79E+00	30.12E+00	29.99E+00	30.81E+00	34.66E+00
POWER (WATTS):	14.64E-01					
CHIP NO6:	30.86E+00	31.77E+00	30.66E+00	30.72E+00	31.43E+00	39.92E+00
POWER (WATTS):	14.62E-01					
CHIP NO7:	33.43E+00	31.83E+00	30.89E+00	30.81E+00	31.12E+00	35.45E+00
POWER (WATTS):	14.80E-01					
CHIP NO8:	32.82E+00	31.45E+00	31.27E+00	31.40E+00	31.22E+00	38.77E+00
POWER (WATTS):	14.87E-01					
CHIP NO9:	32.21E+00	31.07E+00	30.36E+00	30.97E+00	30.30E+00	37.25E+00
POWER (WATTS):	14.74E-01					

HEAT EXCHANGERS TEMPERATURES:	RIGHT	LEFT
BOTTOM:	99.49E-01	99.69E-01
TOP:	99.69E-01	95.79E-01

BACK PLANE TEMPERATURES ARE :

T(55):	21.87E+00
T(56):	23.45E+00
T(57):	24.33E+00
T(72):	23.84E+00
T(73):	23.52E+00
T(74):	23.83E+00
T(75):	24.10E+00
T(76):	23.25E+00
T(77):	23.10E+00

TABLE 5

TEMPERATURE DATA FOR INPUT POWER Q_{in} = 1.9 W

THESE RESULTS ARE STORED IN FILE: D81001130

AMBIENT TEMP WAS: 23 C
VOLTMETER READING WAS: 5.2844 #61
BATH TEMP WAS: 10 C
THIS RUN WAS RECORDED WITH FLOW VIZ

ALL TEMPERATURES ARE IN DEGREES CELCIUS

	CENTER	TOP	RIGHT	LEFT	BOTTOM	BACK
CHIP NO1:	37.45E+00	35.42E+00	35.24E+00	35.29E+00	34.90E+00	39.63E+00
POWER (WATTS):	19.10E-01					
CHIP NO2:	37.46E+00	34.63E+00	35.00E+00	34.29E+00	34.99E+00	42.43E+00
POWER (WATTS):	19.11E-01					
CHIP NO3:	36.60E+00	34.89E+00	35.33E+00	34.33E+00	35.51E+00	40.46E+00
POWER (WATTS):	19.05E-01					
CHIP NO4:	37.22E+00	34.88E+00	35.28E+00	33.81E+00	35.01E+00	40.20E+00
POWER (WATTS):	18.86E-01					
CHIP NO5:	36.70E+00	33.55E+00	34.01E+00	33.86E+00	34.97E+00	39.83E+00
POWER (WATTS):	18.94E-01					
CHIP NO6:	35.05E+00	36.55E+00	34.59E+00	34.95E+00	35.73E+00	48.38E+00
POWER (WATTS):	18.90E-01					
CHIP NO7:	38.33E+00	36.17E+00	35.13E+00	34.99E+00	35.34E+00	40.79E+00
POWER (WATTS):	19.15E-01					
CHIP NO8:	37.38E+00	35.81E+00	35.42E+00	35.57E+00	35.43E+00	45.03E+00
POWER (WATTS):	19.23E-01					
CHIP NO9:	36.47E+00	35.22E+00	34.36E+00	35.10E+00	34.40E+00	43.13E+00
POWER (WATTS):	19.07E-01					

HEAT EXCHANGERS TEMPERATURES:	RIGHT	LEFT
BOTTOM:	99.84E-01	10.02E+00
TOP:	95.29E-01	92.47E-01

BACK PLANE TEMPERATURES ARE :

T(55):	23.54E+00
T(56):	25.35E+00
T(57):	26.58E+00
T(72):	25.81E+00
T(73):	25.38E+00
T(74):	25.72E+00
T(75):	26.29E+00
T(76):	25.04E+00
T(77):	24.85E+00

TABLE 6

TEMPERATURE DATA FOR INPUT POWER Q_{in} = 2.3 W

THESE RESULTS ARE STORED IN FILE: D81001740

AMBIENT TEMP WAS: 23 C
VOLTMETER READING WAS: 5.8093 #61
BATH TEMP WAS: 10 C
THIS RUN WAS RECORDED WITH FLOW VIZ

ALL TEMPERATURES ARE IN DEGREES CELCIUS

	CENTER	TOP	RIGHT	LEFT	BOTTOM	BACK
CHIP NO1:	42.48E+00	39.94E+00	39.75E+00	39.90E+00	39.39E+00	45.05E+00
POWER (WATTS):	23.07E-01					
CHIP NO2:	42.44E+00	39.26E+00	39.57E+00	38.83E+00	39.51E+00	48.58E+00
POWER (WATTS):	23.08E-01					
CHIP NO3:	41.90E+00	39.50E+00	40.09E+00	38.99E+00	40.59E+00	46.17E+00
POWER (WATTS):	23.00E-01					
CHIP NO4:	42.09E+00	39.24E+00	39.82E+00	38.09E+00	39.48E+00	45.71E+00
POWER (WATTS):	22.78E-01					
CHIP NO5:	41.49E+00	37.80E+00	38.35E+00	38.17E+00	39.60E+00	45.28E+00
POWER (WATTS):	22.88E-01					
CHIP NO6:	39.67E+00	41.33E+00	38.98E+00	39.52E+00	40.48E+00	56.04E+00
POWER (WATTS):	22.82E-01					
CHIP NO7:	43.53E+00	40.80E+00	39.71E+00	39.58E+00	39.89E+00	46.53E+00
POWER (WATTS):	23.12E-01					
CHIP NO8:	42.48E+00	40.36E+00	40.09E+00	40.20E+00	39.57E+00	51.52E+00
POWER (WATTS):	23.22E-01					
CHIP NO9:	41.70E+00	39.86E+00	38.85E+00	39.61E+00	38.95E+00	49.58E+00
POWER (WATTS):	23.03E-01					

HEAT EXCHANGERS TEMPERATURES:	RIGHT	LEFT
BOTTOM:	10.00E+00	10.04E+00
TOP:	10.14E+00	10.06E+00

BACK PLANE TEMPERATURES ARE :

T(55):	25.69E+00
T(56):	27.76E+00
T(57):	29.42E+00
T(72):	28.37E+00
T(73):	27.87E+00
T(74):	28.23E+00
T(75):	29.04E+00
T(76):	27.41E+00
T(77):	27.19E+00

TABLE 7

TEMPERATURE DATA FOR INPUT POWER Q_{in} = 2.7 W

THESE RESULTS ARE STORED IN FILE: D81011130

AMBIENT TEMP WAS: 23 C
VOLTMETER READING WAS: 5.344 *61
BATH TEMP WAS: 10 C
THIS RUN WAS RECORDED WITH FLOW VIZ

ALL TEMPERATURES ARE IN DEGREES CELCIUS

	CENTER	TOP	RIGHT	LEFT	BOTTOM	BACK
CHIP NO1:	46.68E+00	43.58E+00	43.37E+00	43.69E+00	43.06E+00	49.81E+00
POWER (WATTS):	27.60E-01					
CHIP NO2:	46.25E+00	43.02E+00	43.14E+00	42.04E+00	42.86E+00	53.82E+00
POWER (WATTS):	27.61E-01					
CHIP NO3:	45.70E+00	43.18E+00	43.85E+00	42.33E+00	44.32E+00	50.88E+00
POWER (WATTS):	27.52E-01					
CHIP NO4:	46.22E+00	42.88E+00	43.55E+00	41.56E+00	43.20E+00	50.62E+00
POWER (WATTS):	27.26E-01					
CHIP NO5:	45.45E+00	40.81E+00	41.67E+00	41.55E+00	43.18E+00	49.94E+00
POWER (WATTS):	27.37E-01					
CHIP NO6:	43.55E+00	45.08E+00	41.98E+00	43.23E+00	44.00E+00	63.01E+00
POWER (WATTS):	27.29E-01					
CHIP NO7:	47.86E+00	44.69E+00	43.43E+00	43.20E+00	43.56E+00	51.81E+00
POWER (WATTS):	27.66E-01					
CHIP NO8:	46.05E+00	43.92E+00	43.56E+00	43.77E+00	43.34E+00	57.24E+00
POWER (WATTS):	27.78E-01					
CHIP NO9:	44.78E+00	43.22E+00	41.99E+00	42.90E+00	41.90E+00	55.35E+00
POWER (WATTS):	27.55E-01					

HEAT EXCHANGERS TEMPERATURES:	RIGHT	LEFT
BOTTOM:	99.27E-01	99.49E-01
TOP:	10.00E+00	98.46E-01

BACK PLANE TEMPERATURES ARE :

T(55):	26.87E+00
T(56):	29.09E+00
T(57):	31.13E+00
T(72):	29.93E+00
T(73):	29.30E+00
T(74):	29.77E+00
T(75):	30.78E+00
T(76):	28.82E+00
T(77):	28.57E+00

TABLE 8

TEMPERATURE DATA FOR INPUT POWER Q_{in} = 3.1 W

THESE RESULTS ARE STORED IN FILE: D81011515

AMBIENT TEMP WAS: 23 C
VOLTMETER READING WAS: 6.8019 #61
BATH TEMP WAS: 10 C
THIS RUN WAS RECORDED WITH FLOW VIZ

ALL TEMPERATURES ARE IN DEGREES CELCIUS

	CENTER	TOP	RIGHT	LEFT	BOTTOM	BACK
CHIP NO1:	50.27E+00	46.37E+00	46.67E+00	46.36E+00	46.34E+00	54.20E+00
POWER (WATTS):	31.58E-01					
CHIP NO2:	49.47E+00	45.72E+00	45.94E+00	44.88E+00	45.65E+00	58.34E+00
POWER (WATTS):	31.60E-01					
CHIP NO3:	48.49E+00	45.75E+00	46.70E+00	44.97E+00	47.04E+00	54.80E+00
POWER (WATTS):	31.50E-01					
CHIP NO4:	49.72E+00	46.06E+00	46.89E+00	44.65E+00	46.51E+00	55.03E+00
POWER (WATTS):	31.19E-01					
CHIP NO5:	48.67E+00	43.79E+00	44.88E+00	44.50E+00	46.45E+00	54.10E+00
POWER (WATTS):	31.32E-01					
CHIP NO6:	46.42E+00	48.26E+00	44.90E+00	46.17E+00	47.08E+00	68.15E+00
POWER (WATTS):	31.23E-01					
CHIP NO7:	51.67E+00	48.20E+00	46.82E+00	46.51E+00	46.95E+00	56.86E+00
POWER (WATTS):	31.66E-01					
CHIP NO8:	49.44E+00	46.99E+00	46.61E+00	46.80E+00	46.32E+00	62.31E+00
POWER (WATTS):	31.80E-01					
CHIP NO9:	48.20E+00	46.19E+00	44.97E+00	46.00E+00	45.25E+00	60.81E+00
POWER (WATTS):	31.53E-01					

HEAT EXCHANGERS TEMPERATURES:	RIGHT	LEFT
BOTTOM:	10.02E+00	10.05E+00
TOP:	10.09E+00	99.64E-01

BACK PLANE TEMPERATURES ARE :

T(55): 28.58E+00
T(56): 30.93E+00
T(57): 33.10E+00
T(72): 31.64E+00
T(73): 31.01E+00
T(74): 31.47E+00
T(75): 32.56E+00
T(76): 30.46E+00
T(77): 30.21E+00

TABLE 9

REDUCED DATA FOR INPUT POWER Q_{in} = 0.3 W

THE RAW Emf DATA ARE FROM THE FILE: D80700925
THE POWER SETTING PER CHIP WAS: 0.3 WATTS

CHIP	QNET(W)	Tavg-Ts	Nu	%UNC IN Nu
1	27.38E-02	56.09E-01	10.61E+00	20.55E-01
	TEMPERATURE BASED RAYLEIGH NUMBER * E-6 IS: 104.43E-02			
	% UNCERTAINTY IN THE TEMPERATURE BASED RAYLEIGH NUMBER IS :179.04E-02			
	FLUX BASED RAYLEIGH NUMBER * E-7 IS: 110.76E-02			
	% UNCERTAINTY IN FLUX BASED RAYLEIGH NUMBER IS: 100.88E-02			
2	27.38E-02	57.60E-01	10.33E+00	20.14E-01
	TEMPERATURE BASED RAYLEIGH NUMBER * E-6 IS: 107.44E-02			
	% UNCERTAINTY IN THE TEMPERATURE BASED RAYLEIGH NUMBER IS :174.32E-02			
	FLUX BASED RAYLEIGH NUMBER * E-7 IS: 110.98E-02			
	% UNCERTAINTY IN FLUX BASED RAYLEIGH NUMBER IS: 100.88E-02			
3	27.29E-02	57.70E-01	10.28E+00	20.12E-01
	TEMPERATURE BASED RAYLEIGH NUMBER * E-6 IS: 107.63E-02			
	% UNCERTAINTY IN THE TEMPERATURE BASED RAYLEIGH NUMBER IS :174.03E-02			
	FLUX BASED RAYLEIGH NUMBER * E-7 IS: 110.63E-02			
	% UNCERTAINTY IN FLUX BASED RAYLEIGH NUMBER IS: 100.88E-02			
4	27.03E-02	55.15E-01	10.65E+00	20.82E-01
	TEMPERATURE BASED RAYLEIGH NUMBER * E-6 IS: 102.58E-02			
	% UNCERTAINTY IN THE TEMPERATURE BASED RAYLEIGH NUMBER IS :182.08E-02			
	FLUX BASED RAYLEIGH NUMBER * E-7 IS: 109.23E-02			
	% UNCERTAINTY IN FLUX BASED RAYLEIGH NUMBER IS: 100.89E-02			
5	27.14E-02	56.58E-01	10.42E+00	20.42E-01
	TEMPERATURE BASED RAYLEIGH NUMBER * E-6 IS: 105.40E-02			
	% UNCERTAINTY IN THE TEMPERATURE BASED RAYLEIGH NUMBER IS :177.49E-02			
	FLUX BASED RAYLEIGH NUMBER * E-7 IS: 109.86E-02			
	% UNCERTAINTY IN FLUX BASED RAYLEIGH NUMBER IS: 100.89E-02			
6	27.11E-02	58.16E-01	10.13E+00	20.00E-01
	TEMPERATURE BASED RAYLEIGH NUMBER * E-6 IS: 108.54E-02			
	% UNCERTAINTY IN THE TEMPERATURE BASED RAYLEIGH NUMBER IS :172.66E-02			
	FLUX BASED RAYLEIGH NUMBER * E-7 IS: 109.94E-02			
	% UNCERTAINTY IN FLUX BASED RAYLEIGH NUMBER IS: 100.89E-02			
7	27.45E-02	56.19E-01	10.62E+00	20.52E-01
	TEMPERATURE BASED RAYLEIGH NUMBER * E-6 IS: 104.64E-02			
	% UNCERTAINTY IN THE TEMPERATURE BASED RAYLEIGH NUMBER IS :178.71E-02			
	FLUX BASED RAYLEIGH NUMBER * E-7 IS: 111.08E-02			
	% UNCERTAINTY IN FLUX BASED RAYLEIGH NUMBER IS: 100.88E-02			
8	27.56E-02	58.00E-01	10.33E+00	20.04E-01
	TEMPERATURE BASED RAYLEIGH NUMBER * E-6 IS: 108.23E-02			
	% UNCERTAINTY IN THE TEMPERATURE BASED RAYLEIGH NUMBER IS :173.13E-02			
	FLUX BASED RAYLEIGH NUMBER * E-7 IS: 111.75E-02			
	% UNCERTAINTY IN FLUX BASED RAYLEIGH NUMBER IS: 100.87E-02			
9	27.33E-02	57.25E-01	10.37E+00	20.23E-01
	TEMPERATURE BASED RAYLEIGH NUMBER * E-6 IS: 106.74E-02			
	% UNCERTAINTY IN THE TEMPERATURE BASED RAYLEIGH NUMBER IS :175.40E-02			
	FLUX BASED RAYLEIGH NUMBER * E-7 IS: 110.70E-02			
	% UNCERTAINTY IN FLUX BASED RAYLEIGH NUMBER IS: 100.88E-02			

TABLE 10

REDUCED DATA FOR INPUT POWER Q_{in} = 0.7 W

THE RAW Emf DATA ARE FROM THE FILE: D80701535
THE POWER SETTING PER CHIP WAS: 0.7 WATTS

CHIP	QNET(W)	Tavg-Ts	Nu	%UNC IN Nu
1	70.30E-02	11.51E+00	13.32E+00	13.35E-01

TEMPERATURE BASED RAYLEIGH NUMBER * E-6 IS: 228.83E-02
% UNCERTAINTY IN THE TEMPERATURE BASED RAYLEIGH NUMBER IS :872.27E-03
FLUX BASED RAYLEIGH NUMBER * E-7 IS: 304.72E-02
% UNCERTAINTY IN FLUX BASED RAYLEIGH NUMBER IS: 101.05E-02

2	70.32E-02	11.51E+00	13.32E+00	13.35E-01

TEMPERATURE BASED RAYLEIGH NUMBER * E-6 IS: 228.84E-02
% UNCERTAINTY IN THE TEMPERATURE BASED RAYLEIGH NUMBER IS :872.24E-03
FLUX BASED RAYLEIGH NUMBER * E-7 IS: 304.80E-02
% UNCERTAINTY IN FLUX BASED RAYLEIGH NUMBER IS: 101.05E-02

3	70.09E-02	11.51E+00	13.28E+00	13.35E-01

TEMPERATURE BASED RAYLEIGH NUMBER * E-6 IS: 228.78E-02
% UNCERTAINTY IN THE TEMPERATURE BASED RAYLEIGH NUMBER IS :872.44E-03
FLUX BASED RAYLEIGH NUMBER * E-7 IS: 303.80E-02
% UNCERTAINTY IN FLUX BASED RAYLEIGH NUMBER IS: 101.06E-02

4	69.41E-02	11.36E+00	13.32E+00	13.43E-01

TEMPERATURE BASED RAYLEIGH NUMBER * E-6 IS: 225.48E-02
% UNCERTAINTY IN THE TEMPERATURE BASED RAYLEIGH NUMBER IS :883.80E-03
FLUX BASED RAYLEIGH NUMBER * E-7 IS: 300.34E-02
% UNCERTAINTY IN FLUX BASED RAYLEIGH NUMBER IS: 101.07E-02

5	69.70E-02	11.23E+00	13.53E+00	13.49E-01

TEMPERATURE BASED RAYLEIGH NUMBER * E-6 IS: 222.64E-02
% UNCERTAINTY IN THE TEMPERATURE BASED RAYLEIGH NUMBER IS :893.83E-03
FLUX BASED RAYLEIGH NUMBER * E-7 IS: 301.13E-02
% UNCERTAINTY IN FLUX BASED RAYLEIGH NUMBER IS: 101.06E-02

6	69.61E-02	11.34E+00	13.38E+00	13.44E-01

TEMPERATURE BASED RAYLEIGH NUMBER * E-6 IS: 224.97E-02
% UNCERTAINTY IN THE TEMPERATURE BASED RAYLEIGH NUMBER IS :885.56E-03
FLUX BASED RAYLEIGH NUMBER * E-7 IS: 301.12E-02
% UNCERTAINTY IN FLUX BASED RAYLEIGH NUMBER IS: 101.07E-02

7	70.49E-02	11.57E+00	13.28E+00	13.32E-01

TEMPERATURE BASED RAYLEIGH NUMBER * E-6 IS: 230.19E-02
% UNCERTAINTY IN THE TEMPERATURE BASED RAYLEIGH NUMBER IS :867.69E-03
FLUX BASED RAYLEIGH NUMBER * E-7 IS: 305.75E-02
% UNCERTAINTY IN FLUX BASED RAYLEIGH NUMBER IS: 101.05E-02

8	70.78E-02	11.62E+00	13.28E+00	13.30E-01

TEMPERATURE BASED RAYLEIGH NUMBER * E-6 IS: 231.24E-02
% UNCERTAINTY IN THE TEMPERATURE BASED RAYLEIGH NUMBER IS :864.18E-03
FLUX BASED RAYLEIGH NUMBER * E-7 IS: 307.15E-02
% UNCERTAINTY IN FLUX BASED RAYLEIGH NUMBER IS: 101.05E-02

9	70.17E-02	11.34E+00	13.49E+00	13.43E-01

TEMPERATURE BASED RAYLEIGH NUMBER * E-6 IS: 225.08E-02
% UNCERTAINTY IN THE TEMPERATURE BASED RAYLEIGH NUMBER IS :885.19E-03
FLUX BASED RAYLEIGH NUMBER * E-7 IS: 303.58E-02
% UNCERTAINTY IN FLUX BASED RAYLEIGH NUMBER IS: 101.06E-02

TABLE 11

REDUCED DATA FOR INPUT POWER Q_{in} = 1.1 W

THE RAW Emf DATA ARE FROM THE FILE: D80711035
THE POWER SETTING PER CHIP WAS: 1.1 WATTS

CHIP	QNET(W)	Tavg-Ts	Nu	%UNC IN Nu
1	11.45E-01	16.67E+00	15.01E+00	11.77E-01

TEMPERATURE BASED RAYLEIGH NUMBER * E-6 IS: 343.22E-02
% UNCERTAINTY IN THE TEMPERATURE BASED RAYLEIGH NUMBER IS :602.88E-03
FLUX BASED RAYLEIGH NUMBER * E-7 IS: 515.31E-02
% UNCERTAINTY IN FLUX BASED RAYLEIGH NUMBER IS: 101.06E-02

2	11.46E-01	16.59E+00	15.08E+00	11.78E-01

TEMPERATURE BASED RAYLEIGH NUMBER * E-6 IS: 341.44E-02
% UNCERTAINTY IN THE TEMPERATURE BASED RAYLEIGH NUMBER IS :605.54E-03
FLUX BASED RAYLEIGH NUMBER * E-7 IS: 515.06E-02
% UNCERTAINTY IN FLUX BASED RAYLEIGH NUMBER IS: 101.06E-02

3	11.42E-01	16.56E+00	15.06E+00	11.79E-01

TEMPERATURE BASED RAYLEIGH NUMBER * E-6 IS: 340.72E-02
% UNCERTAINTY IN THE TEMPERATURE BASED RAYLEIGH NUMBER IS :606.64E-03
FLUX BASED RAYLEIGH NUMBER * E-7 IS: 513.21E-02
% UNCERTAINTY IN FLUX BASED RAYLEIGH NUMBER IS: 101.06E-02

4	11.31E-01	16.41E+00	15.05E+00	11.82E-01

TEMPERATURE BASED RAYLEIGH NUMBER * E-6 IS: 337.05E-02
% UNCERTAINTY IN THE TEMPERATURE BASED RAYLEIGH NUMBER IS :612.23E-03
FLUX BASED RAYLEIGH NUMBER * E-7 IS: 507.35E-02
% UNCERTAINTY IN FLUX BASED RAYLEIGH NUMBER IS: 101.07E-02

5	11.35E-01	16.05E+00	15.45E+00	11.89E-01

TEMPERATURE BASED RAYLEIGH NUMBER * E-6 IS: 328.29E-02
% UNCERTAINTY IN THE TEMPERATURE BASED RAYLEIGH NUMBER IS :626.12E-03
FLUX BASED RAYLEIGH NUMBER * E-7 IS: 507.35E-02
% UNCERTAINTY IN FLUX BASED RAYLEIGH NUMBER IS: 101.07E-02

6	11.34E-01	15.92E+00	15.55E+00	11.92E-01

TEMPERATURE BASED RAYLEIGH NUMBER * E-6 IS: 325.25E-02
% UNCERTAINTY IN THE TEMPERATURE BASED RAYLEIGH NUMBER IS :631.11E-03
FLUX BASED RAYLEIGH NUMBER * E-7 IS: 505.88E-02
% UNCERTAINTY IN FLUX BASED RAYLEIGH NUMBER IS: 101.07E-02

7	11.48E-01	16.81E+00	14.93E+00	11.74E-01

TEMPERATURE BASED RAYLEIGH NUMBER * E-6 IS: 346.68E-02
% UNCERTAINTY IN THE TEMPERATURE BASED RAYLEIGH NUMBER IS :597.78E-03
FLUX BASED RAYLEIGH NUMBER * E-7 IS: 517.48E-02
% UNCERTAINTY IN FLUX BASED RAYLEIGH NUMBER IS: 101.06E-02

8	11.53E-01	16.76E+00	15.03E+00	11.75E-01

TEMPERATURE BASED RAYLEIGH NUMBER * E-6 IS: 345.42E-02
% UNCERTAINTY IN THE TEMPERATURE BASED RAYLEIGH NUMBER IS :599.62E-03
FLUX BASED RAYLEIGH NUMBER * E-7 IS: 519.33E-02
% UNCERTAINTY IN FLUX BASED RAYLEIGH NUMBER IS: 101.05E-02

9	11.43E-01	16.28E+00	15.34E+00	11.84E-01

TEMPERATURE BASED RAYLEIGH NUMBER * E-6 IS: 333.97E-02
% UNCERTAINTY IN THE TEMPERATURE BASED RAYLEIGH NUMBER IS :617.04E-03
FLUX BASED RAYLEIGH NUMBER * E-7 IS: 512.18E-02
% UNCERTAINTY IN FLUX BASED RAYLEIGH NUMBER IS: 101.06E-02

TABLE 12

REDUCED DATA FOR INPUT POWER Q_{in} = 1.5 W

THE RAW Emf DATA ARE FROM THE FILE: D80720730
THE POWER SETTING PER CHIP WAS: 1.5 WATTS

CHIP	QNET(W)	Tavg-Ts	Nu	%UNC IN Nu
1	14.59E-01	19.05E+00	16.76E+00	11.41E-01
	TEMPERATURE BASED RAYLEIGH NUMBER * E-6 IS: 401.43E-02			
	% UNCERTAINTY IN THE TEMPERATURE BASED RAYLEIGH NUMBER IS :527.67E-03			
	FLUX BASED RAYLEIGH NUMBER * E-7 IS: 672.71E-02			
	% UNCERTAINTY IN FLUX BASED RAYLEIGH NUMBER IS: 101.12E-02			
2	14.59E-01	19.08E+00	16.74E+00	11.40E-01
	TEMPERATURE BASED RAYLEIGH NUMBER * E-6 IS: 402.25E-02			
	% UNCERTAINTY IN THE TEMPERATURE BASED RAYLEIGH NUMBER IS :526.77E-03			
	FLUX BASED RAYLEIGH NUMBER * E-7 IS: 673.17E-02			
	% UNCERTAINTY IN FLUX BASED RAYLEIGH NUMBER IS: 101.12E-02			
3	14.54E-01	19.35E+00	16.45E+00	11.37E-01
	TEMPERATURE BASED RAYLEIGH NUMBER * E-6 IS: 409.23E-02			
	% UNCERTAINTY IN THE TEMPERATURE BASED RAYLEIGH NUMBER IS :519.31E-03			
	FLUX BASED RAYLEIGH NUMBER * E-7 IS: 673.03E-02			
	% UNCERTAINTY IN FLUX BASED RAYLEIGH NUMBER IS: 101.12E-02			
4	14.40E-01	18.73E+00	16.83E+00	11.45E-01
	TEMPERATURE BASED RAYLEIGH NUMBER * E-6 IS: 393.35E-02			
	% UNCERTAINTY IN THE TEMPERATURE BASED RAYLEIGH NUMBER IS :536.67E-03			
	FLUX BASED RAYLEIGH NUMBER * E-7 IS: 661.82E-02			
	% UNCERTAINTY IN FLUX BASED RAYLEIGH NUMBER IS: 101.13E-02			
5	14.46E-01	18.39E+00	17.20E+00	11.49E-01
	TEMPERATURE BASED RAYLEIGH NUMBER * E-6 IS: 385.00E-02			
	% UNCERTAINTY IN THE TEMPERATURE BASED RAYLEIGH NUMBER IS :546.38E-03			
	FLUX BASED RAYLEIGH NUMBER * E-7 IS: 662.05E-02			
	% UNCERTAINTY IN FLUX BASED RAYLEIGH NUMBER IS: 101.13E-02			
6	14.44E-01	18.59E+00	16.99E+00	11.47E-01
	TEMPERATURE BASED RAYLEIGH NUMBER * E-6 IS: 389.86E-02			
	% UNCERTAINTY IN THE TEMPERATURE BASED RAYLEIGH NUMBER IS :540.68E-03			
	FLUX BASED RAYLEIGH NUMBER * E-7 IS: 662.46E-02			
	% UNCERTAINTY IN FLUX BASED RAYLEIGH NUMBER IS: 101.13E-02			
7	14.62E-01	19.27E+00	16.60E+00	11.38E-01
	TEMPERATURE BASED RAYLEIGH NUMBER * E-6 IS: 407.23E-02			
	% UNCERTAINTY IN THE TEMPERATURE BASED RAYLEIGH NUMBER IS :521.42E-03			
	FLUX BASED RAYLEIGH NUMBER * E-7 IS: 676.12E-02			
	% UNCERTAINTY IN FLUX BASED RAYLEIGH NUMBER IS: 101.11E-02			
8	14.68E-01	19.48E+00	16.50E+00	11.35E-01
	TEMPERATURE BASED RAYLEIGH NUMBER * E-6 IS: 412.33E-02			
	% UNCERTAINTY IN THE TEMPERATURE BASED RAYLEIGH NUMBER IS :516.06E-03			
	FLUX BASED RAYLEIGH NUMBER * E-7 IS: 680.47E-02			
	% UNCERTAINTY IN FLUX BASED RAYLEIGH NUMBER IS: 101.11E-02			
9	14.56E-01	19.09E+00	16.69E+00	11.40E-01
	TEMPERATURE BASED RAYLEIGH NUMBER * E-6 IS: 402.60E-02			
	% UNCERTAINTY IN THE TEMPERATURE BASED RAYLEIGH NUMBER IS :526.39E-03			
	FLUX BASED RAYLEIGH NUMBER * E-7 IS: 671.79E-02			
	% UNCERTAINTY IN FLUX BASED RAYLEIGH NUMBER IS: 101.12E-02			

TABLE 13

REDUCED DATA FOR INPUT POWER Q_{in} = 1.9 W

THE RAW Emf DATA ARE FROM THE FILE: D80721810
THE POWER SETTING PER CHIP WAS: 1.9 WATTS

CHIP	QNET(W)	Tavg-Ts	Nu	%UNC IN Nu
1	18.99E-01	24.92E+00	16.75E+00	10.88E-01

TEMPERATURE BASED RAYLEIGH NUMBER * E-6 IS: 565.77E-02
% UNCERTAINTY IN THE TEMPERATURE BASED RAYLEIGH NUMBER IS :403.27E-03
FLUX BASED RAYLEIGH NUMBER * E-7 IS: 947.69E-02
% UNCERTAINTY IN FLUX BASED RAYLEIGH NUMBER IS: 101.07E-02

2	19.00E-01	24.72E+00	16.89E+00	10.89E-01

TEMPERATURE BASED RAYLEIGH NUMBER * E-6 IS: 560.03E-02
% UNCERTAINTY IN THE TEMPERATURE BASED RAYLEIGH NUMBER IS :406.56E-03
FLUX BASED RAYLEIGH NUMBER * E-7 IS: 945.98E-02
% UNCERTAINTY IN FLUX BASED RAYLEIGH NUMBER IS: 101.07E-02

3	18.94E-01	24.68E+00	16.86E+00	10.90E-01

TEMPERATURE BASED RAYLEIGH NUMBER * E-6 IS: 559.04E-02
% UNCERTAINTY IN THE TEMPERATURE BASED RAYLEIGH NUMBER IS :407.13E-03
FLUX BASED RAYLEIGH NUMBER * E-7 IS: 942.52E-02
% UNCERTAINTY IN FLUX BASED RAYLEIGH NUMBER IS: 101.08E-02

4	18.75E-01	24.53E+00	16.80E+00	10.91E-01

TEMPERATURE BASED RAYLEIGH NUMBER * E-6 IS: 554.73E-02
% UNCERTAINTY IN THE TEMPERATURE BASED RAYLEIGH NUMBER IS :409.65E-03
FLUX BASED RAYLEIGH NUMBER * E-7 IS: 931.79E-02
% UNCERTAINTY IN FLUX BASED RAYLEIGH NUMBER IS: 101.09E-02

5	18.83E-01	23.88E+00	17.32E+00	10.95E-01

TEMPERATURE BASED RAYLEIGH NUMBER * E-6 IS: 536.40E-02
% UNCERTAINTY IN THE TEMPERATURE BASED RAYLEIGH NUMBER IS :420.80E-03
FLUX BASED RAYLEIGH NUMBER * E-7 IS: 928.99E-02
% UNCERTAINTY IN FLUX BASED RAYLEIGH NUMBER IS: 101.08E-02

6	18.80E-01	23.83E+00	17.32E+00	10.95E-01

TEMPERATURE BASED RAYLEIGH NUMBER * E-6 IS: 535.00E-02
% UNCERTAINTY IN THE TEMPERATURE BASED RAYLEIGH NUMBER IS :421.68E-03
FLUX BASED RAYLEIGH NUMBER * E-7 IS: 926.84E-02
% UNCERTAINTY IN FLUX BASED RAYLEIGH NUMBER IS: 101.09E-02

7	19.04E-01	25.23E+00	16.59E+00	10.86E-01

TEMPERATURE BASED RAYLEIGH NUMBER * E-6 IS: 574.77E-02
% UNCERTAINTY IN THE TEMPERATURE BASED RAYLEIGH NUMBER IS :398.25E-03
FLUX BASED RAYLEIGH NUMBER * E-7 IS: 953.30E-02
% UNCERTAINTY IN FLUX BASED RAYLEIGH NUMBER IS: 101.07E-02

8	19.12E-01	25.20E+00	16.68E+00	10.86E-01

TEMPERATURE BASED RAYLEIGH NUMBER * E-6 IS: 573.88E-02
% UNCERTAINTY IN THE TEMPERATURE BASED RAYLEIGH NUMBER IS :398.74E-03
FLUX BASED RAYLEIGH NUMBER * E-7 IS: 957.00E-02
% UNCERTAINTY IN FLUX BASED RAYLEIGH NUMBER IS: 101.07E-02

9	18.96E-01	24.47E+00	17.02E+00	10.91E-01

TEMPERATURE BASED RAYLEIGH NUMBER * E-6 IS: 552.91E-02
% UNCERTAINTY IN THE TEMPERATURE BASED RAYLEIGH NUMBER IS :410.73E-03
FLUX BASED RAYLEIGH NUMBER * E-7 IS: 941.24E-02
% UNCERTAINTY IN FLUX BASED RAYLEIGH NUMBER IS: 101.08E-02

TABLE 14

REDUCED DATA FOR INPUT POWER Q_{in} = 2.3 W

THE RAW Emf DATA ARE FROM THE FILE: D80731030
THE POWER SETTING PER CHIP WAS: 2.3 WATTS

CHIP	QNET(W)	Tavg-Ts	Nu	%UNC IN Nu
1	22.85E-01	28.31E+00	17.76E+00	10.71E-01
	TEMPERATURE BASED RAYLEIGH NUMBER * E-6 IS: 658.53E-02			
	% UNCERTAINTY IN THE TEMPERATURE BASED RAYLEIGH NUMBER IS :355.02E-03			
	FLUX BASED RAYLEIGH NUMBER * E-7 IS: 116.98E-01			
	% UNCERTAINTY IN FLUX BASED RAYLEIGH NUMBER IS: 101.07E-02			
2	22.86E-01	27.97E+00	17.98E+00	10.73E-01
	TEMPERATURE BASED RAYLEIGH NUMBER * E-6 IS: 648.40E-02			
	% UNCERTAINTY IN THE TEMPERATURE BASED RAYLEIGH NUMBER IS :359.32E-03			
	FLUX BASED RAYLEIGH NUMBER * E-7 IS: 116.60E-01			
	% UNCERTAINTY IN FLUX BASED RAYLEIGH NUMBER IS: 101.07E-02			
3	22.78E-01	27.97E+00	17.93E+00	10.73E-01
	TEMPERATURE BASED RAYLEIGH NUMBER * E-6 IS: 648.36E-02			
	% UNCERTAINTY IN THE TEMPERATURE BASED RAYLEIGH NUMBER IS :359.34E-03			
	FLUX BASED RAYLEIGH NUMBER * E-7 IS: 116.22E-01			
	% UNCERTAINTY IN FLUX BASED RAYLEIGH NUMBER IS: 101.07E-02			
4	22.56E-01	27.87E+00	17.81E+00	10.73E-01
	TEMPERATURE BASED RAYLEIGH NUMBER * E-6 IS: 645.46E-02			
	% UNCERTAINTY IN THE TEMPERATURE BASED RAYLEIGH NUMBER IS :360.59E-03			
	FLUX BASED RAYLEIGH NUMBER * E-7 IS: 114.97E-01			
	% UNCERTAINTY IN FLUX BASED RAYLEIGH NUMBER IS: 101.08E-02			
5	22.65E-01	27.10E+00	18.38E+00	10.77E-01
	TEMPERATURE BASED RAYLEIGH NUMBER * E-6 IS: 622.74E-02			
	% UNCERTAINTY IN THE TEMPERATURE BASED RAYLEIGH NUMBER IS :370.80E-03			
	FLUX BASED RAYLEIGH NUMBER * E-7 IS: 114.48E-01			
	% UNCERTAINTY IN FLUX BASED RAYLEIGH NUMBER IS: 101.08E-02			
6	22.60E-01	27.15E+00	18.31E+00	10.76E-01
	TEMPERATURE BASED RAYLEIGH NUMBER * E-6 IS: 624.26E-02			
	% UNCERTAINTY IN THE TEMPERATURE BASED RAYLEIGH NUMBER IS :370.10E-03			
	FLUX BASED RAYLEIGH NUMBER * E-7 IS: 114.28E-01			
	% UNCERTAINTY IN FLUX BASED RAYLEIGH NUMBER IS: 101.08E-02			
7	22.90E-01	28.72E+00	17.55E+00	10.70E-01
	TEMPERATURE BASED RAYLEIGH NUMBER * E-6 IS: 671.04E-02			
	% UNCERTAINTY IN THE TEMPERATURE BASED RAYLEIGH NUMBER IS :349.89E-03			
	FLUX BASED RAYLEIGH NUMBER * E-7 IS: 117.80E-01			
	% UNCERTAINTY IN FLUX BASED RAYLEIGH NUMBER IS: 101.07E-02			
8	23.00E-01	28.59E+00	17.71E+00	10.70E-01
	TEMPERATURE BASED RAYLEIGH NUMBER * E-6 IS: 667.05E-02			
	% UNCERTAINTY IN THE TEMPERATURE BASED RAYLEIGH NUMBER IS :351.51E-03			
	FLUX BASED RAYLEIGH NUMBER * E-7 IS: 118.13E-01			
	% UNCERTAINTY IN FLUX BASED RAYLEIGH NUMBER IS: 101.06E-02			
9	22.80E-01	27.68E+00	18.13E+00	10.74E-01
	TEMPERATURE BASED RAYLEIGH NUMBER * E-6 IS: 639.69E-02			
	% UNCERTAINTY IN THE TEMPERATURE BASED RAYLEIGH NUMBER IS :363.12E-03			
	FLUX BASED RAYLEIGH NUMBER * E-7 IS: 115.97E-01			
	% UNCERTAINTY IN FLUX BASED RAYLEIGH NUMBER IS: 101.07E-02			

TABLE 15

REDUCED DATA FOR INPUT POWER Q_{in} = 2.7 W

THE RAW Emf DATA ARE FROM THE FILE: D80731755
THE POWER SETTING PER CHIP WAS: 2.7 wATTS

CHIP	QNET(W)	Tavg-Ts	Nu	%UNC IN Nu
1	27.37E-01	33.28E+00	18.16E+00	10.55E-01
	TEMPERATURE BASED RAYLEIGH NUMBER * E-6 IS: 813.30E-02			
	% UNCERTAINTY IN THE TEMPERATURE BASED RAYLEIGH NUMBER IS :302.08E-03			
	FLUX BASED RAYLEIGH NUMBER * E-7 IS: 147.70E-01			
	% UNCERTAINTY IN FLUX BASED RAYLEIGH NUMBER IS: 101.05E-02			
2	27.39E-01	32.77E+00	18.44E+00	10.56E-01
	TEMPERATURE BASED RAYLEIGH NUMBER * E-6 IS: 796.95E-02			
	% UNCERTAINTY IN THE TEMPERATURE BASED RAYLEIGH NUMBER IS :306.72E-03			
	FLUX BASED RAYLEIGH NUMBER * E-7 IS: 146.98E-01			
	% UNCERTAINTY IN FLUX BASED RAYLEIGH NUMBER IS: 101.05E-02			
3	27.30E-01	32.53E+00	18.52E+00	10.57E-01
	TEMPERATURE BASED RAYLEIGH NUMBER * E-6 IS: 789.23E-02			
	% UNCERTAINTY IN THE TEMPERATURE BASED RAYLEIGH NUMBER IS :308.97E-03			
	FLUX BASED RAYLEIGH NUMBER * E-7 IS: 146.13E-01			
	% UNCERTAINTY IN FLUX BASED RAYLEIGH NUMBER IS: 101.05E-02			
4	27.03E-01	32.75E+00	18.22E+00	10.56E-01
	TEMPERATURE BASED RAYLEIGH NUMBER * E-6 IS: 796.28E-02			
	% UNCERTAINTY IN THE TEMPERATURE BASED RAYLEIGH NUMBER IS :306.91E-03			
	FLUX BASED RAYLEIGH NUMBER * E-7 IS: 145.04E-01			
	% UNCERTAINTY IN FLUX BASED RAYLEIGH NUMBER IS: 101.06E-02			
5	27.15E-01	31.73E+00	18.87E+00	10.59E-01
	TEMPERATURE BASED RAYLEIGH NUMBER * E-6 IS: 763.51E-02			
	% UNCERTAINTY IN THE TEMPERATURE BASED RAYLEIGH NUMBER IS :316.79E-03			
	FLUX BASED RAYLEIGH NUMBER * E-7 IS: 144.06E-01			
	% UNCERTAINTY IN FLUX BASED RAYLEIGH NUMBER IS: 101.06E-02			
6	27.07E-01	31.79E+00	18.78E+00	10.59E-01
	TEMPERATURE BASED RAYLEIGH NUMBER * E-6 IS: 765.48E-02			
	% UNCERTAINTY IN THE TEMPERATURE BASED RAYLEIGH NUMBER IS :316.18E-03			
	FLUX BASED RAYLEIGH NUMBER * E-7 IS: 143.75E-01			
	% UNCERTAINTY IN FLUX BASED RAYLEIGH NUMBER IS: 101.06E-02			
7	27.44E-01	33.82E+00	17.92E+00	10.53E-01
	TEMPERATURE BASED RAYLEIGH NUMBER * E-6 IS: 831.14E-02			
	% UNCERTAINTY IN THE TEMPERATURE BASED RAYLEIGH NUMBER IS :297.22E-03			
	FLUX BASED RAYLEIGH NUMBER * E-7 IS: 148.91E-01			
	% UNCERTAINTY IN FLUX BASED RAYLEIGH NUMBER IS: 101.05E-02			
8	27.56E-01	33.41E+00	18.21E+00	10.54E-01
	TEMPERATURE BASED RAYLEIGH NUMBER * E-6 IS: 817.56E-02			
	% UNCERTAINTY IN THE TEMPERATURE BASED RAYLEIGH NUMBER IS :300.90E-03			
	FLUX BASED RAYLEIGH NUMBER * E-7 IS: 148.90E-01			
	% UNCERTAINTY IN FLUX BASED RAYLEIGH NUMBER IS: 101.04E-02			
9	27.32E-01	32.11E+00	18.77E+00	10.58E-01
	TEMPERATURE BASED RAYLEIGH NUMBER * E-6 IS: 775.54E-02			
	% UNCERTAINTY IN THE TEMPERATURE BASED RAYLEIGH NUMBER IS :313.07E-03			
	FLUX BASED RAYLEIGH NUMBER * E-7 IS: 145.59E-01			
	% UNCERTAINTY IN FLUX BASED RAYLEIGH NUMBER IS: 101.05E-02			

1. Graphical Representation of Reduced Data

The experimental surface temperature data were plotted as a dimensionless Nusselt Number vs. both a temperature based and a flux based Rayleigh Number, Figures 4.15 through 4.32.

Representative error bounds were plotted in Figures 4.15 and 4.16 for input powers of 1.5 and 1.9 watts. All points, with the exception of 1.5 watts were well within the error bounds. The point representing 1.5 watts was either too high on the Nusselt Number axis or too low on the Rayleigh number axis.

The factors affecting the Nusselt Number were h, L & K. Of these three, only h was calculated with uncertainty in this experiment. The factors affecting the Rayleigh Numbers were α, L, ΔT, Q_{net}, β, ν and K. Of these only ΔT and Q_{net} had uncertainties.

Examination of Tables 4 and 12 resulted in no data which appeared to be extreme in either the raw or reduced data sets. One possible explanation for this point is the changing flow patterns around this power input. This may be a transition region from somewhat orderly flow to completely chaotic flow. It is recommended that further investigation of this region of power settings be conducted.

The equations for the best fit lines are very close to each other suggesting that an overall correlation that would produce good approximations is possible.

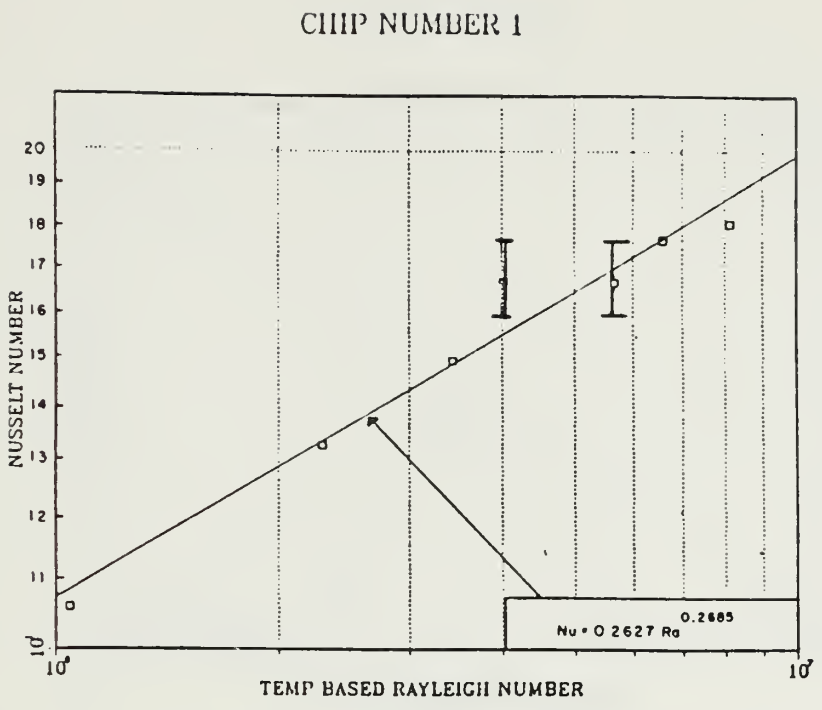

Figure 4.15 Temperature Based Rayleigh Numbers, Chip 1

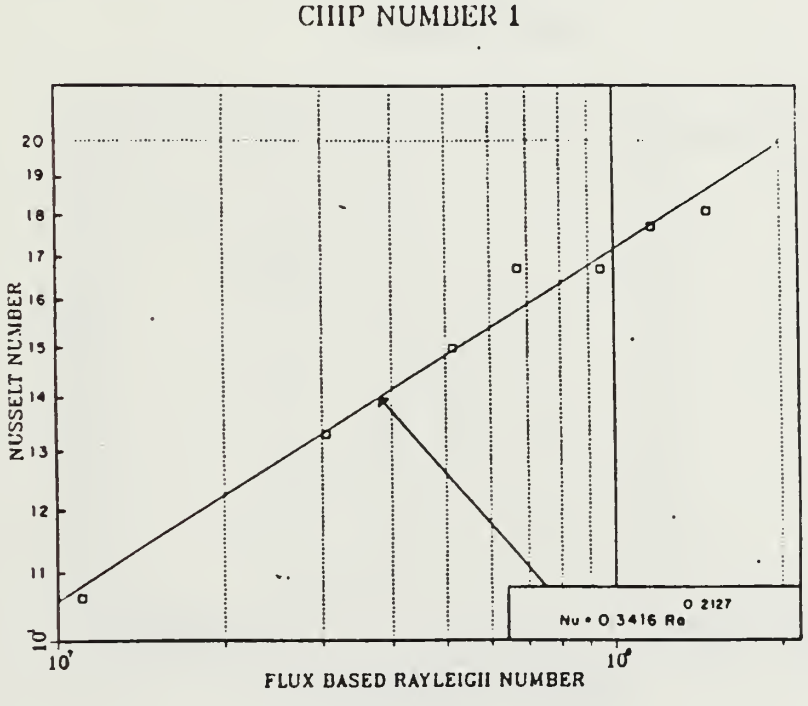

Figure 4.16 Flux Based Rayleigh Numbers, Chip 1

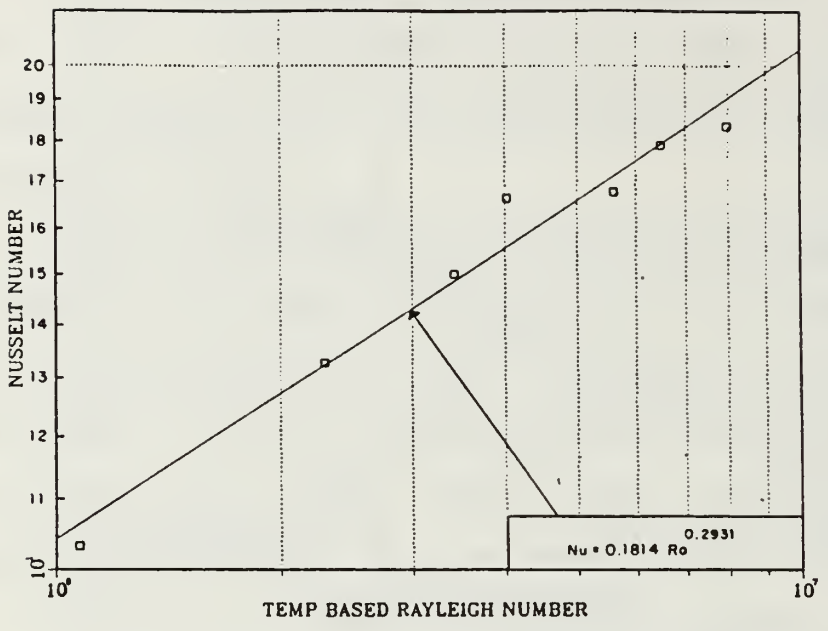

Figure 4.17 Temperature Based Rayleigh Numbers, Chip 2

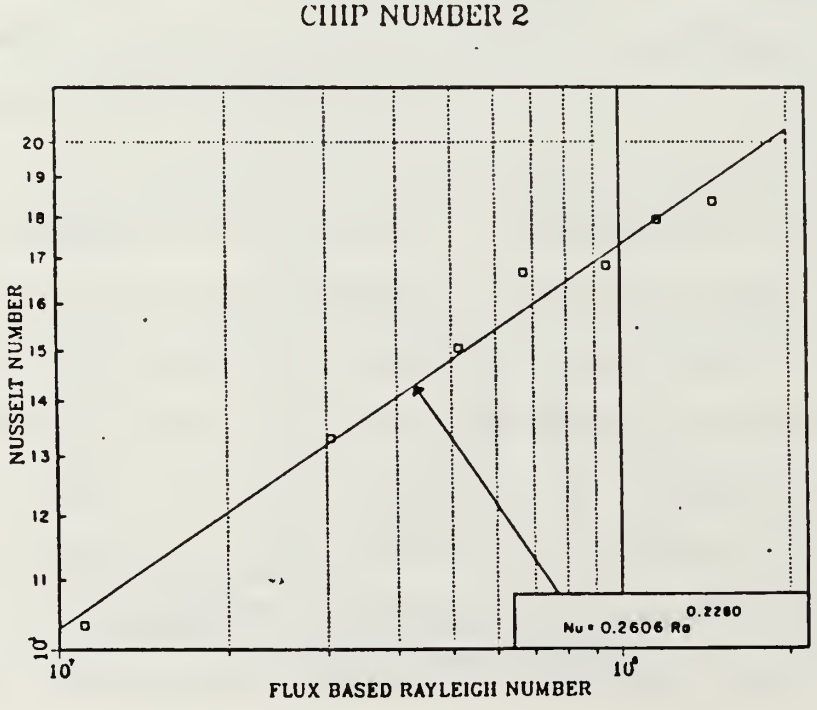

Figure 4.18 Flux Based Rayleigh Numbers, Chip 2

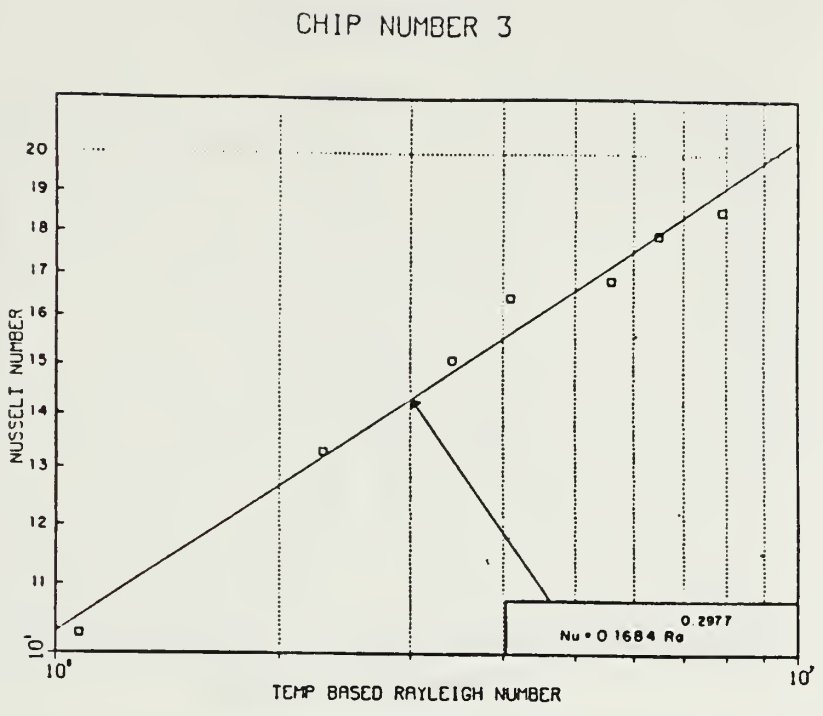

Figure 4.19 Temperature Based Rayleigh Numbers, Chip 3

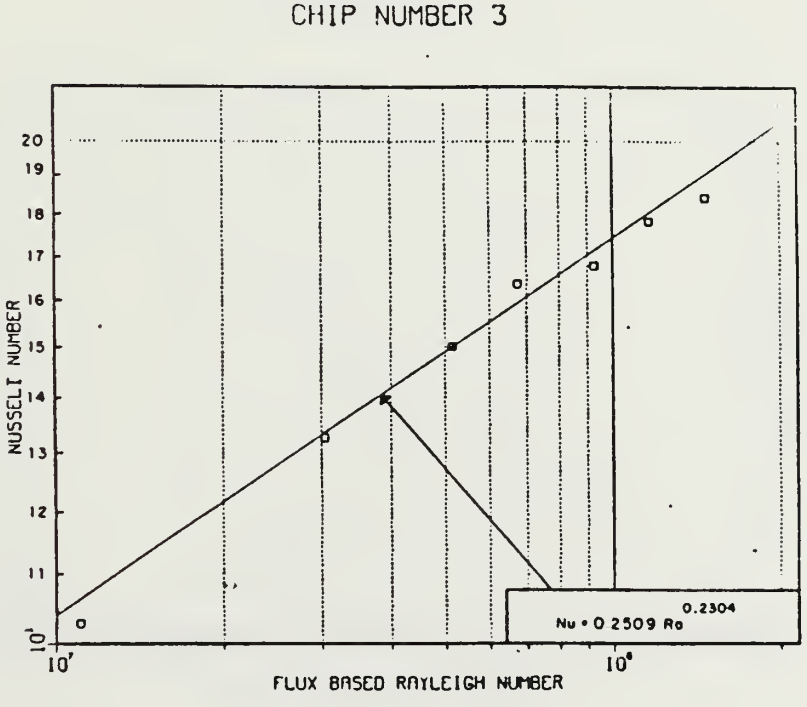

Figure 4.20 Flux Based Rayleigh Numbers, Chip 3

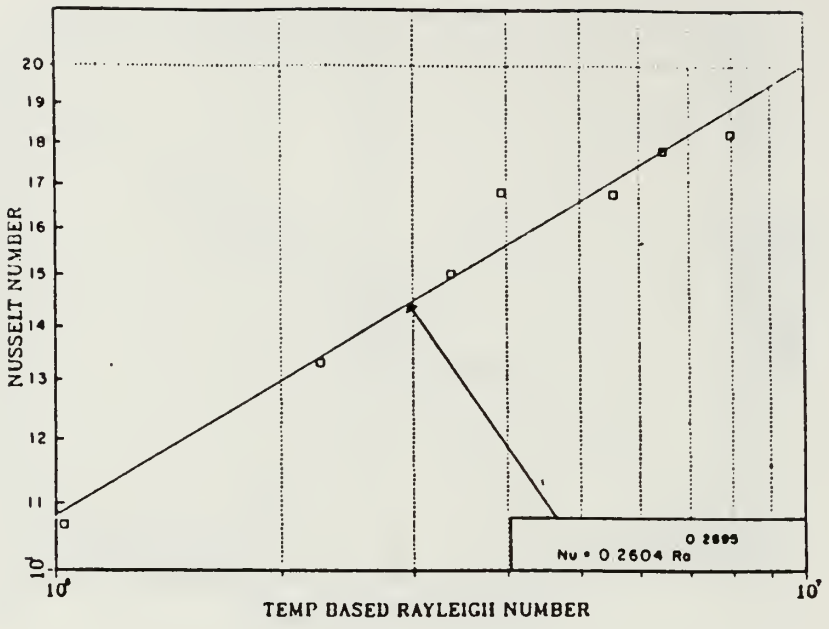

Figure 4.21 Temperature Based Rayleigh Numbers, Chip 4

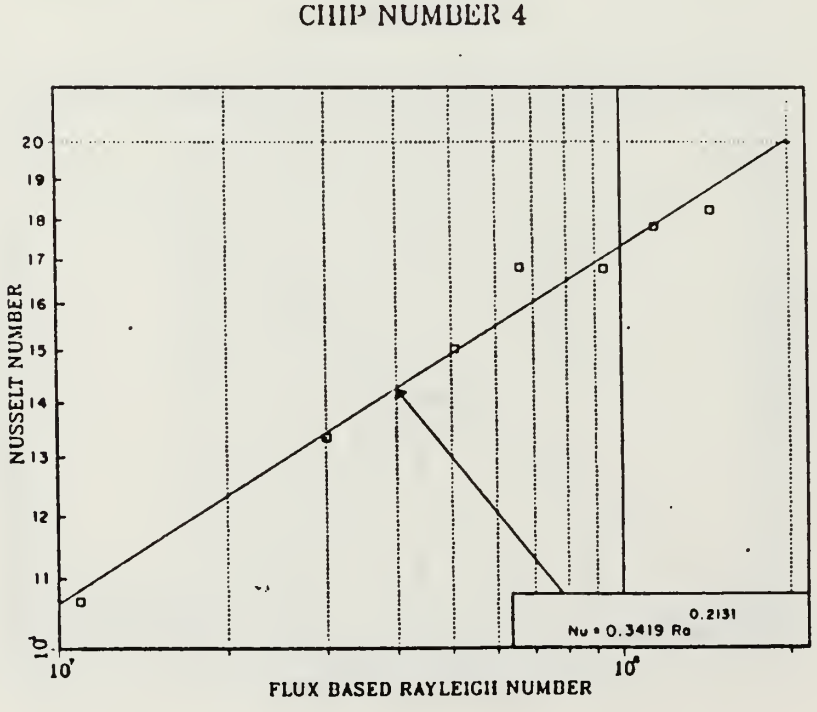

Figure 4.22 Flux Based Rayleigh Numbers, Chip 4

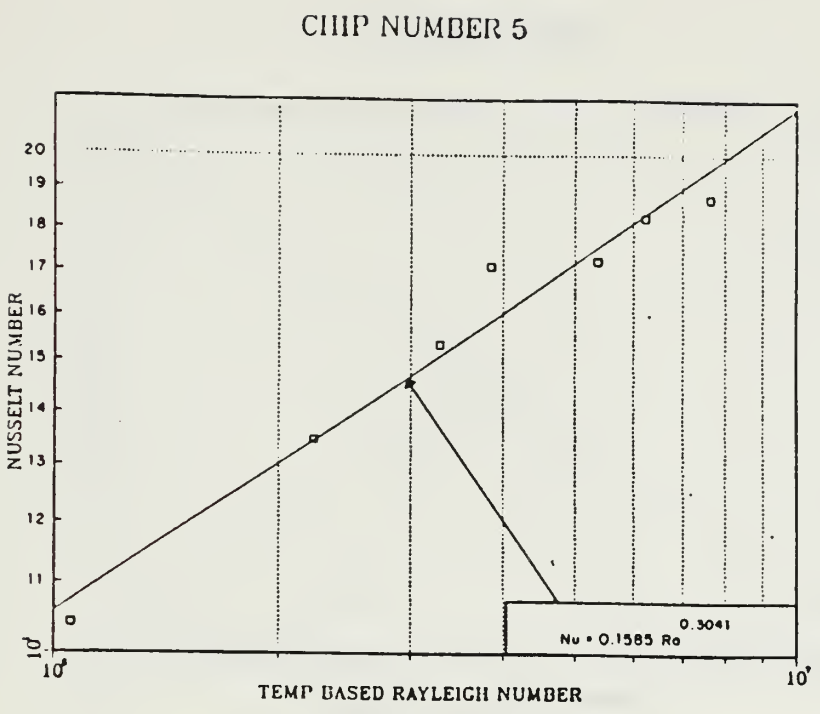

Figure 4.23 Temperature Based Rayleigh Numbers, Chip 5

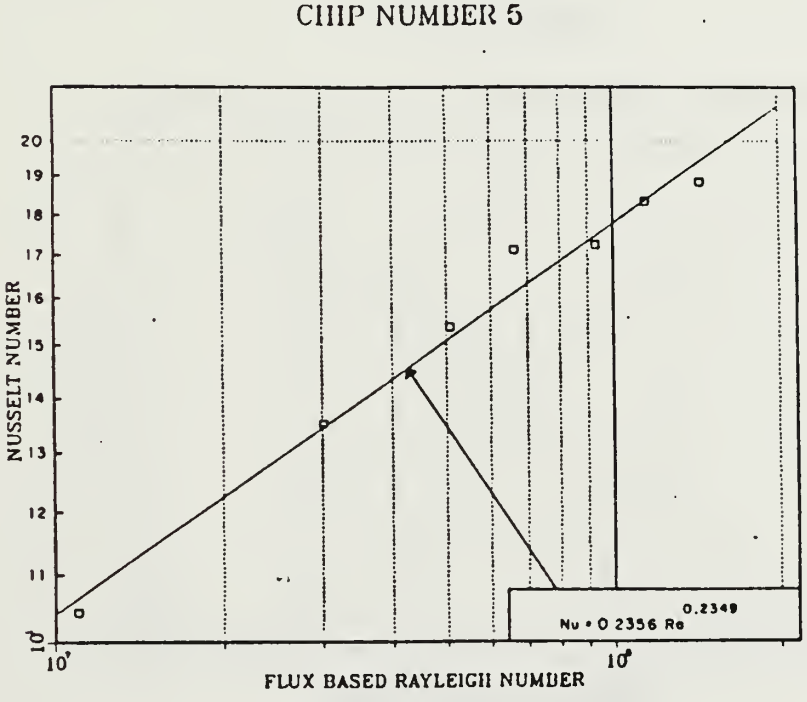

Figure 4.24 Flux Based Rayleigh Numbers, Chip 5

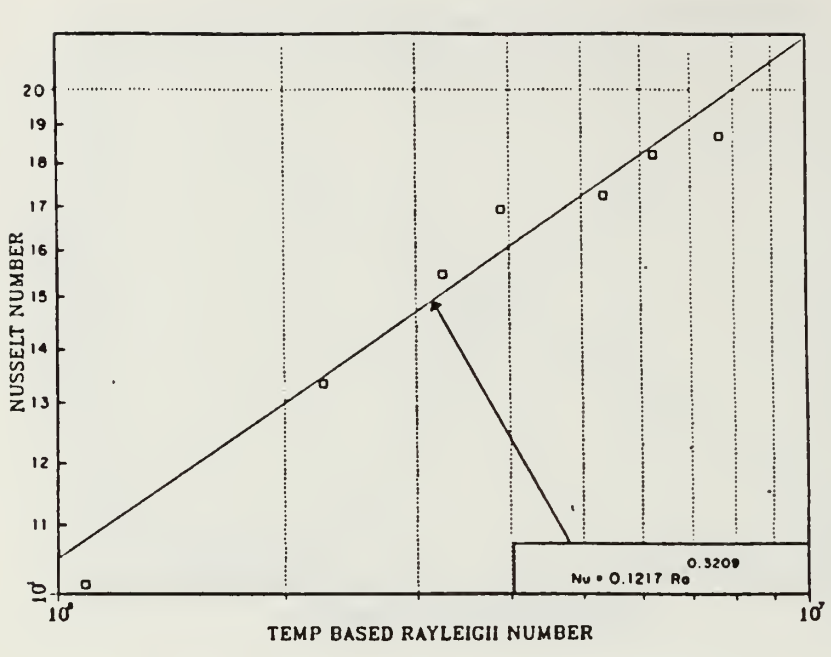

Figure 4.25 Temperature Based Rayleigh Numbers, Chip 6

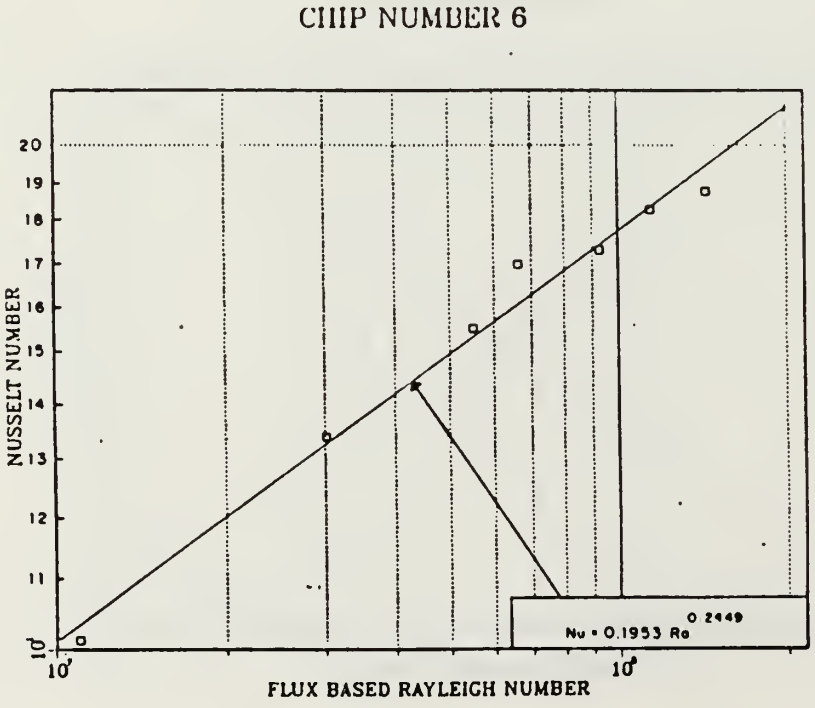

Figure 4.26 Flux Based Rayleigh Numbers, Chip 6

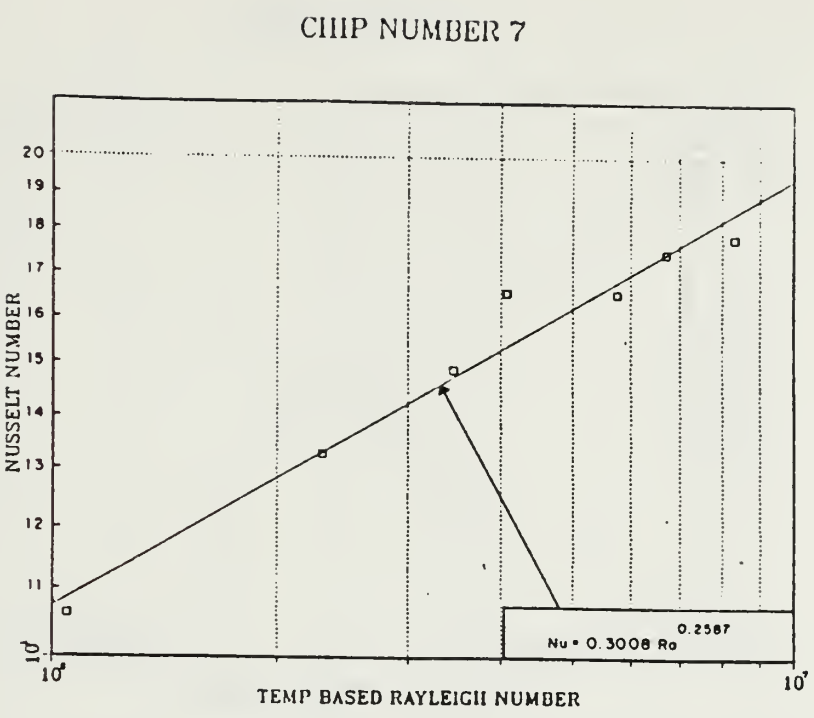

Figure 4.27 Temperature Based Rayleigh Numbers, Chip 7

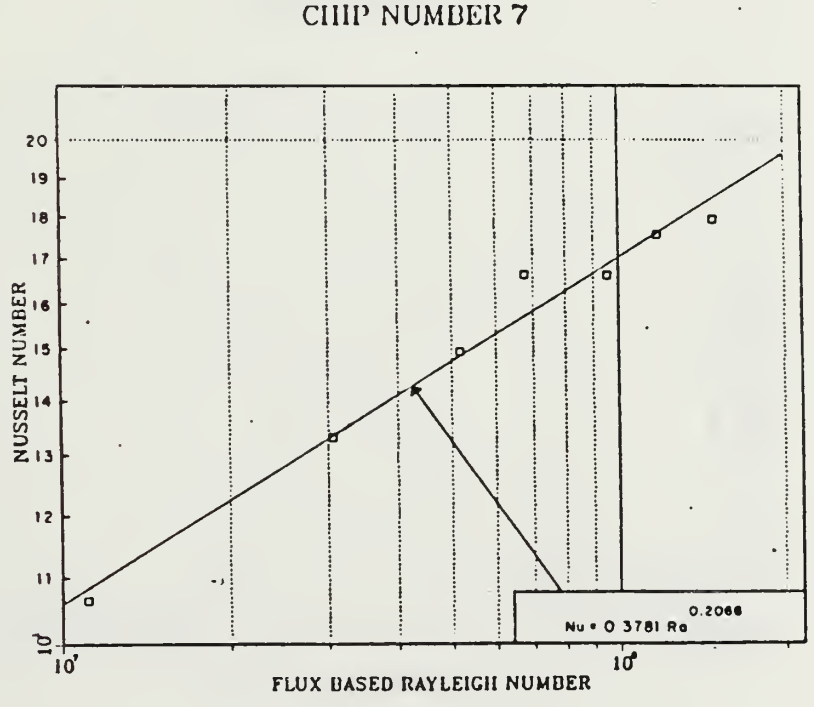

Figure 4.28 Flux Based Rayleigh Numbers, Chip 7

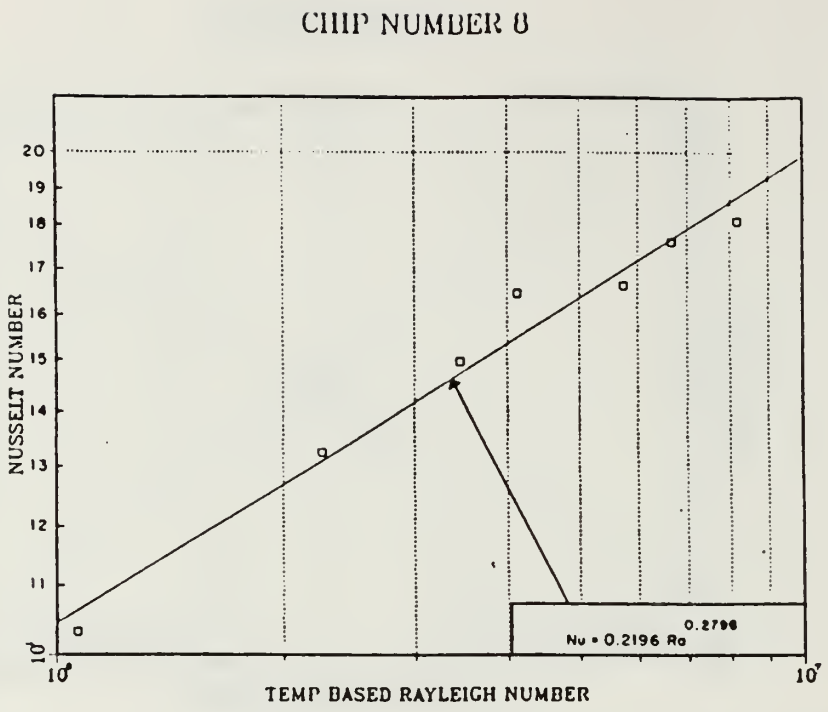

Figure 4.29 Temperature Based Rayleigh Numbers, Chip 8

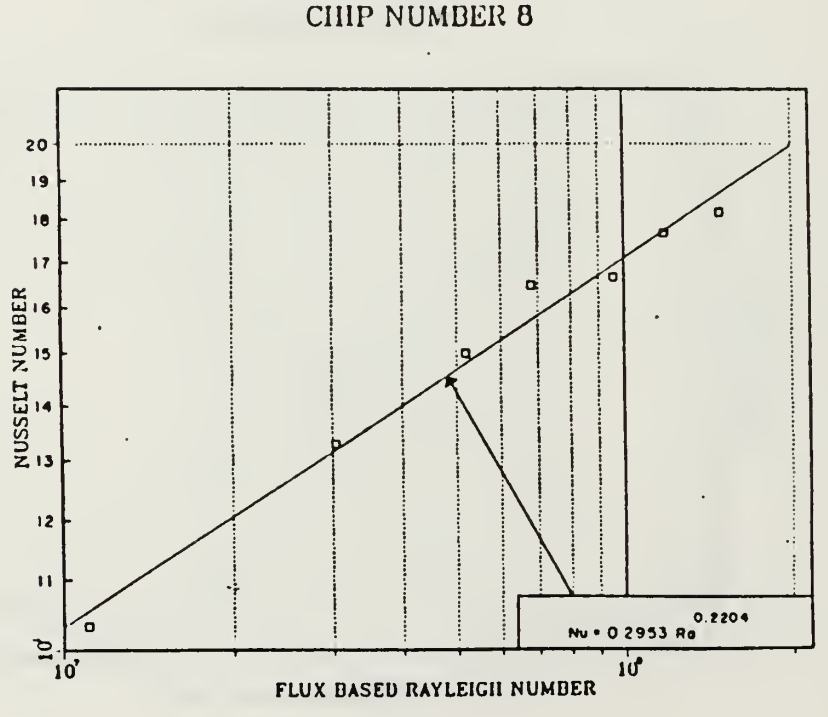

Figure 4.30 Flux Based Rayleigh Numbers, Chip 8

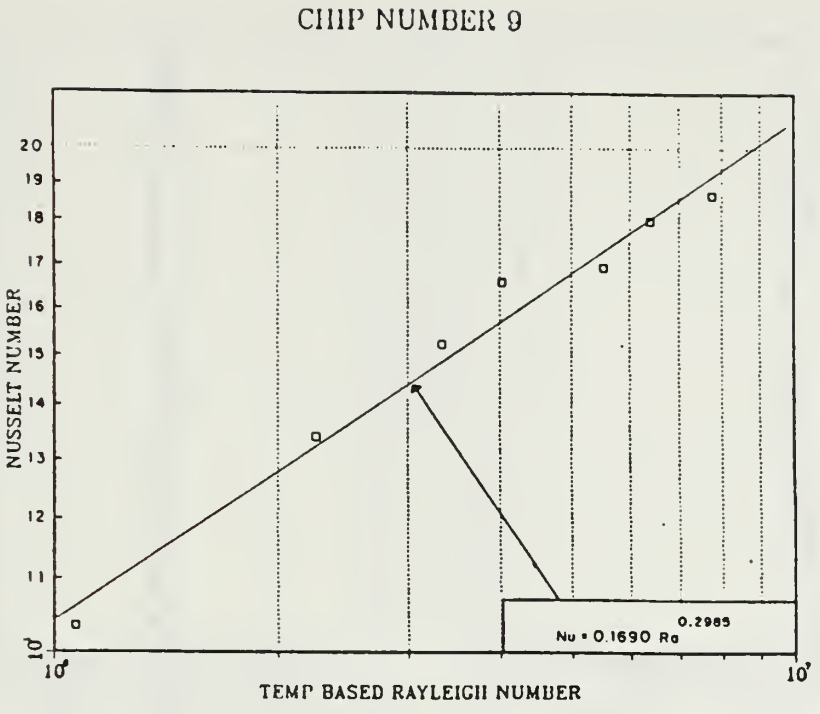

Figure 4.31 Temperature Based Rayleigh Numbers, Chip 9

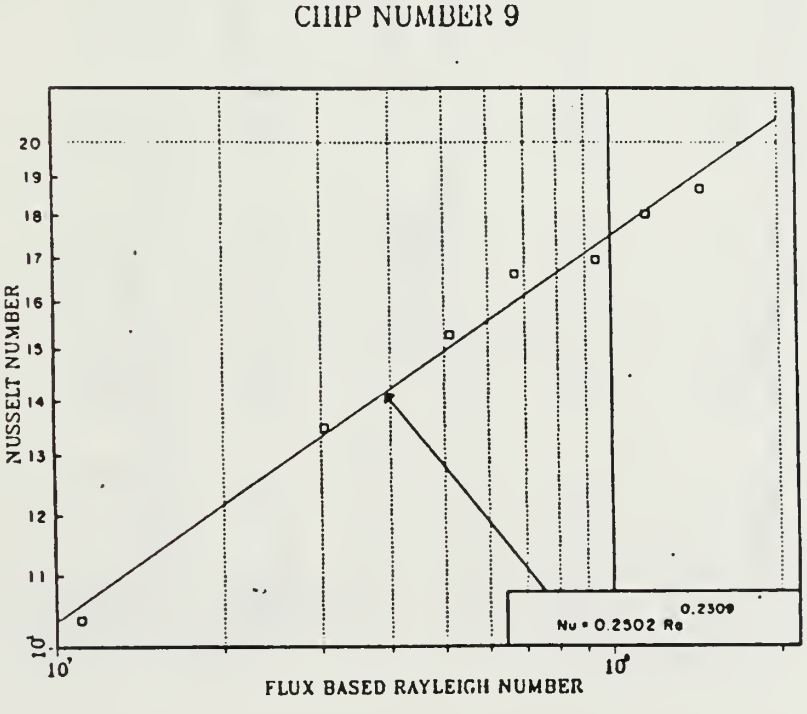

Figure 4.32 Flux Based Rayleigh Numbers, Chip 9

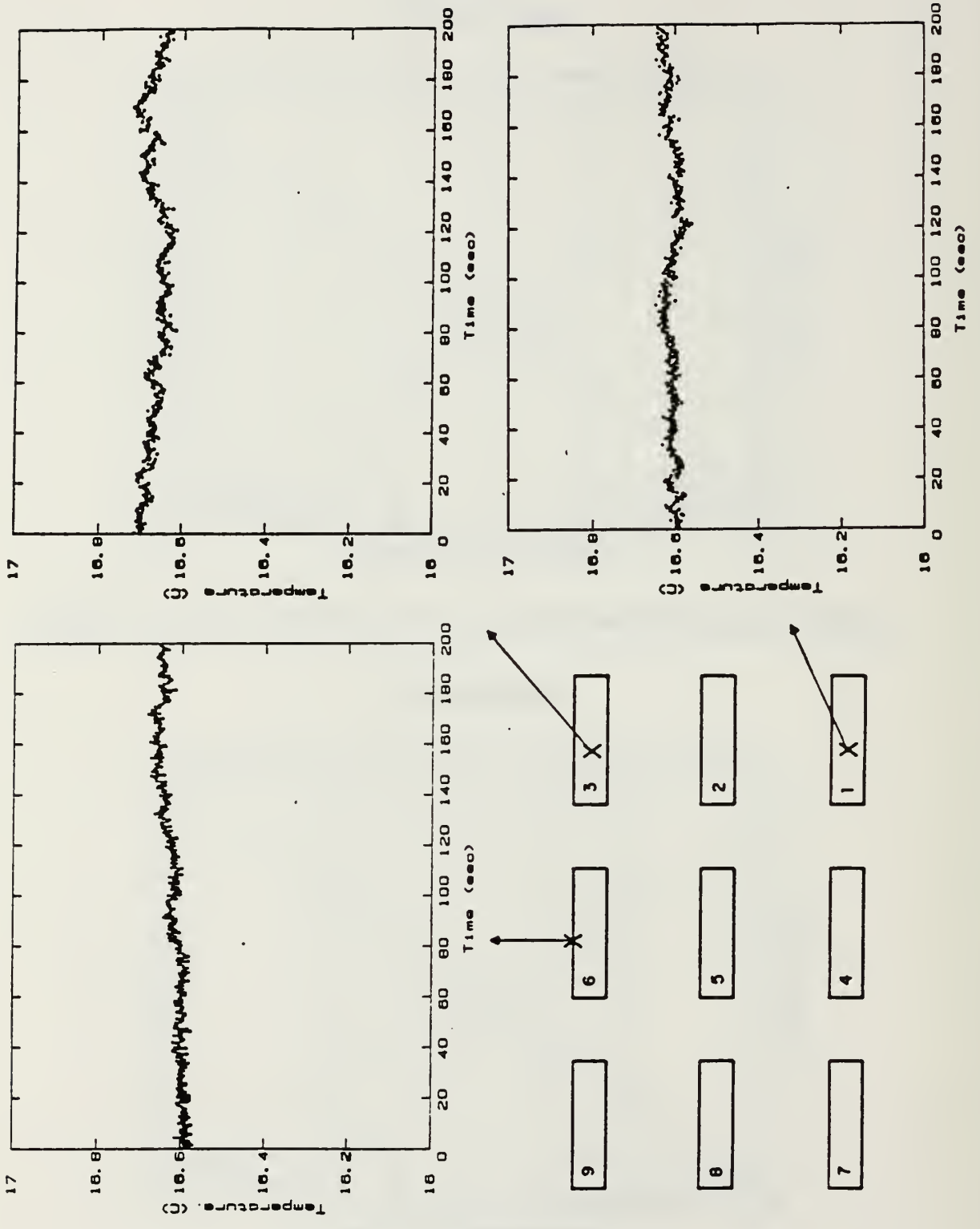

Figure 4.33 Temperature Variation for Input Power 0.3 W

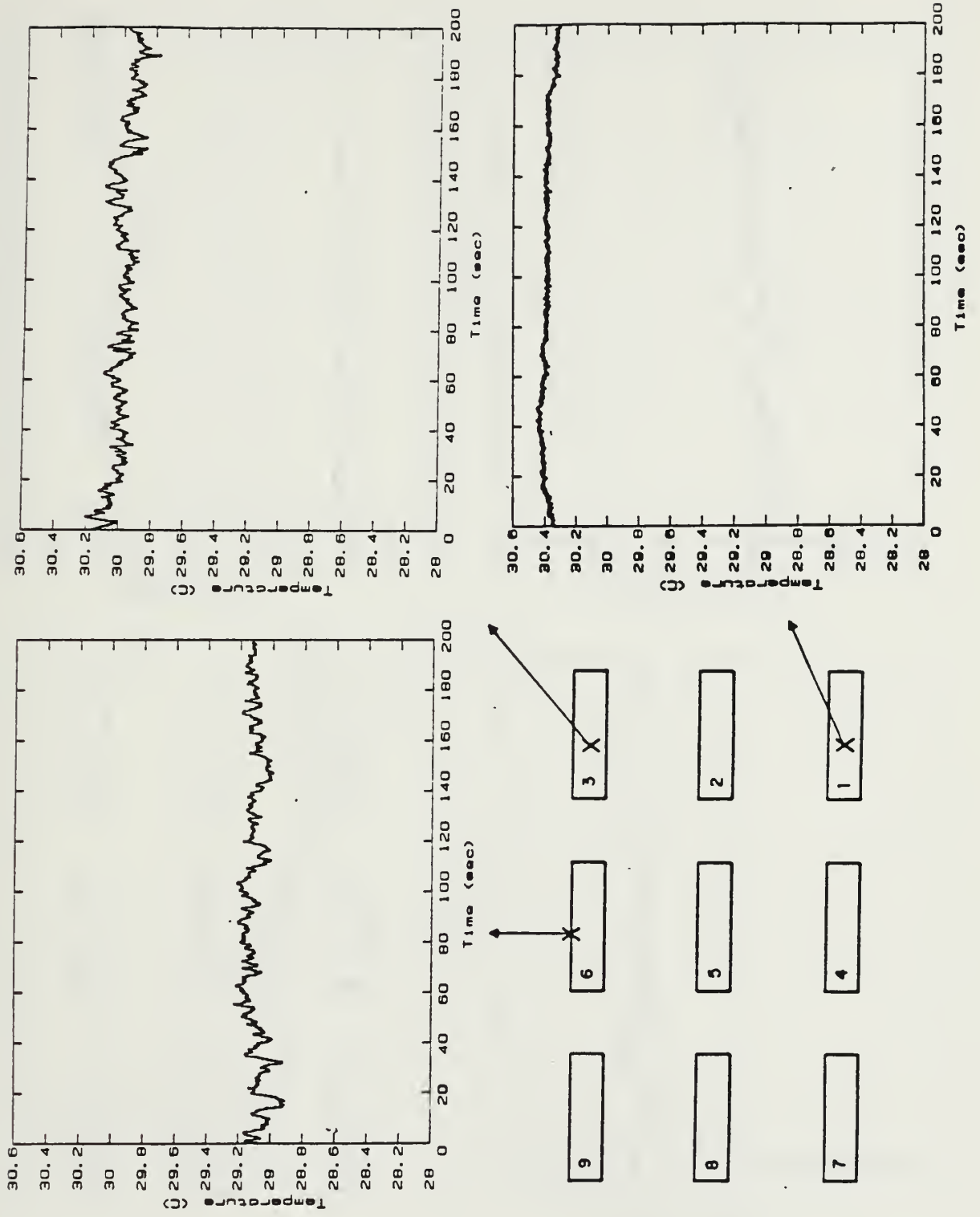

Figure 4.34 Temperature Variation for Input Power 0.7 W

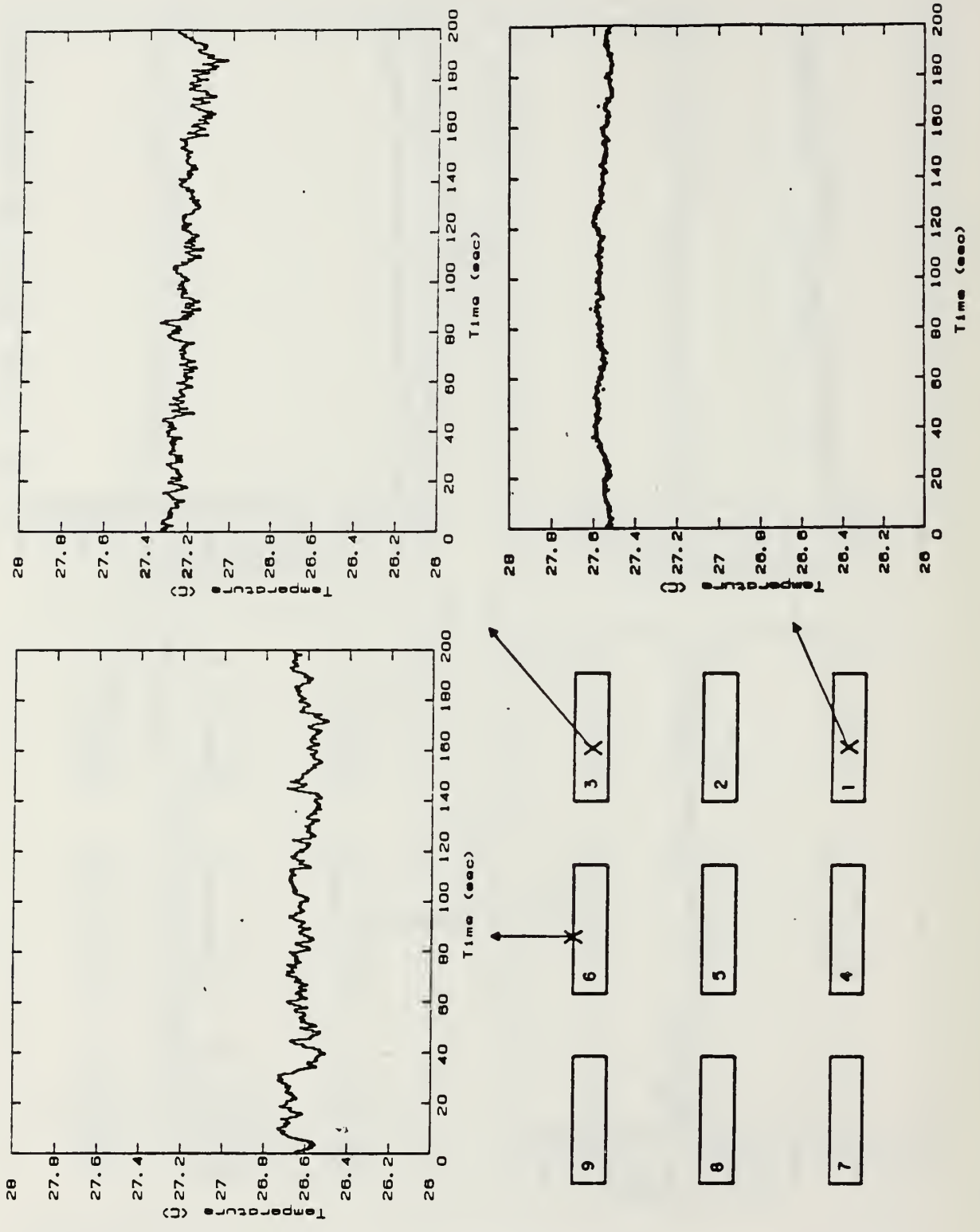

Figure 4.35 Temperature Variation for Input Power 1.1 W

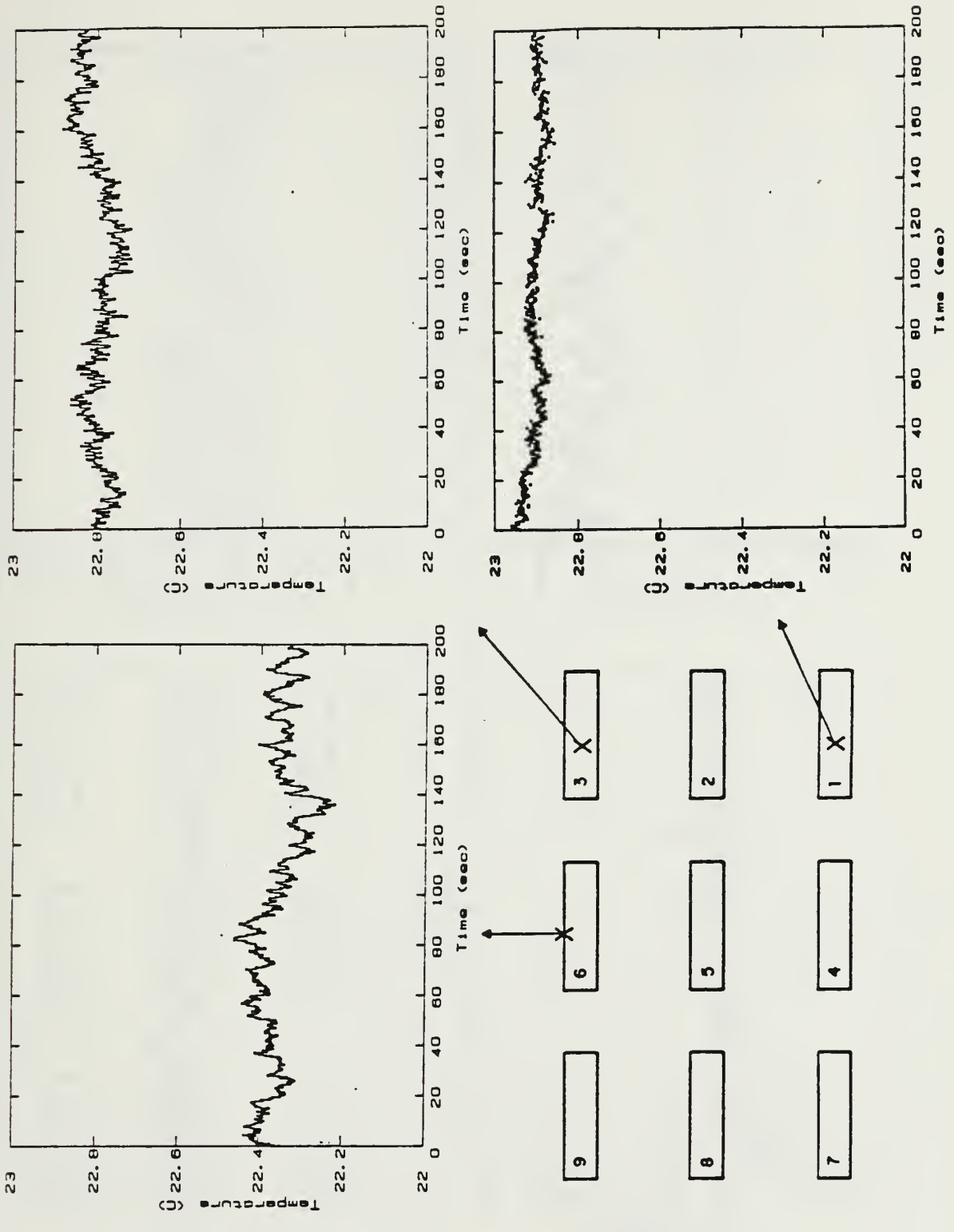

Figure 4.36 Temperature Variation for Input Power 1.5 W

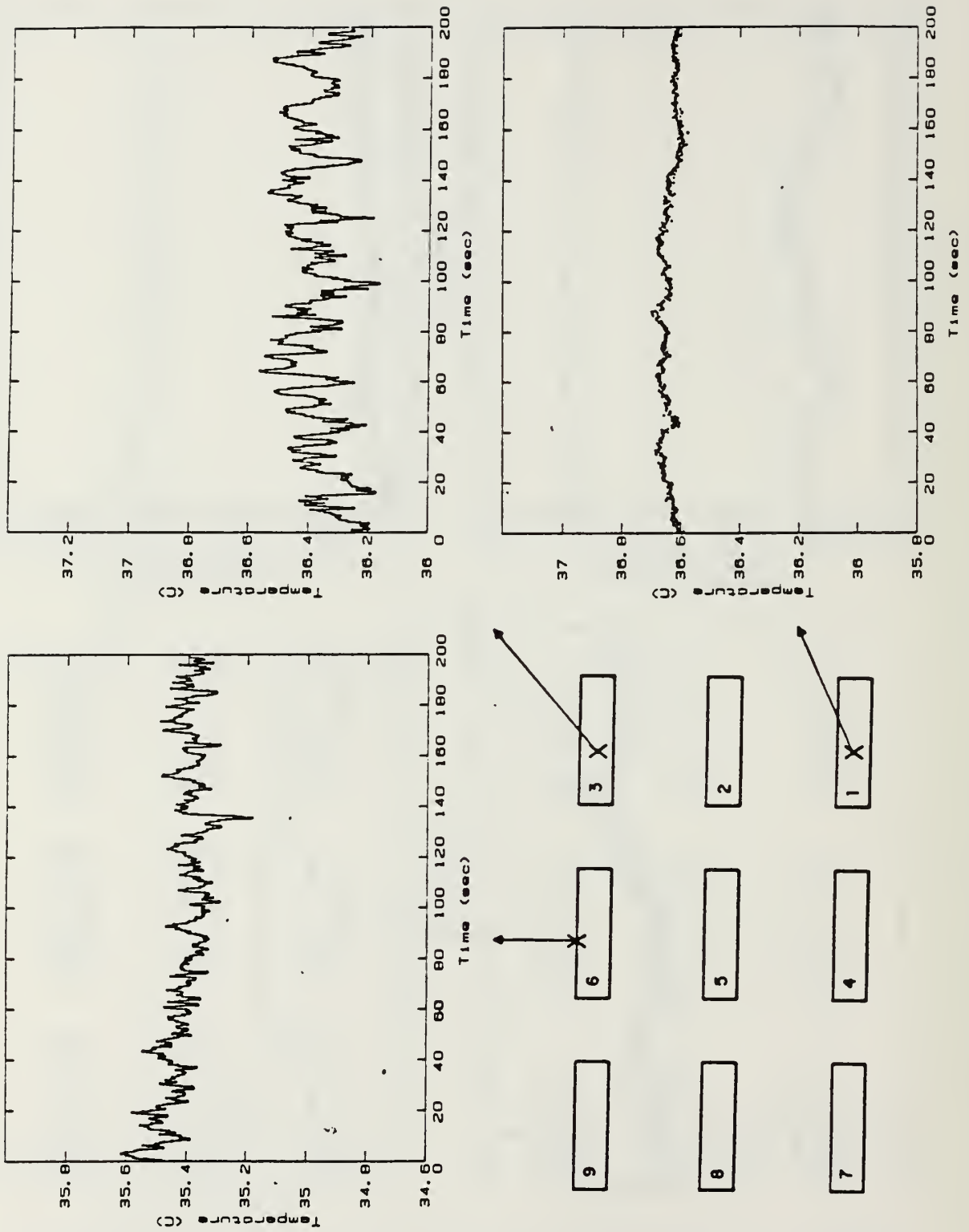

Figure 4.37 Temperature Variation for Input Power 1.9 W

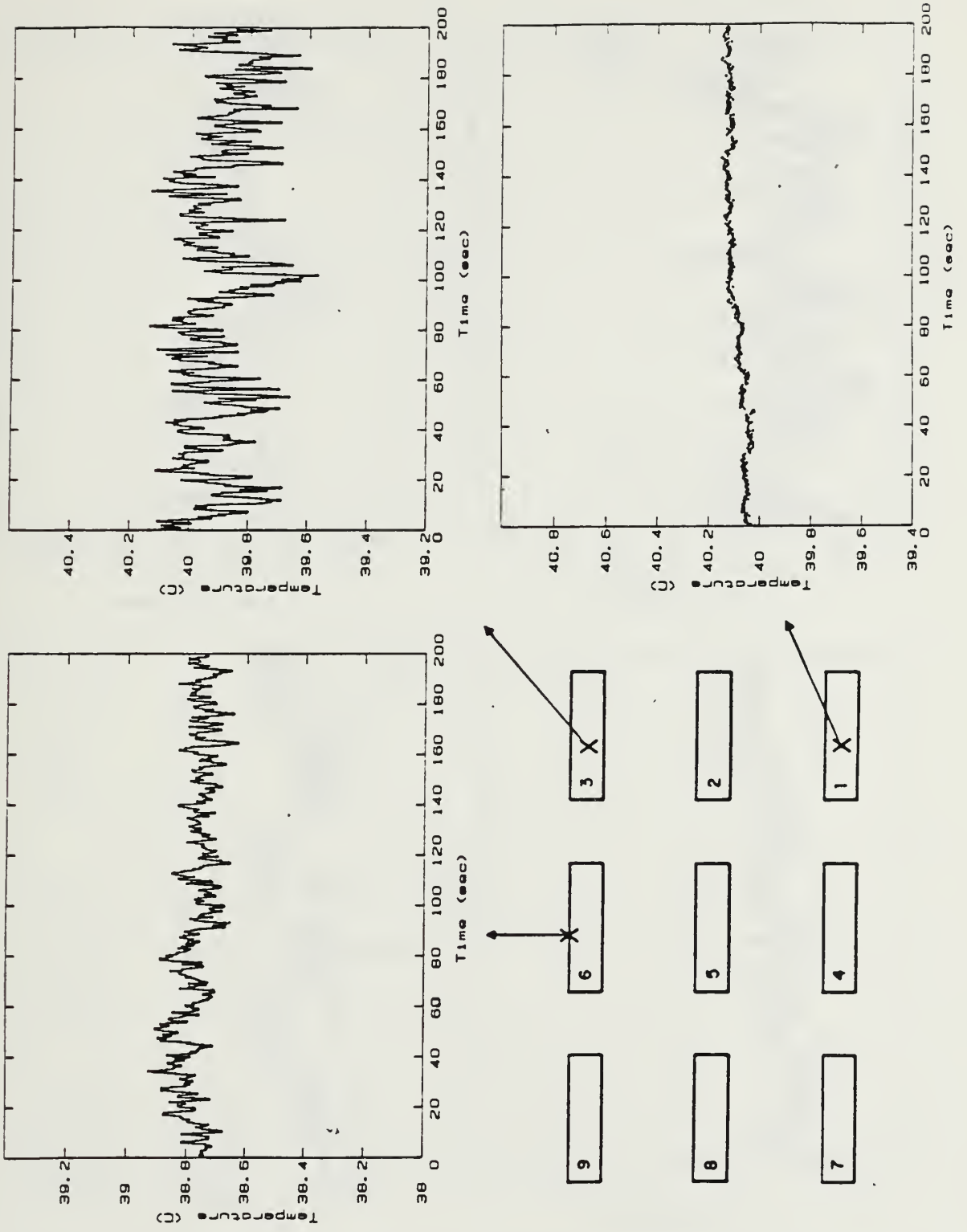

Figure 4.38 Temperature Variation for Input Power 2.3 W

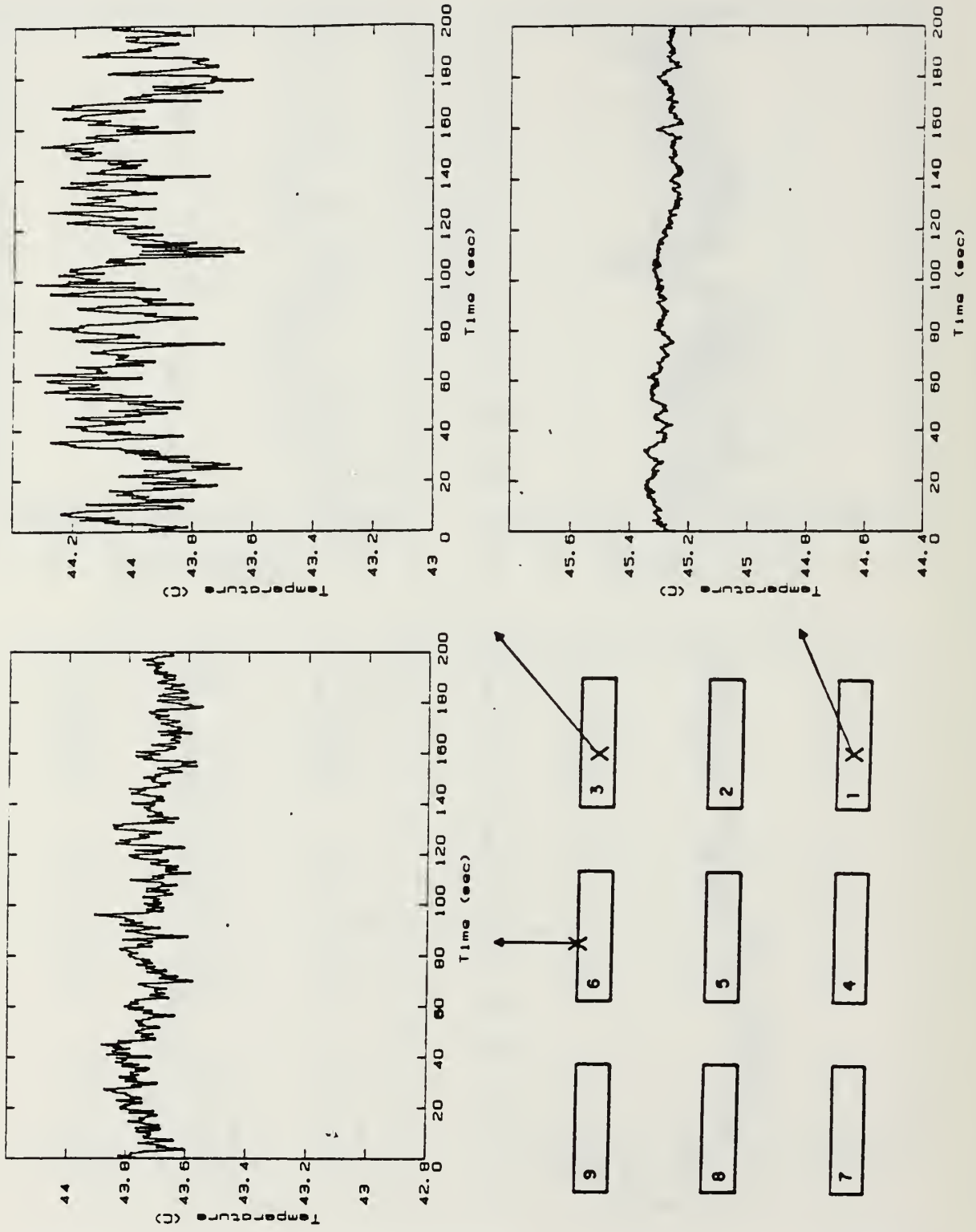

Figure 4.39 Temperature Variation for Input Power 2.7 W

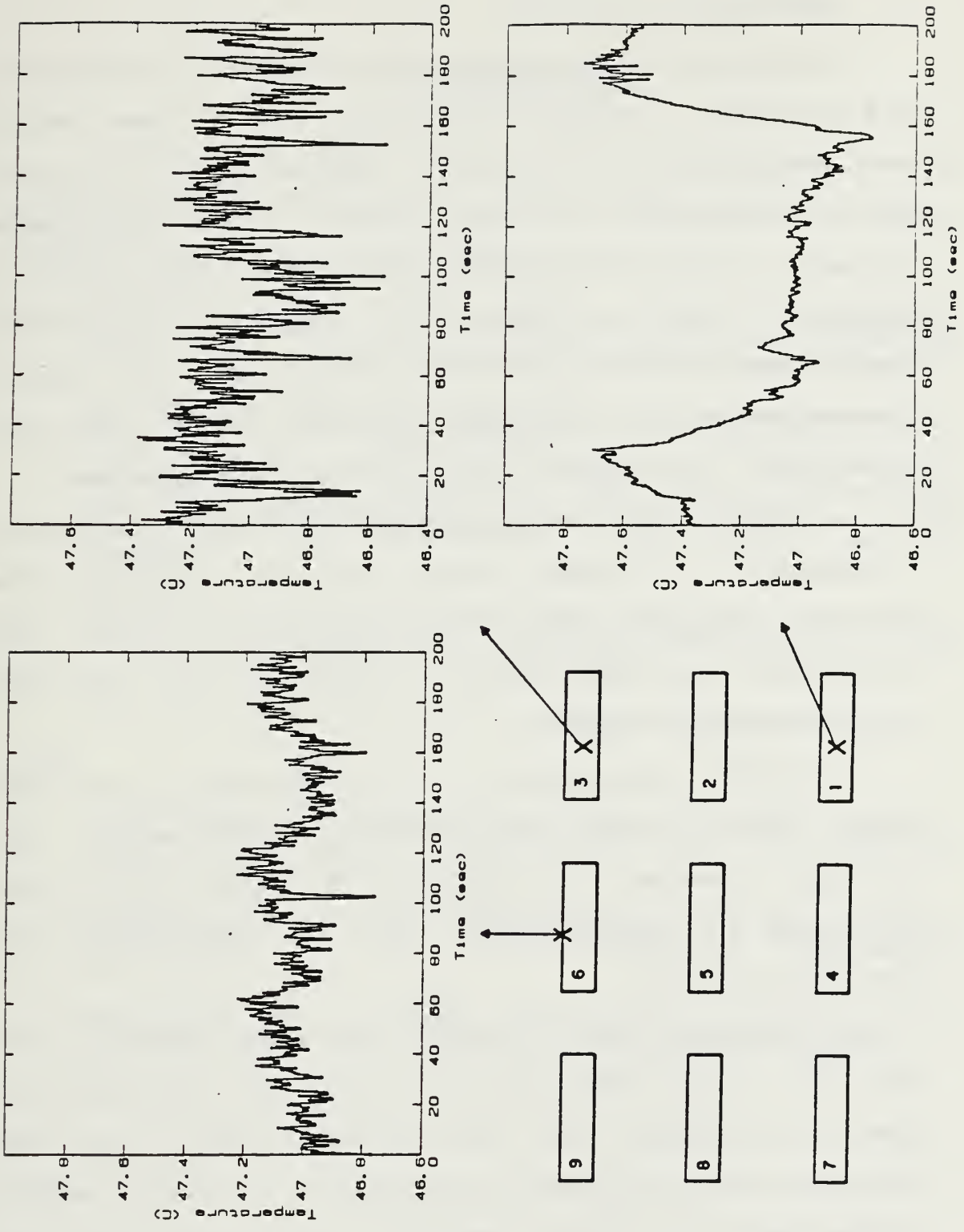

Figure 4.40 Temperature Variation for Input Power 3.1 W

C. TEMPERATURE VARIATIONS

The temperature variations with time were investigated and reported in Figures 4.33 through 4.40. These results were motivated by the studies conducted by Liu, Yang and Kelleher [Liu et al., 1987, pp. 486-97]. Three thermocouple channels, numbers 1, 13 and 32 were scanned individually at a rate of 3 times per second for a period of 200 seconds. These quantitative results were then plotted. The results clearly demonstrate a multiple frequency content signal for most of the power levels investigated in this experiment.

An observation of this experiment was that the output of thermocouple #1 remained steady with time throughout the increase in power levels. The temperature level for this thermocouple was also generally higher than for the other two thermocouples sampled.

A possible explanation for these results is that the cold, stagnant fluid layer created by the bottom heat exchanger prevented the penetration of warmer fluid below the bottom row of components. This is also supported by flow visualization.

One exception is at 3.1 watts. As seen in Figure 4.40, there is a large fluctuation of temperature with time. A possible explanation for this fluctuation may be that the increased energy acquired by the fluid at this power setting enabled the flow to force itself into the stagnant region at the bottom of the chamber.

V. RECOMMENDATIONS

There is a great deal more experimentation to be accomplished with this component configuration. Three possible variations to the chamber are :

- Placing a spacer in the chamber to reduce the chamber width. This would act in the same manner as a shrouding wall and would affect the heat transfer characteristics.

- Setting the bottom heat exchanger to a temperature other than $10^{o}C$. The energy expended to maintain the bottom heat exchanger at $10^{o}C$ is considerable. If reasonable components temperatures can be realized by maintaining the bottom heat exchanger at a higher temperature level then the energy consumption of the system would be reduced.

- Powering different configurations other than the entire array. This could possibly offer some explanation of the flow patterns observed in the chamber.

Other possible improvements to software and hardware are:

- Producing a plotting program that would read the data directly from the data acquisition unit for plots of Nusselt vs. Rayleigh number.

- Implementation of measurement devices that have greater sensitivity to minor fluctuations in temperature variation.

- Development of a program that will perform frequency analysis on the data recorded by the program Fastscan.

APPENDIX A

SAMPLE CALCULATIONS

Throughout this appendix, the sample calculations will be based on component number one with a power input of 0.71 watts.

1. Determination of Input Power

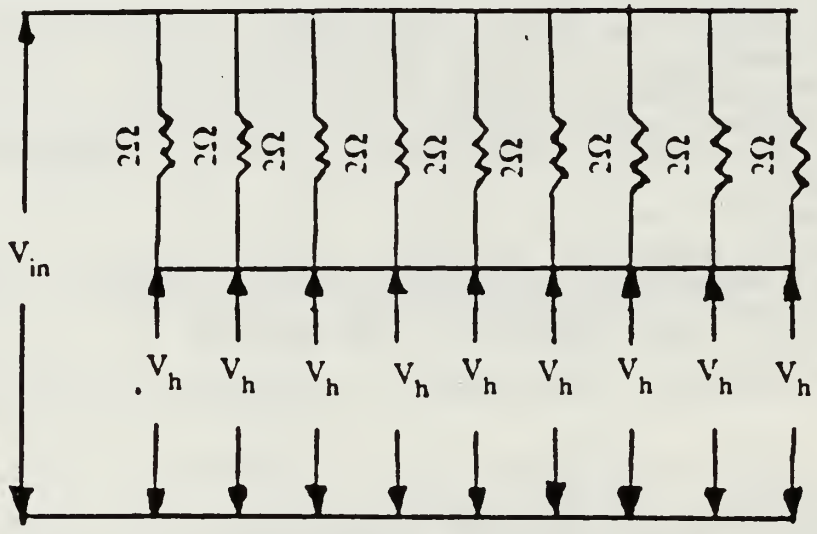

Figure A.1 Electrical Network of Power Input

From Equation (3.4):

$$Q_{in} = ((3.218 - 0.5278)(0.5278))/2$$

2. Estimation of Conduction Loss

Equation 3.3 requires T_s, T_b and R_{con}. T_s and T_b were read directly from thermocouples placed immediately behind the heaters and on the back of the board, respectively. R_{con} was calculated by using the constriction resistance formulas developed by Mikic and repeated in [Kraus and Bar-Cohen, 1983, pp. 76-9]. The conduction losses for components 3, 5 and 7 were then averaged to yield a total conduction loss.

3. Calculation of Nusselt and Rayleigh Numbers

The calculations of the convection coefficient from Equation (3.5) was:

$$Q_{net} = hA(T_{avg} - T_c)$$

$$h = \frac{Q_{net}}{A(T_{avg} - T_c)}$$

$$= \frac{.703}{(5.76 \times 10^{-4})(11.51)}$$

$$= 106.04 \text{ W/m}^2 \text{ }^{o}\text{K}$$

From Equation (3.10):

$$T_{film} = \frac{T_{avg} + T_c}{2}$$

$$= \frac{21.51 + 10}{2}$$

$$T_{film} = 15.75^{o}C$$

Using the relationships of [3-M Manual, 1985, pp. 9-60], the physical properties of FC-75 were:

$$k_f = (.65 - 7.8947 \times 10^{-4} * T_{film})(0.1)$$

$$= 0.0637 \ W/m^{o}C$$

$$\rho = 1000(1.825 - 0.00246 * T_{film})$$

$$= 1823.21 \ Kg/m^3$$

$$c_p = 4180(.241111 + 3.7037 \times 10^{-4} * T_{film})$$

$$= 1032.23 \ J/Kg^{o}C$$

$$\nu = 10^{-6}(1.4074 - 2.964 \times 10^{-2} * T_{film} + 3.8018 \times 10^{-4} * T_{film} - 2.7308 \times 10^{-6} * T_{film} + 8.1679 \times 10^{-9} * T_{film})$$

$$\nu = 1.024 \times 10^{-6} \ m^2/sec$$

$$\beta = \frac{.00246}{1.825 - .00246 * T_{film}}$$

$$\beta = 1.377 \times 10^{-3}$$

Then from Equation (3.1):

$$Nu = \frac{hL}{K_f}$$

$$= \frac{106.04(.008)}{.0637}$$

$$= 13.32$$

$$\alpha = \frac{K}{\rho c_p}$$

$$= \frac{.0637}{1823.2 * 1032.2}$$

$$= 3.38 \times 10^{-8} \text{ m}^2/\text{sec}$$

$$Pr = \frac{\nu}{\alpha}$$

$$= \frac{1.024 \times 10^{-6}}{3.38 \times 10^{-8}}$$

$$= 30.3$$

$$Gr_t = \frac{g\beta L^3 (T_{avg} - T_c)}{\nu^2}$$

$$= \frac{9.81(1.377 \times 10^{-3})(.008)^3(11.51)}{(1.024 \times 10^{-6})^2}$$

$$= 7.592 \times 10^4$$

From Equation (3.11), the temperature based Rayleigh number was:

$$Ra_t = Gr_t * Pr$$

$$= 2.3 \times 10^6$$

From Equation (3.12), the flux based Rayleigh number was:

$$Ra_f = 3.06 \times 10^7$$

APPENDIX B

UNCERTAINTY CALCULATIONS

Uncertainty calculations were evaluated using the root mean square formulation described in [Beckwith, Buck and Marangoni, 1982, pp. 261-292]. The following calculations are for components number one at 0.7 watts (see Table 4.10):

TABLE 16

UNCERTAINTIES IN VARIABLES

Variables	Uncertainties	Reference
L	10^{-5} m	Resolution
T	0.1 ^{o}C	Thermocouple readings
R_p	0.02	1% Variation
K_p	1.5 %	[Touloukian, 1986, p. 970]
V	0.001 V	Resolution

The uncertainty in the net power added to the fluid was:

$$\delta Q_{net} = (\delta Power^2 + \delta Q_{loss}{}^2)^{1/2}$$

where

$$\delta Power = 0.01 * Power$$

$$= .0071 \text{ W}$$

$$\delta Q_{loss} = 0.055 * Q_{loss}$$

$$= .000159 \text{ W}$$

Therefore,

$$\delta Q_{net} = .0071$$

The uncertainty for the other variables used were:

$$\delta T_{sink} = \delta T$$

$$= 0.1 \text{ K}$$

$$\delta T_{film} = (\delta T_{sink}^2 + \delta T_{avg}^2)^{1/2}$$

$$= (.01^2 + 0.1^2)^{1/2}$$

$$= .1414 \text{ K}$$

$$\delta T_{Delt} = (\delta T_{avg}^2 + \delta T_{sink}^2)^{1/2}$$

$$= (0.1^2 + .01^2)^{1/2}$$

$$= .1414 \text{ K}$$

$$\frac{\delta h}{h} = \left[\left(\frac{\delta Q_{net}}{Q_{net}}\right)^2 + \left(\frac{\delta T_{Delt}}{T_{Delt}}\right)^2\right]^{1/2}$$

$$= \left[\left(\frac{.0071}{.703}\right)^2 + \left(\frac{.1414}{11.51}\right)^2\right]^{1/2}$$

$$= .0159$$

$$\frac{\delta Nu}{Nu} = \frac{\delta h}{h}$$

$$= .0159$$

$$\frac{\delta Gr_t}{Gr_t} = \frac{\delta T_{Delt}}{T_{Delt}}$$

$$= \frac{.1414}{11.51}$$

$$= .0123$$

$$\frac{\delta Ra_t}{Ra_t} = \frac{\delta Gr_t}{Gr_t}$$

$$= .0123$$

$$\frac{\delta Ra_f}{Ra_f} = \frac{\delta Q_{net}}{Q_{net}}$$

$$= \frac{.0071}{.703}$$

$$= .0101$$

APPENDIX C

SOFTWARE

1. Acquire

```
10    ! FILE ACQUIRE
20    !
30    ! EDITED BY LT T J BENEDICT, USN
40    !
41    ! READ FILE "READ_ME"
42    !
50    COM /Co/ D(7)
60    DIM Emf(76),Power(9),T(76)
70    !
80    !CORRELATION FACTORS TO CONVERT EMF TO DEGREES CELCIUS
90    DATA 0.10086091,25727.9,-767345.8,78025596,
100   DATA -9247486589,6.98E11,-2.66E13,3.94E14
110   !
120   READ D(*)
130   Rp=2.000
140   PRINTER IS 701
150   BEEP
160   !
170   INPUT "ENTER THE INPUT MODE: 0-SYS, 1-FILE",Im
180   !
190   IF Im=1 THEN
200   BEEP
210   INPUT "ENTER THE NAME OF THE FILE TO BE READ",Oldfile$
211   !
220   PRINT USING "15X,""THESE RESULTS ARE STORED IN FILE :   "",10A";Oldfile$
230   !
240   ELSE
250   BEEP
260   INPUT "ENTER THE NAME OF THE NEW FILE",Newfile$
261   PRINT USING "10X,""THESE RESULTS ARE STORED IN FILE:  "",10A":Newfile$
270   END IF
280   PRINT
290   PRINT
291   !
300   INPUT "ENTER THE AMBIANT TEMP",Temp$
310   PRINT USING "15X,""AMBIENT TEMP WAS:   "",10A":Temp$
320   !
330   INPUT "FLOW VIZ? Y/N",Ans$
340   INPUT "VOLTMETER READING",V$
350   PRINT USING "15X,""VOLTMETER READING WAS:  "",10A";V$
360   !
370   INPUT "ENTER THE BATH TEMP",B$
380   PRINT USING "15X,""BATH TEMP WAS   :"",10A";B$
390   !
400   IF Ans$="Y" THEN PRINT USING "15X,""THIS RUN WAS RECORDED WITH FLOW VIZ"",
10A"
410   !
420   IF Im=1 THEN ASSIGN @File TO Oldfile$
430   PRINT
440   !
450   IF Im=0 THEN
460   CREATE BDAT Newfile$,5
470   ASSIGN @File TO Newfile$
480   END IF
490   !
500   ! READ DATA
510   !
520   IF Im=0 THEN
530   OUTPUT 709;"AR AF00 AL79"
```

```
540   OUTPUT 722:"F1 R1 T1 Z0 FLO"
550   !
560   FOR I=0 TO 76
570   OUTPUT 709:"AS"
580   WAIT 1
590   ENTER 722;Emf(I)
600   BEEP
610   NEXT I
620   !
630   OUTPUT @File;Emf(*)
640   !
650   ELSE
660   ENTER @File;Emf(*)
670   END IF
680   !
690   OUTPUT 709;"TD"
700   !
710   FOR I=0 TO 60
720   Sum=0
730   FOR J=1 TO 7
740   Sum=Sum+D(J)*Emf(I)^J
750   NEXT J
760   T(I)=Sum
770   NEXT I
780   !
790   FOR I=71 TO 76
800   Sum=0
810   FOR J=1 TO 7
820   Sum=Sum+D(J)*Emf(I)^J
830   NEXT J
840   T(I)=Sum
850   NEXT I
860   !
870   ! POWER CALCULATIONS
880   !
890   J=1
900   Volt=Emf(61)
910   !
920   FOR I=62 TO 70
930   Power(J)=Emf(I)*(Volt-Emf(I))/Rp
940   J=J+1
950   NEXT I
960   !
970   BEEP
980   BEEP
990   PRINT USING "14X,""ALL TEMPERATURES ARE IN DEGREES CELCIUS"""
1000  !
1010  PRINT
1020  !
1030  PRINT USING "12X,""CENTER     TOP          RIGHT      LEFT      BOTTOM
   BACK"""
1040  PRINT
1050  PRINT USING "1X,""CHIP NO1: "",5(ZZ.DDE,2X),2X,ZZ.DDE";T(0),T(1),T(2),T(
,T(4),T(5)
1060  PRINT USING "5X,""POWER (WATTS):  "",ZZ.DDE";Power(1)
1061  PRINT
1070  PRINT USING "1X,""CHIP NO2: "",5(ZZ.DDE,2X),2X,ZZ.DDE";T(6),T(7),T(8),T(
,T(10),T(11)
1080  PRINT USING "5X,""POWER (WATTS):  "",ZZ.DDE";Power(2)
1081  PRINT
```

```
1090  PRINT USING "1X,""CHIP NO3: "",5(ZZ.DDE,2X),2X,ZZ.DDE";T(12),T(13),T(14)
(15),T(16),T(17)
1100  PRINT USING "5X,""POWER (WATTS):  "",ZZ.DDE";Power(3)
1101  PRINT
1110  PRINT USING "1X,""CHIP NO4: "",5(ZZ.DDE,2X),2X,ZZ.DDE";T(18),T(19),T(20)
(21),T(22),T(23)
1120  PRINT USING "5X,""POWER (WATTS):  "",ZZ.DDE";Power(4)
1121  PRINT
1130  PRINT USING "1X,""CHIP NO5: "",5(ZZ.DDE,2X),2X,ZZ.DDE";T(24),T(25),T(26)
(27),T(28),T(29)
1140  PRINT USING "5X,""POWER (WATTS):  "",ZZ.DDE";Power(5)
1141  PRINT
1150  PRINT USING "1X,""CHIP NO6: "",5(ZZ.DDE,2X),2X,ZZ.DDE";T(30),T(31),T(32)
(33),T(34),T(35)
1160  PRINT USING "5X,""POWER (WATTS):  "",ZZ.DDE";Power(6)
1161  PRINT
1170  PRINT USING "1X,""CHIP NO7: "",5(ZZ.DDE,2X),2X,ZZ.DDE";T(36),T(37),T(38)
(39),T(40),T(41)
1180  PRINT USING "5X,""POWER (WATTS):  "",ZZ.DDE";Power(7)
1181  PRINT
1190  PRINT USING "1X,""CHIP NO8: "",5(ZZ.DDE,2X),2X,ZZ.DDE";T(42),T(43),T(44)
(45),T(46),T(47)
1200  PRINT USING "5X,""POWER (WATTS):  "",ZZ.DDE";Power(8)
1201  PRINT
1210  PRINT USING "1X,""CHIP NO9: "",5(ZZ.DDE,2X),2X,ZZ.DDE";T(48),T(49),T(50)
(51),T(52),T(53)
1220  PRINT USING "5X,""POWER (WATTS):  "",ZZ.DDE";Power(9)
1230  !
1240  PRINT
1250  PRINT
1260  !
1270  PRINT USING "5X,""HEAT EXCHANGERS TEMPERATURES:     RIGHT      LEFT"""
1280  PRINT USING "10X,""BOTTOM:"",21X,2(ZZ.DDE,2X)";T(58),T(57)
1290  PRINT USING "10X,""TOP:"",24X,2(ZZ.DDE,2X)";T(60),T(59)
1300  PRINT
1310  PRINT
1320  !
1330  PRINT USING "5X,""BACK PLANE TEMPERATURES ARE :"""
1340  PRINT
1350  PRINT USING "10X,""T(55):"",2X,(ZZ.DDE,2X)";T(54)
1360  PRINT USING "10X,""T(56):"",2X,(ZZ.DDE,2X)";T(55)
1370  PRINT USING "10X,""T(57):"",2X,(ZZ.DDE,2X)";T(56)
1380  PRINT USING "10X,""T(72):"",2X,(ZZ.DDE,2X)";T(71)
1390  PRINT USING "10X,""T(73):"",2X,(ZZ.DDE,2X)";T(72)
1400  PRINT USING "10X,""T(74):"",2X,(ZZ.DDE,2X)";T(73)
1410  PRINT USING "10X,""T(75):"",2X,(ZZ.DDE,2X)";T(74)
1420  PRINT USING "10X,""T(76):"",2X,(ZZ.DDE,2X)";T(75)
1430  PRINT USING "10X,""T(77):"",2X,(ZZ.DDE,2X)";T(76)
1440  BEEP
1450  PRINTER IS 1
1460  !
1470  ASSIGN @File TO *
1480  END
```

2. CalcDiel

```
10    ! FILE NAME : CalcDiel
20    !
30    ! EDITED BY : Lt. T BENEDICT, USN
40    !
50    ! THIS PROGRAM ANALYSES THE DATA READ FROM
60    ! A DATA FILE DESINATED BY THE OPERATOR. IT
70    ! REDUCES THE DATA TO CALCUALTIONS OF NET
80    ! POWER, RAYLEIGH NUMBER AND NUSELT NUMBER.
90    !
100   COM /Co/ D(7)
110   !
120   DIM Emf(70),Power(9),T(60),Tavg(9),Ts(9)
130   DIM Tfilm(9),Qnet(9),H(9),K(9),Rho(9),Cp(9)
140   DIM N(9),Nu(9),Ra(9),Delt(9),Alfa(9),Pr(9)
150   DIM Gr(9),Beta(9),Dpow(9),Dts(9)
160   !
170   ! CORRLEATION FACTORS TO CONVERT Emf TO REGREES CELCIUS.
180   DATA 0.10086091,25727.9,-767345.8,78025596,
190   DATA -9247486589,6.98E11,-2.66E13,3.94E14
200   !
210   READ D(*)
220   !
230   ! RESISTANCE OF THE PRECISION RESISTOR IS: 1%
240   Rp=2.00
250   !
260   PRINTER IS 701
270   BEEP
280   BEEP
290   !
300   INPUT "ENTER THE NAME OF THE FILE CONTAINING DATA",Oldfile$
310   PRINT USING "15X,""THE RAW Emf DATA ARE FROM THE FILE:    "",10A";Oldfile$
320   INPUT "ENTER THE POWER SETTING ",Power$
340   PRINT USING "17X,"" THE POWER SETTING PER CHIP WAS:   "",10A";Power$
350   PRINT
370   !
380   BEEP
390   BEEP
400   ASSIGN @File TO Oldfile$
410   ENTER @File;Emf(*)
420   !
430   ! CONVERT Emf TO DEGREES CELCIUS
440   FOR I=0 TO 60
450   Sum=0
460   FOR J=0 TO 7
470   Sum=Sum+D(J)*Emf(I)^J
480   NEXT J
490   T(I)=Sum
500   NEXT I
510   !
520   ! CONVERT Emf TO POWER
530   J=1
540   Volt=Emf(61)
550   FOR I=62 TO 70
560   Power(J)=Emf(I)*(Volt-Emf(I))/Rp
570   Dpow(J)=.01*Power(J)
580   J=J+1
590   NEXT I
600   !
610   ! AREA OF THE BLOCK FACES
620   Acen=1.92E-4
```

```
630   Alef=1.44E-4
640   Arig=1.44E-4
650   Atop=4.8E-5
660   Abot=4.8E-5
670   Atot=5.76E-4
680   !
690   !CALCULATE THE AVERAGE TEMPERATURES OF THE BLOCK FACES
700   !
710   Tavg(1)=(T(0)*Acen+T(1)*Atop+T(2)*Arig+T(3)*Alef+T(4)*Abot)/Atot
720   Tavg(2)=(T(6)*Acen+T(7)*Atop+T(8)*Arig+T(9)*Alef+T(10)*Abot)/Atot
730   Tavg(3)=(T(12)*Acen+T(13)*Atop+T(14)*Arig+T(15)*Alef+T(16)*Abot)/Atot
740   Tavg(4)=(T(18)*Acen+T(19)*Atop+T(20)*Arig+T(21)*Alef+T(22)*Abot)/Atot
750   Tavg(5)=(T(24)*Acen+T(25)*Atop+T(26)*Arig+T(27)*Alef+T(28)*Abot)/Atot
760   Tavg(6)=(T(30)*Acen+T(31)*Atop+T(32)*Arig+T(33)*Alef+T(34)*Abot)/Atot
770   Tavg(7)=(T(36)*Acen+T(37)*Atop+T(38)*Arig+T(39)*Alef+T(40)*Abot)/Atot
780   Tavg(8)=(T(42)*Acen+T(43)*Atop+T(44)*Arig+T(45)*Alef+T(46)*Abot)/Atot
790   Tavg(9)=(T(48)*Acen+T(49)*Atop+T(50)*Arig+T(51)*Alef+T(52)*Abot)/Atot
800   !
810   ! UNCERTAINTY OF THE THERMOCOUPLE READINGS
820   Dt=.1
830   Dtavg=.1
840   !
850   ! RESISTANCE OF PLEXIGLASS AND UNCERTAINTY
860   Rc=764.65
880   !
890   ! CHIP BACK SURFACE TEMPERATURES
900   Ts(1)=T(5)
910   Ts(2)=T(11)
920   Ts(3)=T(17)
930   Ts(4)=T(23)
940   Ts(5)=T(29)
950   Ts(6)=T(35)
960   Ts(7)=T(41)
970   Ts(8)=T(47)
980   Ts(9)=T(53)
990   Tssum=0
1000  FOR J=1 TO 9
1010  Tssum=Tssum+Ts(J)
1020  NEXT J
1030  !
1040  Tsavg=Tssum/9
1050  !
1060  ! CONDUCTION LOSS CALCULATION AND UNCERTAINTY
1070  Qloss3=(T(17)-T(56))/Rc
1080  Qloss5=(T(29)-T(55))/Rc
1090  Qloss7=(T(41)-T(54))/Rc
1100  Qloss=(Qloss3+Qloss5+Qloss7)/3
1110  Dqloss=(Qloss)*.022
1120  !
1130  ! AVERAGE SINK TEMPERATURE CALCULATION
1140  Tsink=(T(57)+T(58)+T(59)+T(60))/4
1150  Dtsink=(Dt/T(58))
1160  L=8.0E-3
1170  !
1180 PRINT USING "1X,""CHIP      QNET(W)          Tavg-Ts            Nu
%UNC IN Nu "",10A"
1190 PRINT
1200  !
1210  !
1220  ! CALCULATION OF NET POWER, Nu, Ra, AND UNCERTAINTIES
```

```
1230  !
1240  FOR J=1 TO 9
1241  PRINTER IS 1
1242  PRINT "J"
1244  PRINT J
1245  PRINTER IS 701
1250  !
1260  ! CALULATION OF Qnet
1270  Qnet(J)=Power(J)-Qloss
1280  Dqnet=(Dpow(J)^2+Dqloss^2)^.5
1290  !
1300  ! CALCULATION OF Tfilm
1310  Tfilm(J)=(Tavg(J)+Tsink)/2
1320  Dtfilm=(Dtsink^2+Dtavg^2)^.5
1330  !
1340  ! CALCULATION OF A DELTA TEMPERATURE
1350  Delt(J)=Tavg(J)-Tsink
1360  Ddelt=(Dtavg^2+Dtsink^2)^.5
1370  !
1380  ! CALCULATION OF CONVECTION COEFFICIENT
1390  H(J)=Qnet(J)/(Atot*Delt(J))
1400  Dh=H(J)*((Dqnet/Qnet(J))^2+(Ddelt/Delt(J))^2)^.5
1410  !
1420  ! CALCULATION OF CONDUCTION COEFFICIENT
1430  K(J)=(.65-7.89474E-4*Tfilm(J))/10
1440  !
1450  ! CALCULATION OF DENSITY
1460  Rho(J)=(1.825-.00246*Tfilm(J))*1000
1470  !
1480  ! CALCULATION OF SPECIFIC HEAT
1490  Cp(J)=(.241111+3.7037E-4*Tfilm(J))*4180
1500  !
1510  ! CALCULATION OF VISCOSITY
1520  N(J)=1.4074-2.964E-2*Tfilm(J)+3.8018E-4*Tfilm(J)^2-2.7308E-6*Tfilm(J)^3+8.
1679E-9*Tfilm(J)^4
1530  N(J)=N(J)*1.E-6
1540  !
1550  ! CALCULATION OF BETA
1560  Beta(J)=.00246/(1.825-.00246*Tfilm(J))
1570  !
1580  ! CALCULATION OF ALPHA
1590  Alfa(J)=K(J)/(Rho(J)*Cp(J))
1600  !
1610  ! CALCULATION OF PRANDTL NUMBER AND UNCERTAINTY
1620  Pr(J)=N(J)/Alfa(J)
1630  !
1640  ! CALCULATION OF NUSSELT NUMBER
1650  Nu(J)=H(J)*L/K(J)
1660  Dnu=Nu(J)*(Dh/H(J))
1670  !
1680  ! CALCULATION OF PERCENT UNCERTAINTY IN NUSSELT NUMBER
1690  Pernu=(Dnu/Nu(J))*100
1700  !
1710  ! CALCULATION OF GRASHOF NUMBER AND UNCERTAINTY
1720  Gr(J)=9.81*Beta(J)*(L^3)*Delt(J)/N(J)^2
1730  Dgr=Gr(J)*(Ddelt/Delt(J))
1740  !
1750  ! CALCULATION OF RAYLEIGH NUMBER AND UNCERTAINTY
1760  Ra(J)=Gr(J)*Pr(J)*1.E-6
1770  Dra=Ra(J)*(Dgr/Gr(J))
1780  !
```

```
1794  ! CALCULATION OF FLUX BASED RAYLEIGH NUMBER
1800  !
1810  Raf(J)=((9.81*Beta(J)*L^4*Qnet(J))/(K(J)*N(J)*Alfa(J)*Atot))*1.E-7
1820  Draf=Raf(J)*(Dqnet/Qnet(J))
1830  !
1840  ! PERCENT UNCERTAINTY IN RAYLEIGH NUMBERS
1850  Perra=(Dra/Ra(J))*100
1860  Perraf=(Draf/Raf(J))*100
1870  !
1880  PRINT USING "1X,D,1X,4(7X,ZZ.DDE,)";J,Qnet(J),Delt(J),Nu(J),Pernu
1890  !
1910  PRINT USING "6X,""TEMPERATURE BASED RAYLEIGH NUMBER * E-6 IS:  "",3D.DDE";
Ra(J)
1920  PRINT USING "6X,""% UNCERTAINTY IN THE TEMPERATURE BASED RAYLEIGH NUMBER I
S :"",DDD.DDE":Perra
1930  PRINT USING "6X,""FLUX BASED RAYLEIGH NUMBER * E-7 IS:  "",3D.DDE";Raf(J)
1940  PRINT USING "6X,""% UNCERTAINTY IN FLUX BASED RAYLEIGH NUMBER IS:  "",DDD.
DDE";Perraf
1950  PRINT
1960  NEXT J
1970  ASSIGN @File TO *
1980  END
```

3. FastScan

```
10    ! PROGRAM FASTSCAN
11    !
20    ! EDITED BY LT. T J BENEDICT
30    !
40    ! THIS PROGRAM SCANS 3 CHANNELS FOR VOLTAGE MEASUREMENTS
60    Ipass=599
70    Pass=0
71    N=0
80    DIM T1(599),V1(2),Y1(599)
81    DIM T2(599),V2(2),Y2(599)
82    DIM T3(599),V3(2),Y3(599)
90    CLEAR 709
100   CLEAR 722
101   !
102   BEEP
103   PRINTER IS 701
105   BEEP
106   INPUT "ENTER THE FIRST FILE NAME:  ",Newfile1$
107   INPUT "ENTER THE SECOND FILE NAME: ",Newfile2$
108   INPUT "ENTER THE THIRD FILE NAME: ",Newfile3$
109   INPUT "ENTER THE VOLTMETER READING: ",V$
113   PRINT USING "15X,""THESE RESULTS ARE NOW STORED ON DISK 'FASTSCAN' "",10A"
114   PRINT
116   PRINT USING "25X,""FILE: "",10A";Newfile1$
117   PRINT
118   PRINT USING "25X,""FILE: "",10A";Newfile2$
119   PRINT
120   PRINT USING "25X,""FILE: "",10A";Newfile3$
121   PRINT
123   WAIT 1
124   BEEP
125   OUTPUT 709;"AE1"
130   WAIT 2
131   BEEP
140   OUTPUT 722;"T4 F1 R1 P0 Z0 1STI S01 1STN"
141   !
142   ! LOOP NUMBER ONE
143   !
150   OUTPUT 709;"AF0 AL0"
160   OUTPUT 709;"AS"
170   BEEP
175   Timedate1=TIMEDATE
180   FOR Jj=0 TO Ipass
200   OUTPUT 722;"T3"
210   ENTER 722;V1(*)
230   T1(Pass)=V1(1)
250   Pass=Pass+1
251   N=N+1
260   NEXT Jj
261   Timedate2=TIMEDATE
262   Totaltime1=Timedate2-Timedate1
263   OUTPUT 722;"AC0"
264   Pass=0
266   !
267   ! LOOP NUMBER TWO
268   !
269   OUTPUT 709;"AF12 AL12"
270   OUTPUT 709;"AS"
271   BEEP
```

```
272   BEEP
274   FOR Jj=0 TO Ipass
275   OUTPUT 722;"T3"
276   ENTER 722;V2(*)
277   T2(Pass)=V2(1)
278   Pass=Pass+1
279   NEXT Jj
280   OUTPUT 722;"AC12"
281   Pass=0
282   !
283   ! LOOP NUMBER THREE
284   !
285   OUTPUT 709;"AF31 AL31"
286   OUTPUT 709;"AS"
287   BEEP
288   BEEP
289   BEEP
291   FOR Jj=0 TO Ipass
292   OUTPUT 722;"T3"
293   ENTER 722;V3(*)
294   T3(Pass)=V3(1)
295   Pass=Pass+1
296   NEXT Jj
297   !
298   ! END LOOPS
299   !
300   PRINT USING "15X,""THE TOTAL TIME ELAPSED WAS (SECONDS):"",2X,(DDD.DDE)";
otaltime1
301   PRINT
302   PRINT USING "15X,""THE TOTAL NUMBER OF SCANS WAS :  "",2X,(DDDD.D,2X)";N
303   PRINT
304   PRINT USING "15X,""THE VOLTMETER READING WAS:  "",10A,";V$
306   PRINTER IS 1
307   BEEP
308   !
309   ! TRANSFER FIRST SCAN DATA
310   !
311   CREATE BDAT Newfile1$,20
312   ASSIGN @File TO Newfile1$
313   OUTPUT @File;T1(*)
314   FOR Ii=0 TO Ipass
320   T1(Ii)=.10086091+25727.9*T1(Ii)-767345.8*T1(Ii)^2+78002556*T1(Ii)^3
340   NEXT Ii
341   !
342   ! TRANSFER SECOND SCAN DATA
343   !
344   CREATE BDAT Newfile2$,20
345   ASSIGN @File TO Newfile2$
346   OUTPUT @File;T2(*)
347   FOR Ii=0 TO Ipass
348   T2(Ii)=.10086091+25727.9*T2(Ii)-767345.8*T2(Ii)^2+78002556*T2(Ii)^3
349   NEXT Ii
350   !
351   ! TRANSFER THIRD SCAN DATA
352   !
353   CREATE BDAT Newfile3$,20
354   ASSIGN @File TO Newfile3$
355   OUTPUT @File;T3(*)
356   FOR Ii=0 TO Ipass
357   T3(Ii)=.10086091+25727.9*T3(Ii)-767345.8*T3(Ii)^2+78002556*T3(Ii)^3
358   NEXT Ii
390   STOP
400   END
```

4. Plot

```
10   !  FILE NAME: PLOT
20   !
30   ! EDITED BY Lt T J BENEDICT
40   !
50   ! THIS PROGRAM PLOTS THE DATA ACQUIRED BY
60   ! PROGRAM "FASTSCAN".
70   !
80    PRINTER IS 705
90    BEEP
100   Xmin=0
110   Xmax=200
120   BEEP
130   INPUT "ENTER MINIMUM AND MAXIMUM Y-VALUES",Ymin,Ymax
140   BEEP
150   Xstep=20
160   BEEP
170   Ystep=.2
180   BEEP
190   PRINT "IN:SP1;IP 2000,2000,8000,7000;"
200   PRINT "SC 0,100,0,100;TL 2,0;"
210   Sfx=100/(Xmax-Xmin)
220   Sfy=100/(Ymax-Ymin)
230   PRINT "PU 0,0 PD"
240   FOR Xa=Xmin TO Xmax STEP Xstep
250   X=(Xa-Xmin)*Sfx
260   PRINT "PA";X,",0; XT;"
270   NEXT Xa
280   PRINT "PA 100,0;PU;"
290   PRINT "PU PA 0,0 PD"
300   FOR Ya=Ymin TO Ymax STEP Ystep
310   Y=(Ya-Ymin)*Sfy
320   PRINT "PA 0,";Y,"YT"
330   NEXT Ya
340   PRINT "PA 0,100 TL 0 2"
350   FOR Xa=Xmin TO Xmax STEP Xstep
360   X=(Xa-Xmin)*Sfx
370   PRINT "PA";X,",100; XT"
380   NEXT Xa
390   PRINT "PA 100,100 PU PA 100,0 PD"
400   FOR Ya=Ymin TO Ymax STEP Ystep
410   Y=(Ya-Ymin)*Sfy
420   PRINT "PD PA 100,",Y,"YT"
430   NEXT Ya
440   PRINT "PA 100,100 PU"
450   PRINT "PA 0,-2 SR 1.5,2"
460   FOR Xa=Xmin TO Xmax STEP Xstep
470   X=(Xa-Xmin)*Sfx
480   PRINT "PA";X,",0;"
490   PRINT "CP -2,-1;LB";Xa;""
500   NEXT Xa
510   PRINT "PU PA 0,0"
520   FOR Ya=Ymin TO Ymax STEP Ystep
530   IF ABS(Ya)<1.E-5 THEN Ya=0
540   Y=(Ya-Ymin)*Sfy
550   PRINT "PA 0,";Y,""
560   PRINT "CP -5,-.25;LB";Ya;""
570   NEXT Ya
580   BEEP
590   Id1=0
600   IF Id1=0 THEN
```

```
610   BEEP
620   Xlabel$="Time (sec)"
630   BEEP
640   Ylabel$="Temperature (C)"
650   PRINT "SR 1.5,2;PU PA 50,-10 CP";-LEN(Xlabel$)/2;"0;LB";Xlabel$;""
660   PRINT "PA -11,50 CP 0,";-LEN(Ylabel$)/2*5/6;"DI 0,1;LB";Ylabel$;""
670   END IF
680   PRINT "CP 0,0"
690   BEEP
700   INPUT "ENTER THE NAME OF THE DATA FILE",D_file$
710   ASSIGN @File TO D_file$
720   BEEP
730   Md=0
740   BEEP
750   Npairs=600
760   BEEP
770   PRINTER IS 1
780   Sym=1
790   PRINTER IS 705
800   PRINT "PU DI"
810   IF Sym=1 THEN PRINT "SM."
820   IF Sym=2 THEN PRINT "SM+"
830   IF Sym=3 THEN PRINT "SMo"
840   IF Md>1 THEN
850   FOR I=1 TO (Md-1)
860   ENTER @File;Xa,Ya
870   NEXT I
880   END IF
890   FOR Xa=0 TO 199 STEP .3333333
900   ENTER @File;Ya
910   Ya=.10086091+25727.9*Ya-767345.8*Ya^2+78002556*Ya^3
920   X=(Xa-Xmin)*Sfx
930   Y=(Ya-Ymin)*Sfy
940   IF Sym>3 THEN PRINT "SM"
950   IF Sym<4 THEN PRINT "SR 1.4,2.4"
960   PRINT "PA",X,Y,"PD"
970   IF Sym>3 THEN PRINT "SR 1.2,1.6"
980   IF Sym=4 THEN PRINT "UC2,4,99,0,-8,-4,0,0,8,4,0,;"
990   IF Sym=5 THEN PRINT "UC3,0,99,-3,-6,-3,6,3,6,3,-6;"
1000  IF Sym=6 THEN PRINT "UC0,5.3,99,3,-8,-6,0,3,8:"
1010  IF Sym=7 THEN PRINT "UC0,-5.3,99,-3,8,6,0,-3,-8:"
1020  NEXT Xa
1021  PRINT "PU"
1030  BEEP
1040  ASSIGN @File TO *
1050  END
```

LIST OF REFERENCES

1. Acharya, S. and Goldstein, R.J., "Natural Convection in an Externally Heated Vertical or Inclined Square Box Containing Internal Energy Sources," Journal of Heat Transfer, November, Vol. 107, 1985.

2. Baker, E., "Liquid Cooling of Microelectronic Devices by Free and Forced Convection," Microelectronics and Reliability, Vol. 11, 1972.

3. Baker, E., "Liquid Immersion Cooling of Small Electronic Devices," Microelectonics and Reliability, Vol. 12, 1973.

4. Bar-Cohen, A., "Thermal Management of Air and Liquid Cooled Multichip Modules," IEEE Transactions on Components, Hybrids and Manufacturing Technology, Vol. CHMT-10, No. 2, June 1987.

5. Beckwith, Buck and Marangoni, Mechanical Measurements, 3rd Edition, Addison-Wesley Publishing Co., 1982.

6. Goel, S. and Jaluria, Y., "Thermal Transport From an Isolated Source On a Vertical or Inclined Surface," Eighth International Heat Transfer Conference, Vol. 3, San Francisco, California, 1986.

7. Han, S.M. and Chen, H., "Numerical Analysis of Transient Natural Convection in a Rectangular Enclosure with a Heat Source," The American Society of Mechanical Engineers, Heat Transfer in Enclosures, Vol. 39, December 1984.

8. Hazard, S.J., Single Phase Liquid Immersion Cooling of Discrete Heat Sources on a Vertical Channel, Master's Thesis, Naval Postgraduate School, Monterey, California, December 1986.

9. Incropera, F.P. and DeWitt, D.P., Fundamentals of Heat and Mass Transfer, John Wiley and Sons, 1981.

10. Jaluria, Y., "Buoyancy Induced Flow Due To Isolated Thermal Sources on a Vertical Surface," Journal of Heat Transfer, Vol. 104, 1982.

11. Jaluria, Y., "Interaction of Natural Convection Wakes Arising From Thermal Sources on a Vertical Surface," ASME HTD, Vol. 32, 1984.

12. Kisimoto, T., Sasaki, E. and Moriya, K., "Gas Cooling Enhancement Technology for Integrated Circuit Components," IEEE Transactions on Components, Hybrids and Manufacturing Technology, Vol. chmt-7, No.3, September 1984.

13. Knock, R.H., Flow Visualization Study of Natural Convection from a Heated Protrusion in a Liquid Filled Rectangular Enclosure, Master's Thesis, Naval Postgraduate School, Monterey, California, December 1983.

14. Kraus, A. and Bar-Cohen, A., Thermal Analysis and Control of Electronic Equipment, Hemisphere Publishing Corp., 1983.

15. Kuhn, D. and Oosthuizen, P.H., "Three Dimensional Transient Natural Convective Flow in a Rectangular Enclosure with Localized Heating," Winter Annual meeting of ASME, ASME HTD, Vol. 63, December 1986.

16. Liu, K.V., Yang, K.T. and Kelleher, M.D., "Three-Dimensional Natural Convection Cooling of an Array of Heated Protrusions in an Enclosure Filled with a Dielectric Fluid," International Symposium on Cooling Technology for Electronic Equipment, Honolulu, Hawaii, March 1987.

17. Liu, K.V., Yang, K.T., Wu,Y.W. and Kelleher, M.D., "Local Oscillatory Surface Temperature Responses in Immersion Cooling of a Components Array by Natural Convection in an Enclosure," Proceedings of the Symposium on Heat and Mass Transfer, October 1987.

18. Milanez, L.F. and Bergles A.E., "Studies on Natural Convection Heat Transfer from Thermal Sources on a Vertical Surface," Proceedings of the Eighth International Heat Transfer Conference, Vol, 3, 1986.

19. Oktay, S., "High Heat from a Small Package," Mechanical Engineering, Vol. 108, March 1986.

20. Oosthuizen, P.H. and Paul, J.T., "Natural Convection Heat Transfer From a Square Element Mounted on the Wall of an Inclined Square Enclosure," AIAA 22nd Thermophysics Conference, Honolulu, Hawaii, June 1977.

21. Ortega, A. and Moffat, R.J., "Heat Transfer from an Array of Simulated Electronic Components: Experimental Results for Free Convection with and Without a Shrouding Wall," Heat Transfer in Electronics Equipment, ASME HTD, Vol. 48, 1985.

22. Pamuk, T., Natural Convection Immersion Cooling of an Array of Simulated Components in an Enclosure Filled with a Dielectric Fluid, Master's Thesis, Naval Postgraduate School, Monterey, California, December 1987.

23. Park, K.A. and Bergles, A.E., "Natural Convection Heat Transfer Characteristics of Simulated Microelectronic Components," Journal of Heat Transfer, Vol. 109, February 1987.

24. Shakerin, S., Bohn, M. and Loehrke, R.I., "Natural Convection in an Enclosure with Discrete Roughness Elements on a Vertical Heated Wall," Proceedings of the International Heat Transfer Conference, Vol. 4, August, 1986.

25. 3-M Corp., Fluorinert Product Manual, Commercial Chemicals Division, St. Paul, Minnesota, 1985.

26. Touloukian, Y.S., Thermophysical Properties of Matter Vol. 2, Thermal Conductivity of Nonmetallic Solids, IFI/Plenum Data Corp., New York, 1970.

INITIAL DISTRIBUTION LIST

		No. Copies
1.	Defense Technical Information Center Cameron Station Alexandria, Virginia 22304-6145	2
2.	Library, Code 0142 Naval Postgraduate School Monterey, California 93943-5002	2
3.	Professor M.D. Kelleher Department of Mechanical Engineering Naval Postgraduate School Monterey, California 93943-5000	2
4.	Professor Y. Joshi Department of Mechanical Engineering Naval Postgraduate School Monterey, California 93943-5000	2
5.	Professor K.T. Yang Department of Aerospace & Mechanical Engineering University of Notre Dame Notre Dame, Indiana 46556	1
7.	Mr. Duane Embree Naval Weapons Support Center Code 6042 Crane, Indiana 47522-5060	1
8.	Mr. Howard Stevens Head, Electrical Systems Division, Code 271 David Taylor Research Center Annapolis, Maryland 21402	1
9.	Mr. William L. Shapleigh CEQ-C Room 11S18 NC-3 2521 Jefferson Davis Highway Arlington, Virginia 22202	1

10. Mr. Joseph Cipriano 1
Executive Director
Weapons and Combat Systems
Directorate (Sea-06)
Naval Sea Systems Command
Washington, D.C. 20362-5101

11. Lt. T.J. Benedict 1
307 Washington Ave.
Niles, Ohio 44446

Thesis
B366435 Benedict
c.1 An advanced study of natural convection immersion cooling of 3 x 3 array of simulated components in an enclosure filled with dielectric liquid.